UCRL 8558
cy 2

UNIVERSITY OF
CALIFORNIA
Ernest O. Lawrence
Radiation Laboratory

BUBBLING FROM PERFORATED PLATES

DISCLAIMER

UCRL-8558
Chemistry - General

UNIVERSITY OF CALIFORNIA

Lawrence Radiation Laboratory
Berkeley, California

Contract No. W-7405-eng-48

BUBBLING FROM PERFORATED PLATES

Robert S. Brown

(Thesis)

December 1958

Printed for the U. S. Atomic Energy Commission

Printed in USA. Price $2.75. Available from the
Office of Technical Services
U.S. Department of Commerce
Washington 25, D. C.

BUBBLING FROM PERFORATED PLATES

Contents

BUBBLING FROM PERFORATED PLATES

Robert S. Brown

Lawrence Radiation Laboratory and Department of Chemical Engineering
University of California, Berkeley, California

December 1958

ABSTRACT

A 6-inch-square column was used to investigate certain operating characteristics of perforated plates. The amplitude and frequency of the pressure fluctuations in the chamber under the plates were studied. The time-average pressure drop across a plate and dumping rate of liquid through the holes were also investigated. Various gas-liquid systems were used to study the effects of the physical properties of the system. The effect of a plate having single 0.25-in.-diam. hole and multihole plates with holes of 0.25-, 0.375-, and 0.50-inch diam. on 2-, 3-, and 4-diam. triangular spacings were studied. The frequencies varied from 10,000 to 100,000 $hr.^{-1}$ and the amplitude ranged from 0.8 to 18 lbs_f/ft^2. The total pressure drop minus the clear-liquid head varied from 0.8 to 13 lbs_f/ft^2. Time-average dumping rates with all the holes assumed to be operating ranged from 0.001 to 0.1 ft/sec, and time-average gas velocities covered the range from 5.0 to 100 ft/sec.

Correlations of the frequency and pressure drop were obtained. No theoretical or empirical approach gave an adequate correlation for the amplitude, however.

The dumping data from single-hole plates were correlated in terms of the frequency, amplitude, and pressure drop by the application of the theory of flow through a sharp-edged orifice. The multihole dumping was found to result from a complicated interaction of the bubbling from neighboring holes. However, no theoretical or empirical approach adequately correlated the data.

Some dumping data were obtained on a 2- by 2-ft tower, and a possible method of correlation proposed.

BUBBLING FROM PERFORATED PLATES

I. INTRODUCTION

In recent years there has been a considerable revival of interest in perforated-plate trays equipped with downcomers for use in distillation and absorption columns. Until recently, it had been thought that the operative range of gas velocity was too narrow for flexible operation. However, the recent studies of Arnold et al.,[1] Mayfield et al.,[2] Zenz,[3] and Hunt et al.[4] show that this is definitely not the case. A comparative study of bubble-cap trays and perforated-plate trays equipped with downcomers was performed by Jones and Pyle.[5] Their results show somewhat lower pressure drop, definitely lower entrainment, and higher efficiency for the perforated-plate trays. These results are also substantiated by the results of Arnold,[1] Mayfield,[2] and Hunt.[4] Thus, as Jones and Pyle have pointed out,[5] perforated-plate trays have definite economic advantages over bubble-cap trays.

In these studies of the operating characteristics of perforated-plate trays,[1-4] little effort has been applied to the prediction of how much liquid will dump through the holes. A more detailed review of these reports and others appears in a later section. However, it suffices to say here that all the previous efforts have been directed toward defining some minimum vapor velocity. Below this velocity, the tray dumps liquid, and its operation is generally unsatisfactory.

However, as Hunt[6] and Umholtz[7] have pointed out, there is a three-fold change in gas velocity from the point when the holes first begin to dump liquid to the point when they are running full of liquid. Thus, one could arbitrarily define the minimum vapor velocity anywhere in this region although the usual definition is the point where dumping first occurs.

The question that is of greater interest and which has a more meaningful answer in terms of column operation is: what is the dumping rate under a given set of geometric and flow conditions? The purpose of this work then, is to answer in so far as possible the above question through an investigation of the bubbling and other fluid-mechanical factors which influence the dumping.

A. Literature Review

Frequency of Bubbling

In the past ten years, many articles have appeared dealing with bubble formation from single-hole plates and rising of bubbles through liquids.[8-12] Most of these studies have been directed toward predicting the bubble diameter and its terminal rising velocity in terms of geometry and the various physical properties of the system.

The principal path of attack has been to determine the frequency of bubble formation. Then, for a known volumetric gas-feed rate, the bubble volume was determined by the use of the relation

$$V_B = Q_g^o / F, \qquad (1)$$

where V_B is the bubble volume, Q_g^o the time-average volumetric gas flow, and F the frequency. The bubbles were assumed to be spherical, and the diameters thus obtained were empirically correlated against the gas and liquid physical properties and the geometry of the system.

The frequency was determined in a variety of ways. van Krevelin and Hoftijzer[12] used low flow rates and actually counted the bubbles. Davidson,[8] Calderbank,[9] and Quigley et al.[11] used a "Strobotac" to determine the bubbling frequency. Calderbank[9] used a second method which involved the use of a platinum wire probe. One lead was inserted in the liquid pool; the other lead was placed in the bubble path, and the probe was connected to a pulse counter. Thus, by counting the number of pulses over a known time interval, the frequency was determined. Robinson[10] took high-speed movies of the bubbles. A timing mark was placed on the film and by counting the bubbles between the timing marks the frequency was obtained. Hughes determined the frequency of the pressure fluctuations which is the same as the bubbling frequency for a single-hole plate.[13]

Robinson proposes that there are three bubbling mechanisms.[10] The first is valid at low gas-flow rates less than 0.01 ft^3/hr into chambers of 0.01 to 0.1 ft^3. The surface forces are in balance with the buoyancy

forces and the frequency is a linear function of gas velocity. The second mechanism is a transition region where the frequency is a function of the gas and liquid properties, chamber volume, and orifice size. The third mechanism applies at gas flows greater than 1 ft^3/hr into chambers of 0.01 to 0.1 ft^3 which is the region of real interest. Here Robinson proposes that the frequency is independent of the liquid properties and depends only on the geometry of the apparatus and the sonic velocity of the gas.[10]

For this third region, Robinson proposes a correlation for the bubbling frequency in terms of the resonant frequency for the chamber-orifice system, volumetric gas-flow rate, and orifice diameter. The expression for the resonant frequency derived by Lord Rayleigh is used.[14] He finds the frequency to be independent of the liquid physical properties. No mention is made of any effect of the liquid head. The resulting correlation is

$$F = 0.0316 \left\{ \frac{Q_g^o \; c}{D_o^3 \sqrt{2\pi}} \left[\frac{A_o}{V_c \left(L + 1/2 \sqrt{\pi A_o} \right)} \right]^{1/2} \right\}^{1/2} , \qquad (2)$$

where D_o = diameter of the hole, A_o = area of the hole, L = thickness of the plate, and V_c = volume of the chamber under the plate.

Amplitude of Pressure Fluctuations

Davidson[8] and more recently Hughes and co-workers[13] have pointed out that the volume of the chamber under the plate is a very important factor in the formation of a bubble. This effect can also be seen by combining Eqs. (1) and (2). This fact had been overlooked by several investigators.[9,11,12] Hughes carried this observation several steps further by placing strain gauges on the side of the chamber.[13] Thus, he was able to measure the pressure fluctuations in this chamber. Data at low gas-flow rates were taken on single-hole plates. Under these conditions, Hughes finds the maximum pressure change in the chamber to equal $4\gamma/D_o$ where γ is the surface tension. However, at higher flow rates, the amplitude of the fluctuations is greater because the pressure difference across the interface is greater than the equilibrium surface-tension

presure difference. This is a result of the dynamic nature of the gas-liquid interface. However, Hughes presented no data on the amplitudes or frequencies of the pressure fluctuations at these higher gas flows.

B. Experimental Studies

The Present Problem

From these discussions of the work that has already been reported, it is apparent that there is still much to be understood. In particular, frequency, amplitude, and pressure-drop data on plates with small numbers of holes are not available at the higher flows (greater than 5 ft./sec. through the holes). Therefore, these variables were investigated in the hope of obtaining a better understanding of the bubbling process.

Experimental Apparatus and Procedure

The apparatus, shown schematically in Fig. 1, was designed to obtain information on the bubbling process and dumping mechanism. The main test section consisted of a lucite box 1/4 inch thick, 6 inches on a side, and 19 inches high. The plate was located 6 inches above the floor of the column. Lucite was used to allow visual observation of the bubbling and dumping. The front of the column was removable so that different plates could be inserted. This feature also made it possible to place lucite blocks in the chamber below the plate, and thus the effect of chamber volume on the dumping rate could be determined. The plates were also made of lucite, and all holes were drilled and reamed to size, thus assuring square edges.

Gas was supplied from the building compressor in the case of air and from cylinders in the cases of helium, argon, and freon 114. The gas flow was determined by the pressure drop across a previously calibrated orifice. Diameters of 1/8, 1/4, 1/2, and 3/4 in. were used. Several manometers were connected in parallel to give a greater range of flows for a given orifice. The smaller diameter orifices were used wherever possible to define the volume of the chamber under the plate more accurately. The temperature of the entering gas was measured by a copper-constantan thermocouple inserted in the gas line just below the orifice.

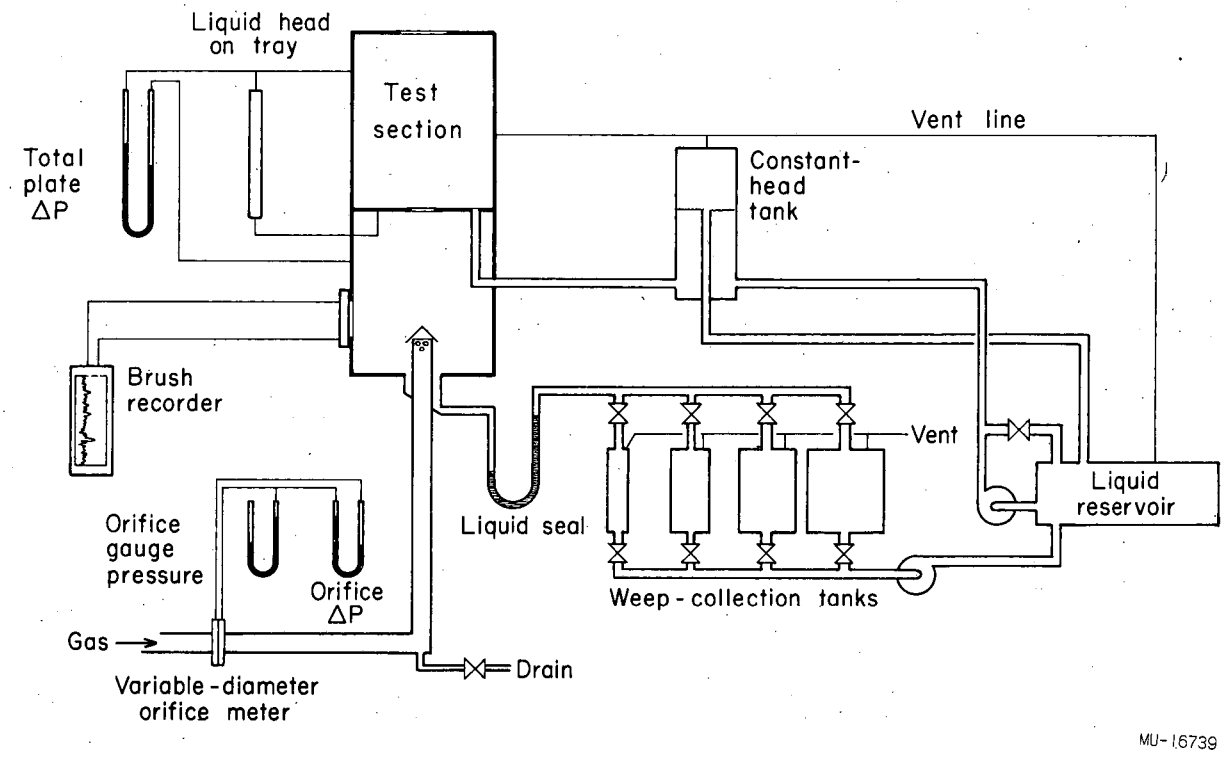

Fig. 1. Schematic diagram of 6-in. column.

The exit gases were vented to atmosphere and were not recirculated.

The liquid on the plate was supplied by a constant-head system which is shown in Fig. 1. The head of liquid on the plate was controlled by the height of the stand pipe in the center of the constant-head tank. The head was measured by a sight gauge which could be flushed out to remove any gas bubbles trapped in the lines.

Samples of the liquids before and after use in the equipment (except water) were taken and their physical properties determined. The surface tension was determined with a standard tensiometer, the viscosity with a calibrated Ostwald viscometer, and the density by weighing a known volume of material. These properties are reported in Table I. There were no appreciable differences in the properties of the liquids before and after use, and the values reported are the average of the two measurements.

The dumping rate was determined by collecting the liquid in one of the four calibrated collecting tanks. By measuring the level change over a known period of time and knowing the area of the tank, the time average dumping rate was calculated. These tanks had volumes 6.2, 11, 99, and 275 $in.^3$ and were all 14 in. high. The level in the tank could be read to ±0.2 in.

The liquid seal, as shown in Fig. 1, was required to seal off the tanks from the chamber volume. Therefore, the volume of these tanks was not considered in calculating the chamber volume.

The fluctuations of the gauge pressure in the chamber under the plate were determined by measuring the change of the strain on a 0.0025-in.-thick aluminum diaphragm stretched tightly across a 2-in.-diam. hole in the side of the chamber. Two Baldwin-Lima-Hamilton Corp. SR-4 Type C-5 strain gauges, with a resistance of 350 ohms, were glued to the diaphragm and were connected in a Wheatstone-bridge circuit as shown in Fig. 2. Resistors A and D were on the diaphragm and B and C were used for temperature compensation. Using two resistors on the diaphragm gave a bridge with twice the sensitivity of a one-resistor diaphragm. The bridge output was amplified twice and then recorded on a Brush recorder.

Table I

Physical Properties of Liquids
(All measurements at 25 ± 0.2° C)

Liquid	Density (gr/cc)	Viscosity (cp)	Surface tension (dynes/cm)
Water	1.0	0.90	72.5
Kerosene	0.795	1.71	27.9
≈ 58% Glycerine in H_2O	1.15	8.10	53.7
≈ 81% Glycerine in H_2O	1.21	52.2	54.5
1,1,1-Trichloroethane	1.31	0.79	29
≈ 50% K_2CO_3 50% H_2O	1.53	7.71	31.9

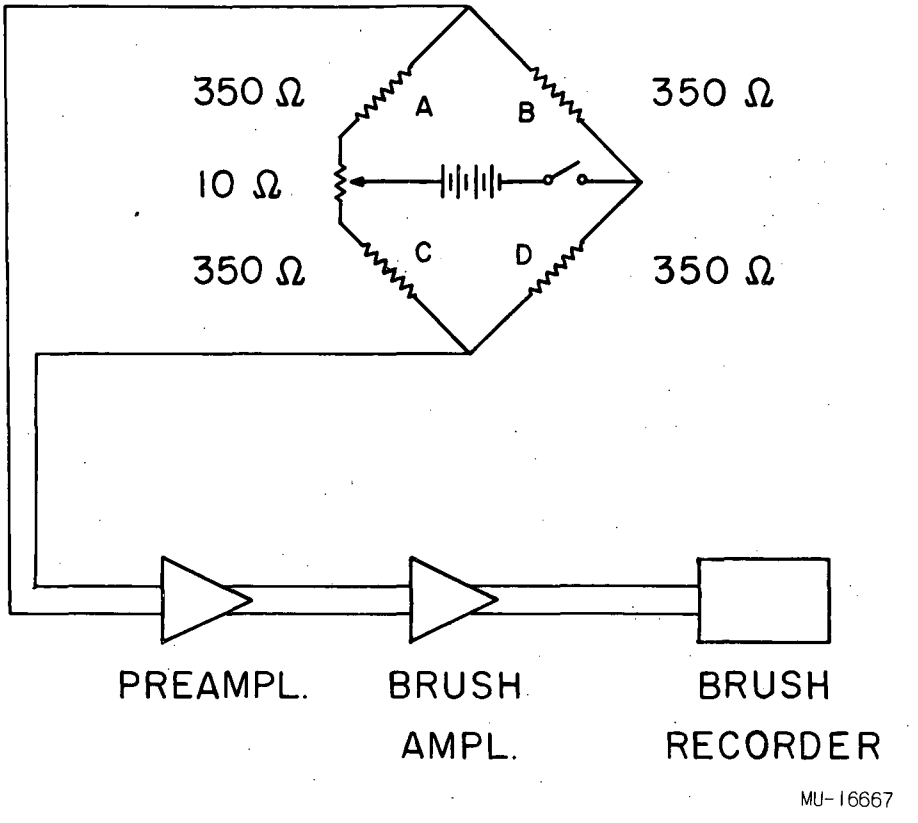

Fig. 2. Pressure-fluctuation measuring circuit. (Bridge powered by 7 Mallory 4 RM-4R batteries.)

Thus, pressure changes of ±0.2 lbs_f/ft^2 could be detected. The 10-ohm balancing resistor provided a means of bucking out the time-average pressure, and thus a higher amplification could be used and the fluctuating component recorded with greater accuracy. The entire circuit, including the strain gauges, was shielded, and this shielding was grounded to minimize the effect of 60 cps pickup.

All the manometers were constructed of 3/8-in. o.d. Tygon tubing and were connected to 5-in.-diam. reservoirs. The high-pressure line was connected to the reservoir and the low-pressure side to the other end of the manometer. Thus, all the pressure difference could be measured by the change in liquid level in the Tygon tubing which could be read to ±0.2 in. This arrangement made it more convenient to mount the manometers on a panel board.

With plates having less than 29 holes, liquid flowed violently from one side of the column to the other. The dumping was greatly increased as the liquid sloshed over a particular hole. This type of action does not occur in columns with a large number of holes in the plate, and therefore is an undesired effect. In order to eliminate this effect, a sheet of copper with a 4.5-in.-diam. hole in the center and many small holes around the outside edge was placed in the liquid pool. The height of this copper sheet was adjustable and was placed as close to the liquid surface as possible. However, the distance from the sheet to the liquid surface had no effect on the dumping rate, provided the sheet was at least one inch above the plate. Also, the diameter of the center hole did not affect the dumping rate. This arrangement essentially guided the bubbling column and put a damper on the side-to-side liquid flow. Thus, the action of plates with a small number of holes approximated the operation of plates with a large number of holes.

Fig. 3 shows an over-all picture of the apparatus. The test section with the diaphragm holder can be seen in the upper left section. The collecting tanks are directly below the test section. The constant-head tank and manometer system are shown on the panel board to the right. The box at the base of the panel contains the batteries, temperature-

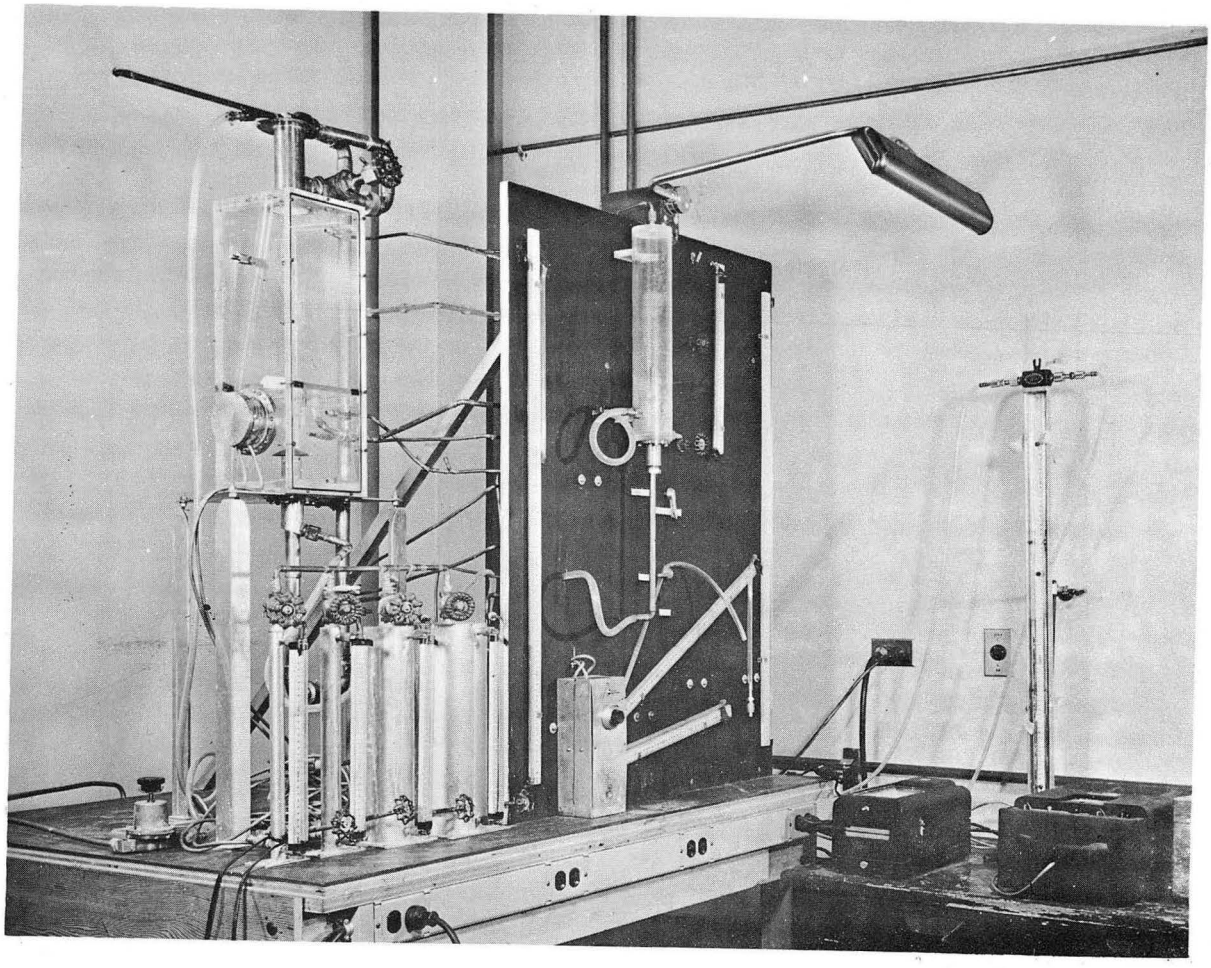

ZN-2115

Fig. 3. Over-all view of 6-in. column.

compensating resistors and balancing resistor for the diaphragm circuit. The Brush recorder and amplifier are shown at the extreme right.

Fig. 4 shows a close-up of the chamber under the plate. The larger pipe on the right feeds liquid to the plate, and the others are pressure taps. The diaphragm can be seen on the left. The plate and gas inlet pipe are also visible.

The column was started up by first turning on the gas flow. Then the liquid was fed to the constant-head tank, and the head on the plate allowed to build up to the desired value. Ten minutes were allowed for steady state to be reached. The weep collection tank which would give the maximum level change over the 4-min. collection period was selected and the proper valve settings made. The level in the tank was recorded at the start, mid-point, and end of the collection period. The total pressure drop across the plate, liquid head, gas temperature, average chamber pressure, and gas flow rate were also recorded at each of these points. At some convenient point during the run, the pressure fluctuations were recorded for approximately 4 sec. The amplifier gain and chart speed were also recorded. At the conclusion of the run, the weep-collection tank was emptied and the gas flow changed to the next desired point. Five minutes were allowed for steady state to be reached between points. In this way, a series of five to ten points was obtained for a given geometry and liquid-gas system.

Upon completion of a series of runs, the column was shut down. The liquid phase, gas phase, or geometry was changed as desired, and a new series of runs were made according to the procedure outlined above.

In this way, the following variables were investigated:

1. Gas velocity.
2. Liquid head on the plate.
3. Hole diameter.
4. Hole spacing.
5. Ratio of total hole area to column area.
6. Gas properties.
7. Liquid properties.
8. Volume of the chamber under the plate.

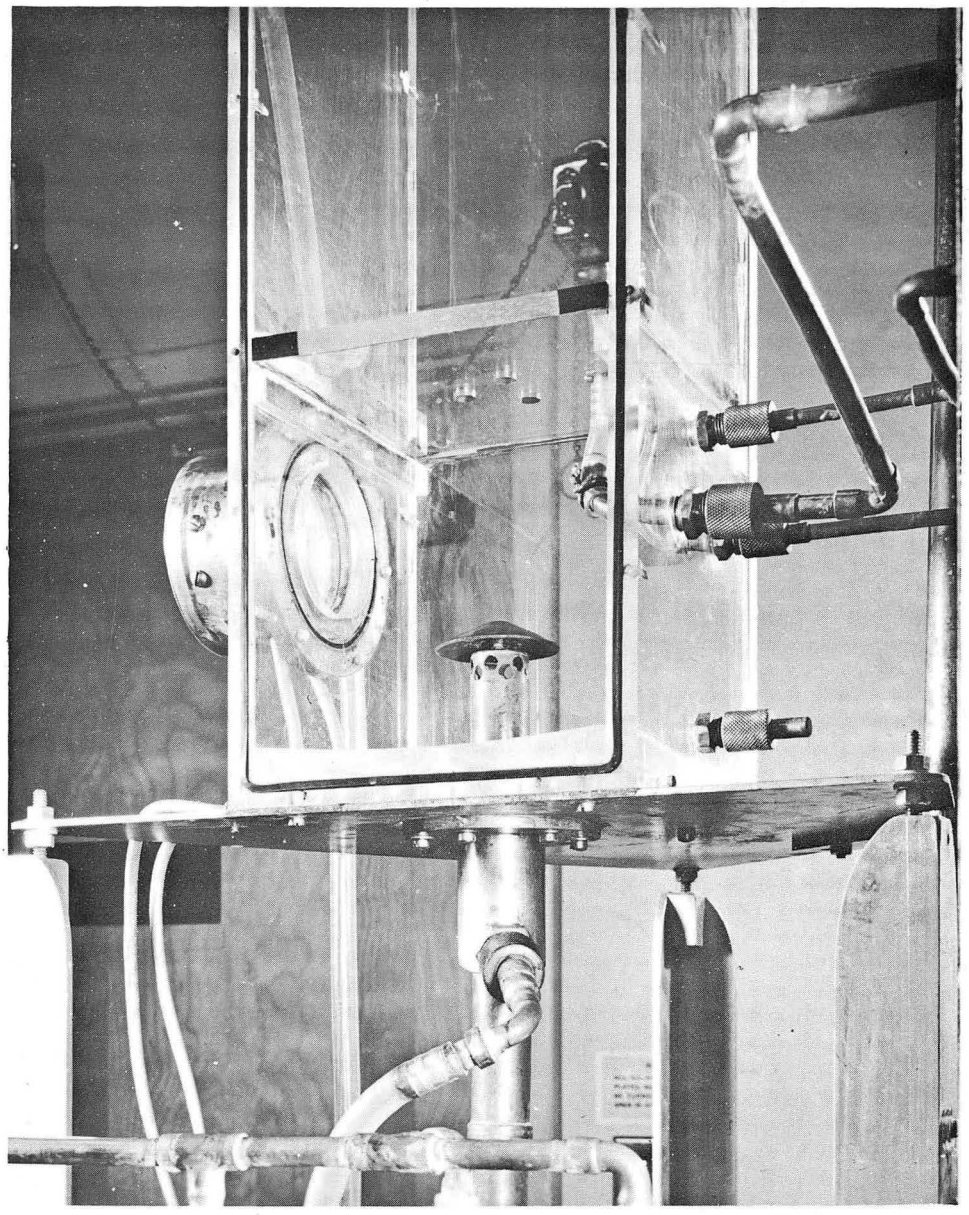

ZN-2114

Fig. 4. Close-up of test section in 6-in. column.

Table I shows the range of liquid properties covered experimentally and Table II shows the physical properties of the various gases. The data on the various geometries used are shown in Table III. The time-average gas velocity through the holes was varied from 4 ft/sec to 100 ft/sec. The head of liquid on the plate was varied from 2 to 4 in. because Hughmark and O'Connell recommended this range as good design limits.[15]

Table II

Physical Properties of Gases
(All data at 68±2°F)

Gas	Density[a] lbs_f/ft^3	Viscosity lb/ft sec x 10^3	Sonic velocity ft/sec
Helium	0.0103	0.132[16]	3180[17]
Air	0.0742	0.123[16]	1130[17]
Argon	0.103	0.149[16]	1010[17]
Freon-114	0.445	0.077[18]	424[b]

[a] Calculated from ideal gas law.

[b] Calculated from adiabatic expansion of ideal gas at constant temperature assuming $C_p/C_v = 1.15$

Table III

Dimensions of Geometries Used

Hole diam. (in.)	Plate thickness. (in.)	Hole spacing (in.)	Number of holes	Chamber volume(in^3)
1/4	1/4	1	3	262
1/4	3/4	1	3	262
1/4	1/4	1	3	91.5
1/4	1/4	1	7	262
1/4	1/4	1	7	91.5
1/4	1/4	1	7	142
1/4	1/4	1	3	142
3/8	3/8	1 1/2	3	262
1/2	1/2	2	3	276
1/2	1/2	1 1/2	3	276
3/8	3/8	1 1/8	3	262
1/4	1/4	3/4	3	262
3/8	3/8	3/4	3	262
1/2	1/2	1	3	262
1/4	1/4	1	29	276
1/4	1/4	1/2	3	262
1/4	1/4	3/4	41	290
1/4	1/4	3/4	49	290

Same as 49-hole plate with baffle around edge of holes added.

Theoretical Interpretation of Results

Hughes and co-workers have presented an excellent simplified picture of the bubbling process.[13] Their approach is to describe the pressure and flow changes during bubble formation in terms of an electrical analog. This analog is shown in Fig. 5. It consists of a constant current source which represents the gas flowing into the chamber below the plate. The capacitor is made analogous to the chamber under the plate and the resistor represents the resistance of the plate to gas flow. Currents are similar to flows and voltages are analogous to pressures.

Start at the point when the bubble first begins to form. The pressure in the chamber under the plate rises because the flow out of the chamber is less than the flow into it. Another way of viewing this period in the cycle is to say that, initially, the rate of bubble growth is small, but it increases with time. Thus, as the bubble grows, more and more gas is required to continue its growth. At some point the flow out of the chamber becomes greater than the flow into it, and the chamber pressure falls. This decrease in pressure continues until there is no potential remaining to support bubble growth. At this point, the bubble breaks off, and liquid seals off the hole. Because the flow into the chamber is constant and there is no outflow, the chamber pressure rises, and the process is then repeated.

Ideally, the solution to this flow problem would be to solve the force-balance, mass-balance, and analog equations for the chamber pressure and bubble volume as functions of time. The boundary condition would be to equate the pressure in the bubble to some theoretical break-off pressure. From such a solution, the minimum point in the pressure wave and the final bubble volume could be calculated. The frequency could then be calculated using Eq.(1). By integrating the pressure wave, the time-average pressure could be determined.

However, this solution cannot be obtained analytically for three reasons. First, the force-balance equation as developed by Hughes contains two nonlinear terms.[13] Also, the flow through the plate is in the

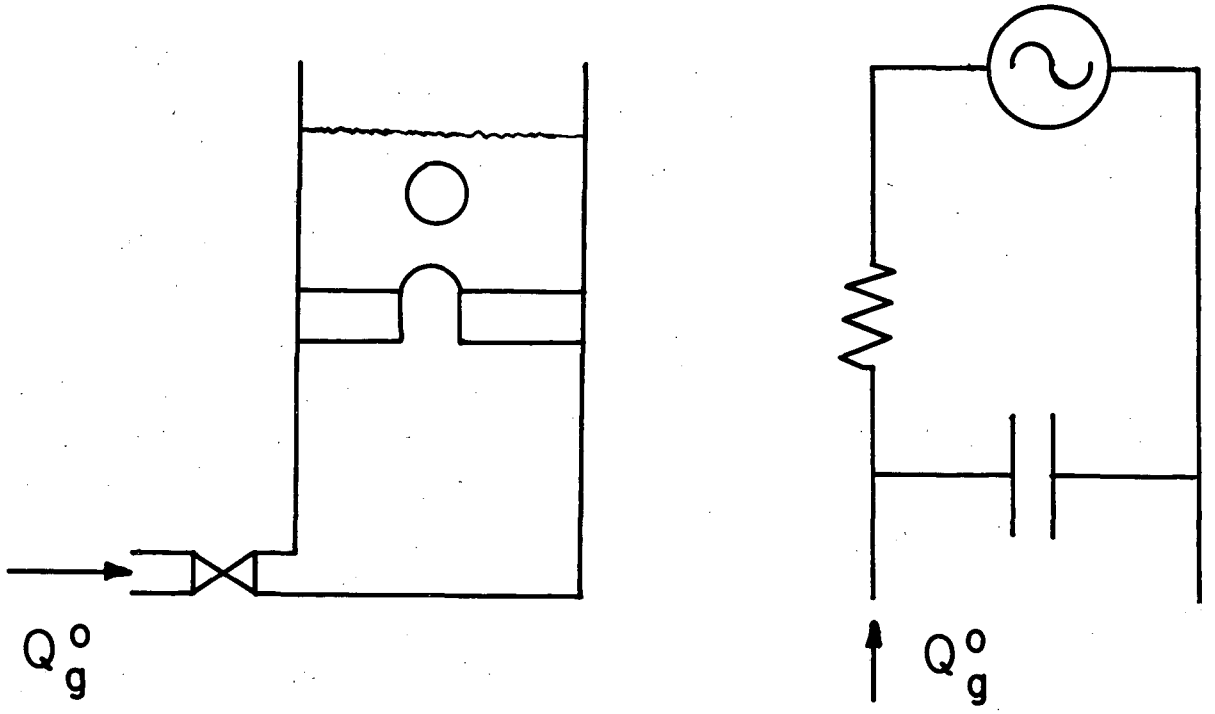

Fig. 5. Electrical analog to bubbling.

turbulent region for part of the cycle which introduces another nonlinear term. Secondly, it must be assumed that individual spherical bubbles are formed. However, this is not the case in actual practice. Thirdly, the prediction of the break-off pressure is not possible in such a violently moving system. Therefore, prediction of the amplitude and frequency is not possible from purely theoretical considerations because the equations are too difficult to solve.

The next logical step, then, is to examine the data for an empirical correlation.

Frequency

Correlation of frequency data. Fig. 6 shows the effect of the chamber volume and the number of holes on the frequency of the pressure fluctuations. This plot clearly shows that the volume per hole is the correct correlating parameter. There is no effect of the number of neighbors a particular hole sees as might have been expected for plates with a small number of holes. The data for the 29-hole plate are slightly low when the volume-per-hole criterion is used. There is no explanation for this anomaly. However, the effect is small and can be neglected for all practical purposes, as will be shown when the correlation of the data is developed.

When different gases were used, the frequency data shown in Fig. 7 were obtained. These data indicate a slight effect of the gas properties on the frequency, although the specific property is not immediately apparent. Cross plots of frequency vs gas density and frequency vs gas kinematic viscosity, both at constant gas flows, were made. However, no definite conclusions can be drawn from these plots, either. Both parameters appear applicable. This point will be discussed further when the general correlation is developed.

Thought was given to a compressibility effect which is measured by the Mach number. However, since the velocities found in the system are low compared to the sonic velocity, this effect was neglected in the further analysis of the data.

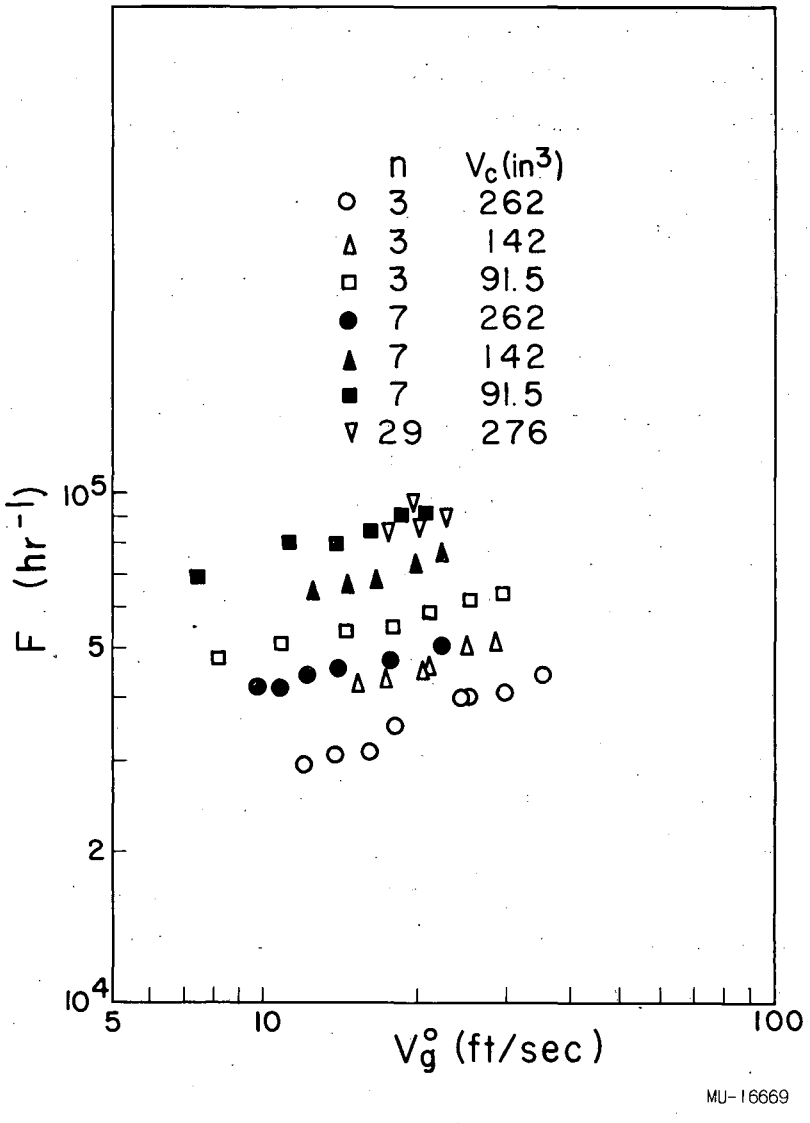

Fig. 6. Effect of chamber volume on frequency.
(Air-water system, D_o = 0.25 in., D = 1.0 in., h_L = 2.0 in.)

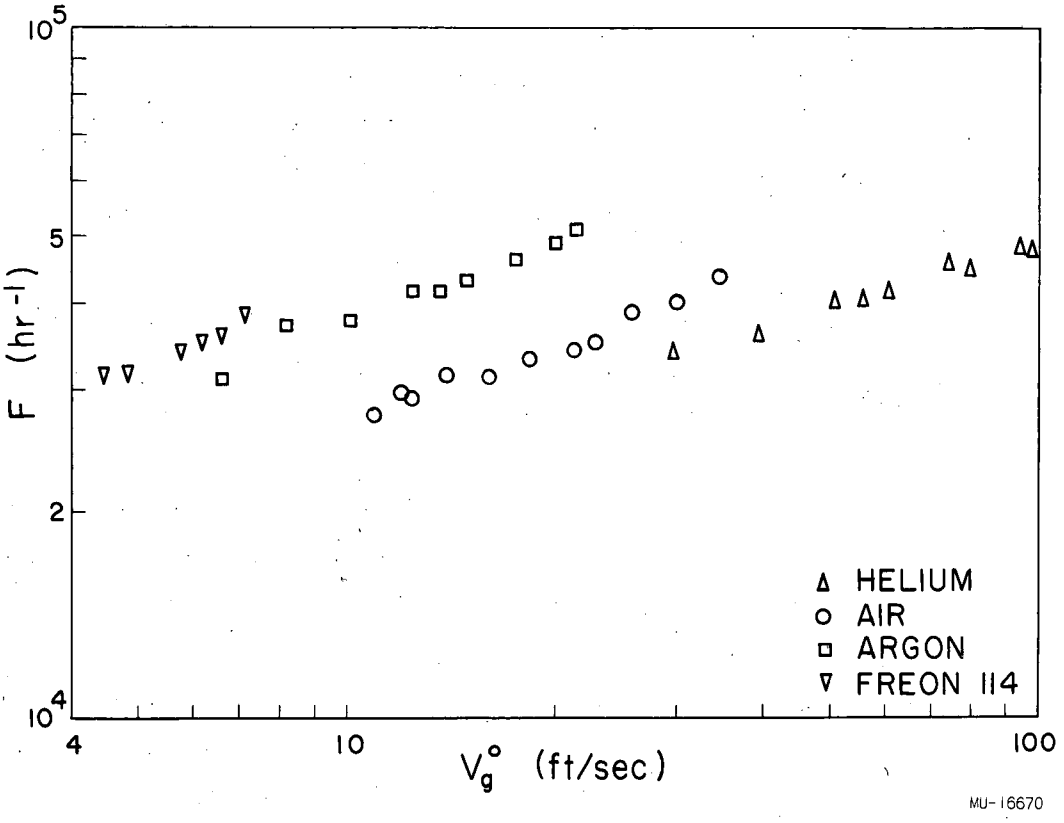

Fig. 7. Effect of gas properties on frequency. (Water as liquid, V_c = 262 in^3., h_L = 2.0 in., D_o = 0.25 in., n = 3, D ≅ 1.0 in.)

In Fig. 8, data for holes of different diameters and different spacings are presented. This plot shows that the frequency is practically independent of the hole diameter and depends almost entirely on the distance between holes. The data for 0.50-in.-diam. holes on 1.5-in. spacings fall on top of the data for 0.375-in.-diam. holes on 1.5-in. centers. The same is true for 0.25-in.-diam. and 0.375-in.-diam. holes on 1.0-in. centers. This really says that the characteristic dimension of the system is the distance that the gas "bubbles" can expand horizontally.

Fig. 9 shows the data obtained when different liquids were placed on the plate. When these data are compared with the table of measured liquid properties (Table I) it is apparent that the significant liquid property is the density. The viscosity has no effect, since the data for the glycerine-water solutions are very close to the pure-water data. Surface tension appears to have little if any effect on the frequency, although this is not obvious from these results.

To develop a correlation of the frequency data, consider the electrical analogy of the bubbling process as presented by Hughes et al.[13] Also, assume that the bubble breaks off from the plate when the pressure inside the bubble reaches a certain level. It seems logical to assume that this break-off pressure is independent of the chamber volume. Also, since the volume of the bubble increases with increasing chamber volume,[13] the time required for the pressure to build up to the release pressure is longer for larger chambers. Hence, fewer bubbles can form in a given period of time and thus the frequency goes down as the chamber volume is increased. Therefore, it seems reasonable to say that the ratio of the total volume of all the bubbles to the chamber volume is an important variable in determining the frequency. This "volume number", Φ, can be expressed by the dimensionless group

$$\Phi = n A_o V_g^o / V_c F , \qquad (3)$$

where n is the number of holes and V_g^o is Q_g^o / nA_o.

The frequency is also affected by the resistance presented by the plate to gas flow. Suppose there are two plates with different pressure-

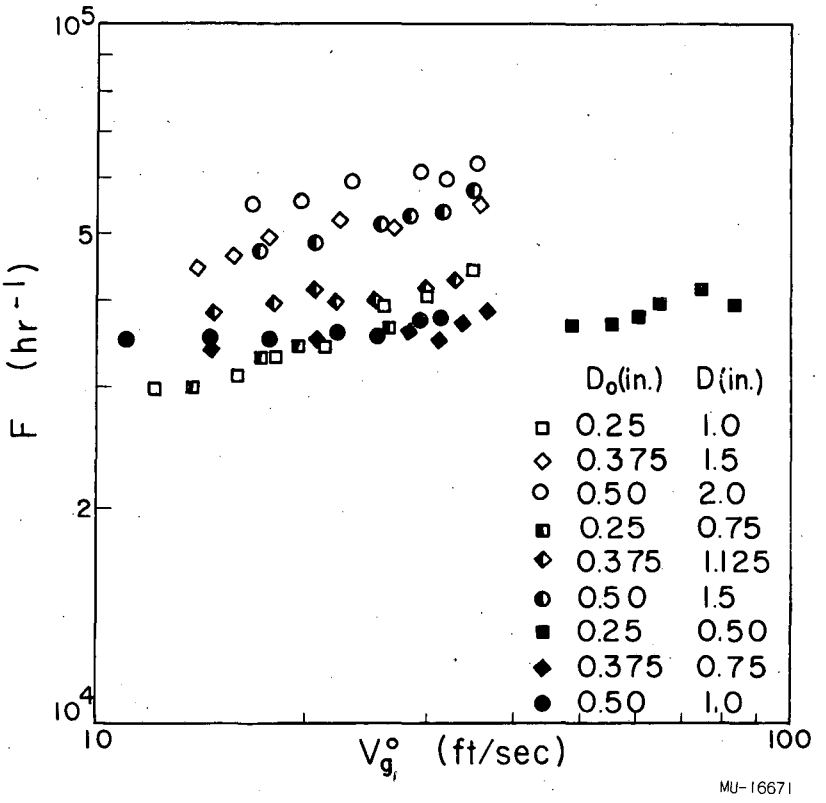

Fig. 8. Effect of hole diameter and spacing on frequency. (Air-water system, V_c = 262 in^3., n = 3, h_L = 2.0 in.)

$$\frac{n A_o V_g^o}{V_c F} \propto \left(\frac{nD^3}{V_c}\right)\left(\frac{D_o}{D}\right)^2 \left(\frac{V_g^o}{DF}\right) \quad . \tag{6}$$

Substituting Eq. (6) into Eq. (4) gives the expression

$$\frac{DF}{V_g^o} = A \left(\frac{nD^3}{V_c}\right)^a \left(\frac{D_o V_g^o \rho_g}{\mu_g}\right)^b \left(\frac{\rho_g}{\rho_L}\right)^c \left(\frac{D}{D_o}\right)^d \quad . \tag{7}$$

The constants in Eq. (7) were determined by the method of least squares. Substituting these constants into Eq. (7) gives the relation

$$\frac{DF}{V_g^o} = 46{,}700 \left(\frac{nD^3}{V_c}\right)^{0.46} \left(\frac{D_o V_g^o \rho_g}{\mu_g}\right)^{-0.69} \left(\frac{\rho_g}{\rho_L}\right)^{0.84} \left(\frac{D}{D_o}\right)^{-0.54} \quad . \tag{8}$$

Discussion of frequency correlation. A comparison of the experimentally measured frequency number, DF/V_g^o vs that calculated from Eq. (8) is shown in Figs. 11 through 14. The results of this comparison show that 95% of the total variation in the frequency number has been accounted for by Eq. (8). The remaining 5% must be explained by some other effect, such as a variable that was omitted from the analysis, experimental error, or a combination of both. Further analysis of this comparison shows that the average deviation is ±10% when based on the calculated frequency number. These figures are based on 215 points.

On the basis of this comparison, Eq. (8) can be used with some confidence to predict the frequency of the pressure fluctuations for multihole plates. However, for single-hole plates the effective distance between holes goes to infinity. Under this condition, Eq. (8) predicts a frequency of zero. Therefore, Eq. (8) does not have a sufficient theoretical basis to allow extrapolation to the limiting condition of a single-orifice plate.

Because of this failure of Eq. (8) for single-hole plates, a comparison with Robinson's correlation[10] is not really valid. However, it is of interest to note the different effect of the chamber volume in

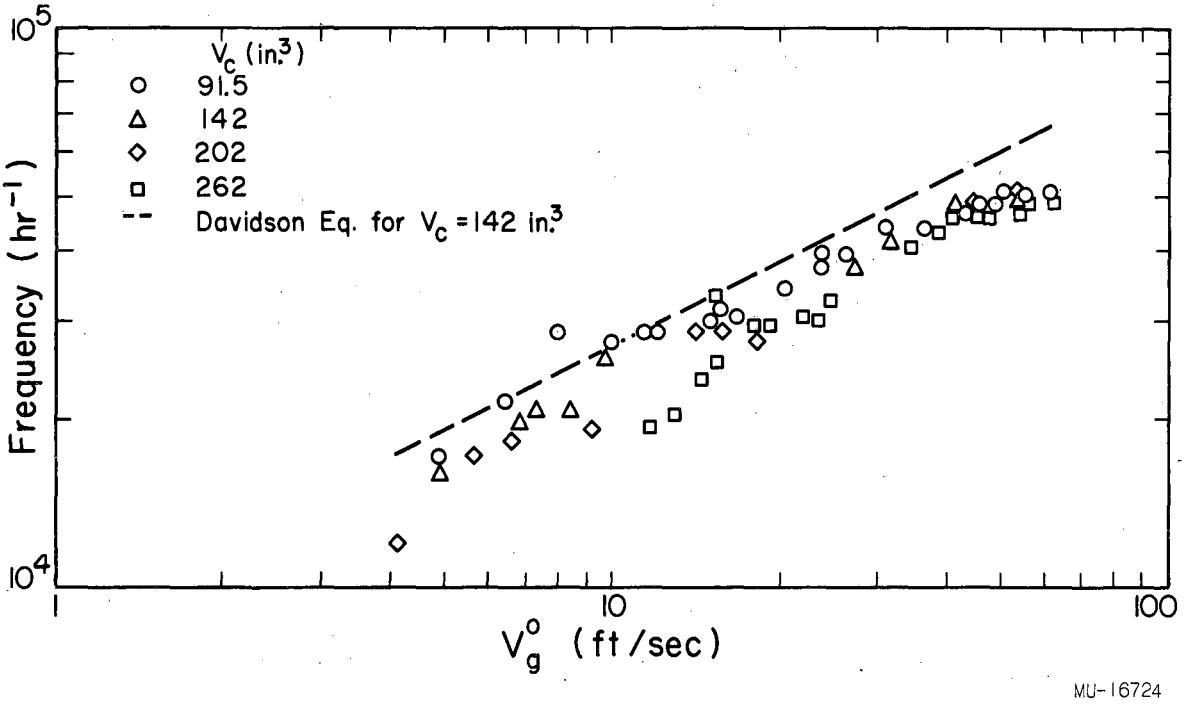

Fig. 10. Single-hole frequency. (Air-water system, D_o = 0.25 in.)

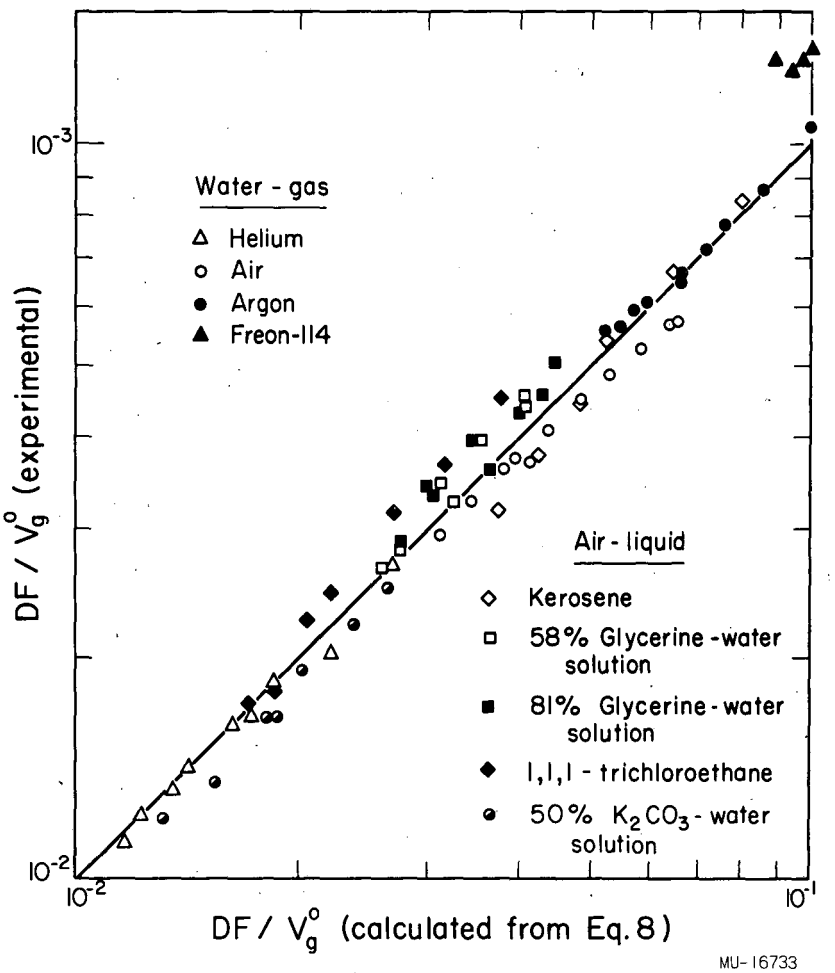

Fig. 11. Correlation of effects of gas and liquid properties on frequency. (V_c = 262 in^3., D_o = 0.25 in., D = 1.0 in., h_L = 2.0 in.)

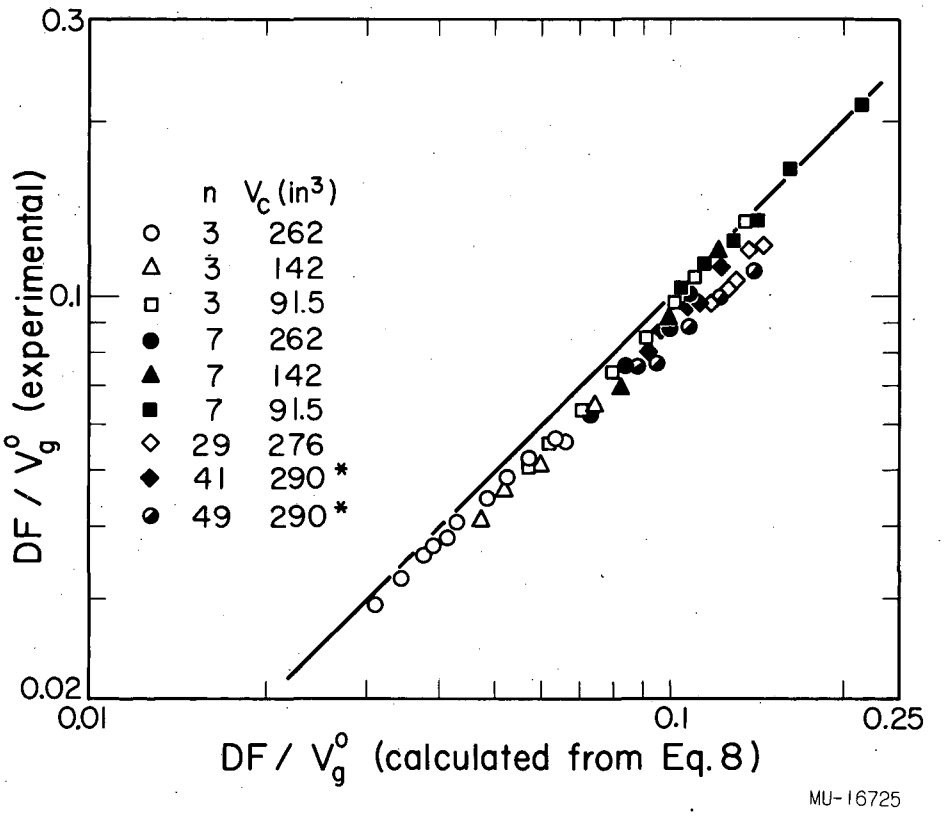

Fig. 12. Correlation of effect of chamber volume on frequency. (Air-water system, h_L = 2.0 in., D_o = 0.25 in., D = 1.0 in., *D = 0.75 in.)

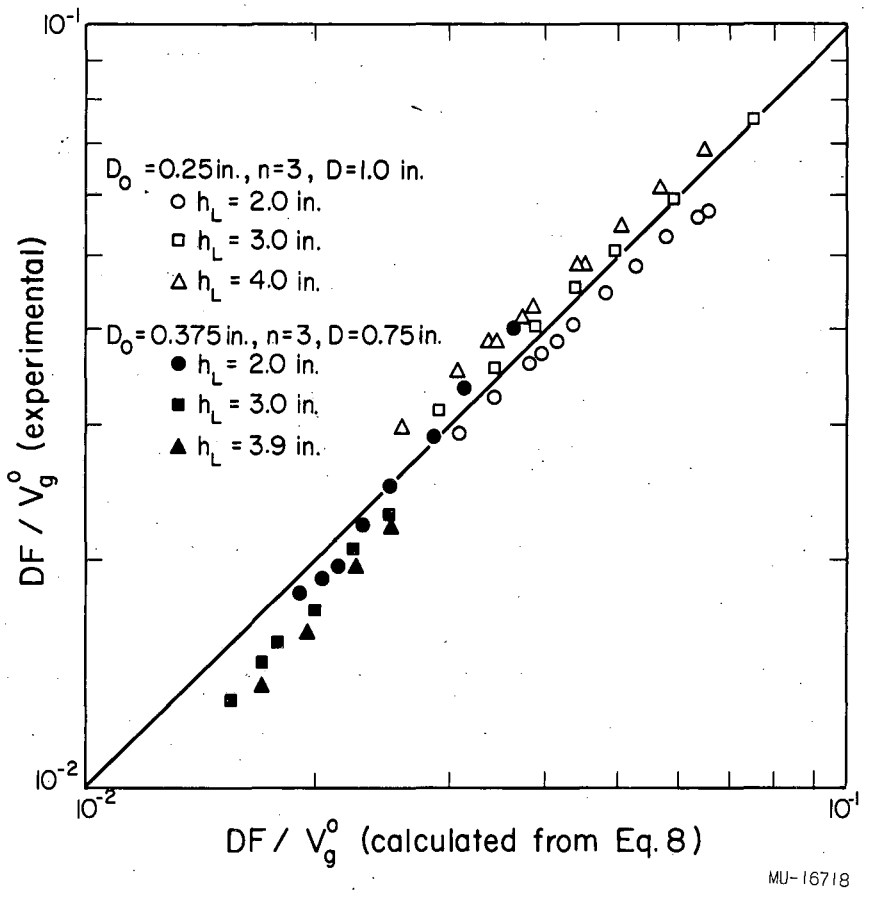

Fig. 13. Correlation of liquid-head effect on frequency. (Air-water system, V_c = 262 in^3.)

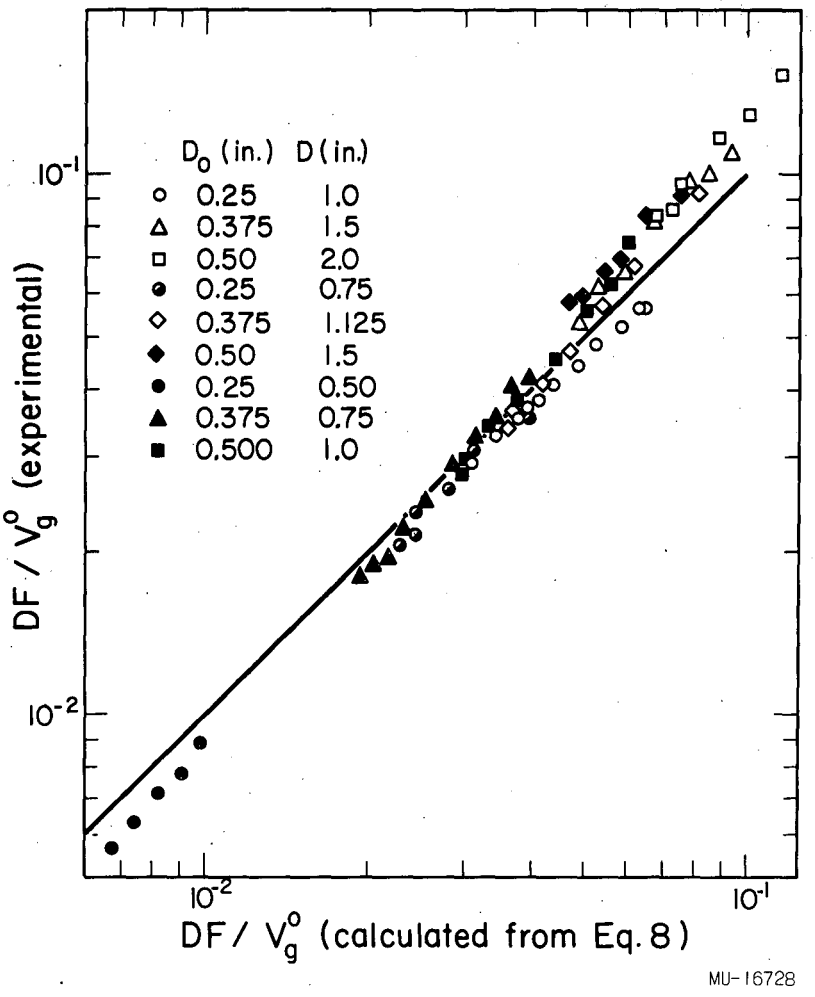

Fig. 14. Correlation of effect of hole diameter and spacing on frequency. (Air-water system, V_c = 262 in^3., n = 3, h_L = 2.0 in.)

these two cases. Robinson found the exponent to be -0.25, and Eq. (8) predicts -0.46 even though the same range of volumes was covered experimentally.

As was mentioned, some single-hole frequency data were obtained and the results are shown in Fig. 10. It is apparent from these results that the volume effect predicted by Robinson's correlation[10] does not agree with the volume effect found in this work. However, Robinson used smaller chambers than were used in the single-hole portion of this work. On the basis of the Hughes' analog[13] it seems reasonable to expect the volume effect to decrease and eventually drop out for very large chambers. Therefore, the failure of Robinson's correlation at higher chamber volumes is not unreasonable.

Sufficient single-hole data were not taken to check Robinson's suggestion that the frequency is independent of the liquid physical properties. Nevertheless, Eq. (8) shows that this theory is in error for the multihole case. It is possible, however, for the liquid density effect to come in as a result of using two or more holes.

Conclusion about frequency. There are two main conclusions that can be drawn from this frequency work. The first is that Eq. (8) predicts the frequency of the pressure fluctuations for multihole plates with good accuracy. However, this frequency is not necessarily the same as the bubbling frequency. Secondly, more theoretical understanding of the bubbling from single-orifice plates is required before the differences between Robinson's correlation[10] and the data obtained in this study can be reconciled.

Amplitude of Pressure Fluctuations

Correlation of pressure-fluctuation amplitudes. Because of the emphasis on dumping in this work, the amplitude is defined here as the average maximum dip of the chamber pressure below the time-average pressure. The reason for this definition will be obvious when the dumping is considered theoretically. To calculate these amplitudes, the time-average pressure was determined by integrating the pressure waves.

Accurate measurement of the time-average pressure with the diaphragm circuit was impossible because of drift in the bridge resistance over a period of time. Therefore, the integration procedure was used. The verage minimum point in the pressure wave was obtained by averaging approximately 40 individual points. This average was then subtracted from the time average to obtain the amplitude reported here. The time average was determined to ±1 chart division, and the average difference was approximately 7 chart divisions. The average expected accuracy of the results, therefore, is ±15%. Naturally, the uncertainty increases as the average amplitude decreases and can go to ±30% for amplitudes in the region of 1.0 to 2.0 lbs_f/ft^2.

Let us first consider the average amplitude, and the variations about the average later. The data obtained using different gases are shown in Fig. 15. It is difficult to draw any definite conclusions about the effect of gas properties on the amplitude from this plot. It seems possible to make either of two conclusions. The first is that the average amplitude, $\bar{P}_f$, is a function of gas flow and independent of gas properties. The second is that the amplitude is independent of gas flow and depends only on the gas properties. The scatter is just too large to draw any definite conclusions. Other than by measurement errors, no explanation for this scatter can be found.

The effect of the liquid head on the average amplitude is shown in Fig. 16. This plot indicates that the amplitude is independent of the head but increases with increasing gas flow.

Figure 17 shows the data obtained when different liquids were used. Comparison of these data with the frequency data obtained at the same time indicates that the amplitude increases as the frequency decreases. This suggests that the ratio of the average amplitude to the maximum possible pressure change in the chamber, $\bar{\rho}_g c^2 Q_g^o/g_c V_c F$, is one possible correlating parameter. Here, $\bar{\rho}_g$ is the average gas density, c is the sonic velocity in the gas, and g_c is the gravity constant. Figure 17 also indicates that the average amplitude increases as the gas flow increases.

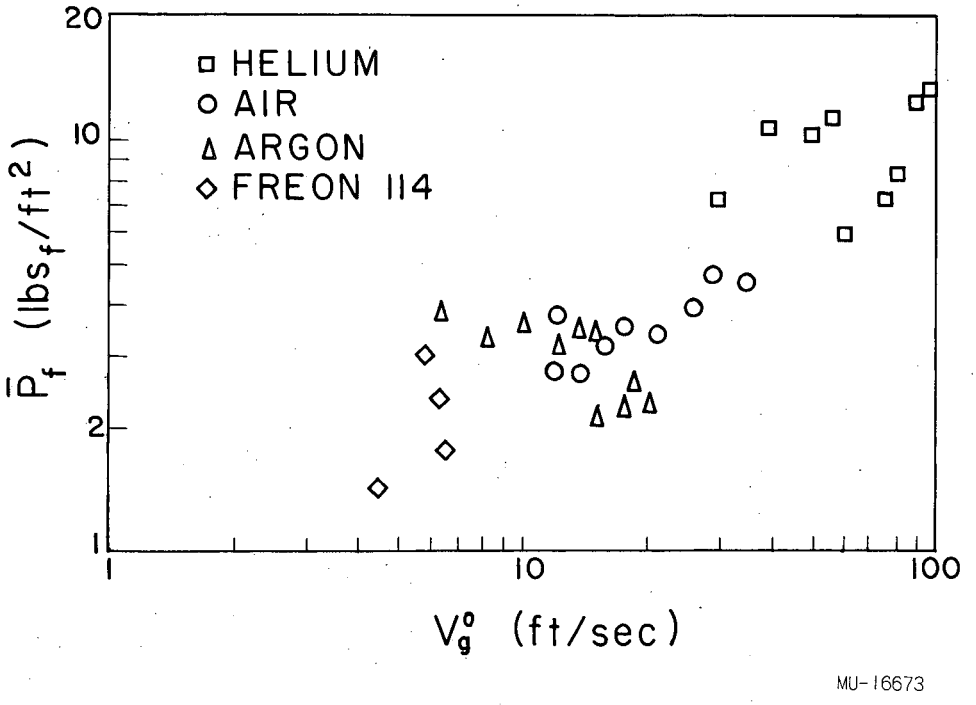

Fig. 15. Effect of gas properties on average amplitude of pressure fluctuations. (Water as liquid, V_c = 262 in^3., D_o = 0.25 in., D = 1.0 in., n = 3, h_L = 2.0 in.)

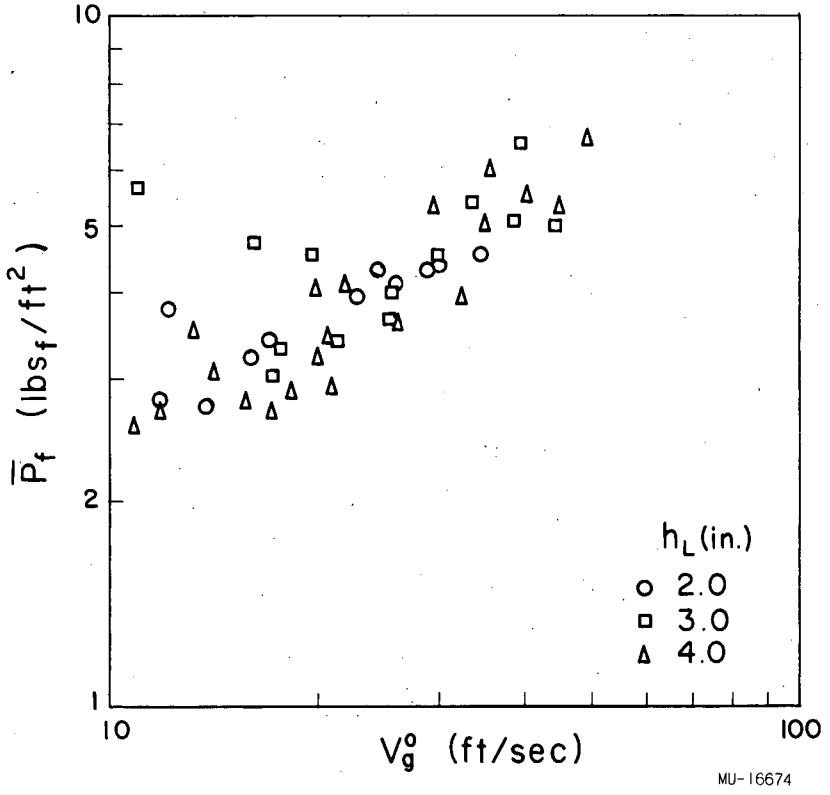

Fig. 16. Effect of liquid head on average amplitude of pressure fluctuations. (Air-water system, V_c = 262 in^3., n = 3, D_o = 0.25 in., D = 1.0 in., h_L = 2.0 in.)

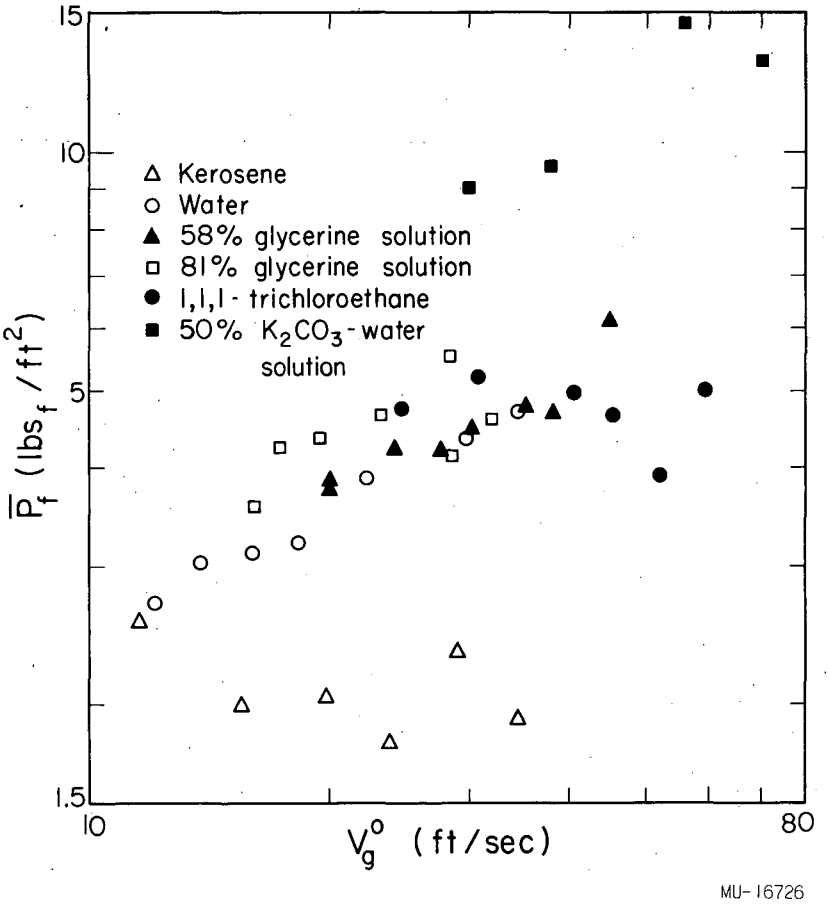

Fig. 17. Effect of liquid properties on average amplitude of pressure fluctuations. (Air as gas, V_c = 262 in^3., n = 3, D_o = 0.25 in., D = 1.0 in., h_L = 2.0 in.)

The data obtained when different chamber volumes were used are shown in Fig. 18. This plot shows that the average amplitude is related to the chamber volume, although it is not a simple functional relationship. This suggests an interaction between the frequency, chamber volume, and the number of holes to give the resultant effect shown in Fig. 18.

The single-hole amplitudes are shown in Fig. 19. This plot shows the amplitude to be a function of volume at the higher flows but independent of volume at the lower flows. Thus, the effect of volume on the amplitude is a function of the gas flow. This effect does not appear in the multihole data shown in Fig. 18.

Fig. 20 shows the data obtained when a large number of holes were used and for comparison the three- and seven-hole plate data are shown. There is no consistent effect of the number of holes. Rather, there is apparently a change in mechanism or controlling parameter. This causes the 29-, 41-, and 49-hole data to be grouped together and the three- and seven-hole data to be in a different group.

The results that were obtained when different hole diameters and hole spacings were used are shown in Fig. 21. These variables also seem to have an effect on the amplitude which is apparently a diameter-spacing interaction. Certainly no simple functional relationships are apparent from this plot.

Variations in amplitude. Figure 22 shows a typical pressure trace that was obtained under a single-hole plate. It can be seen from this figure that the pressure fluctuations do not have a constant amplitude. There is considerable variation in its value. This is caused by the lack of uniformity in the bubbling process. Actually, except at low rates of feeding gas into the chamber ($Q_g^o/A_o < 10$ ft/sec), single bubbles are not formed. The situation is more one of a gas column which oscillates in the horizontal direction in the liquid. Upon occasion, these oscillations are so large that the gas column collapses and dumping occurs. These ocsillations have a random nature and thus cause the random pressure fluctuations. For contrast, Fig. 23 shows a typical pressure trace in the region where single bubbles are formed.

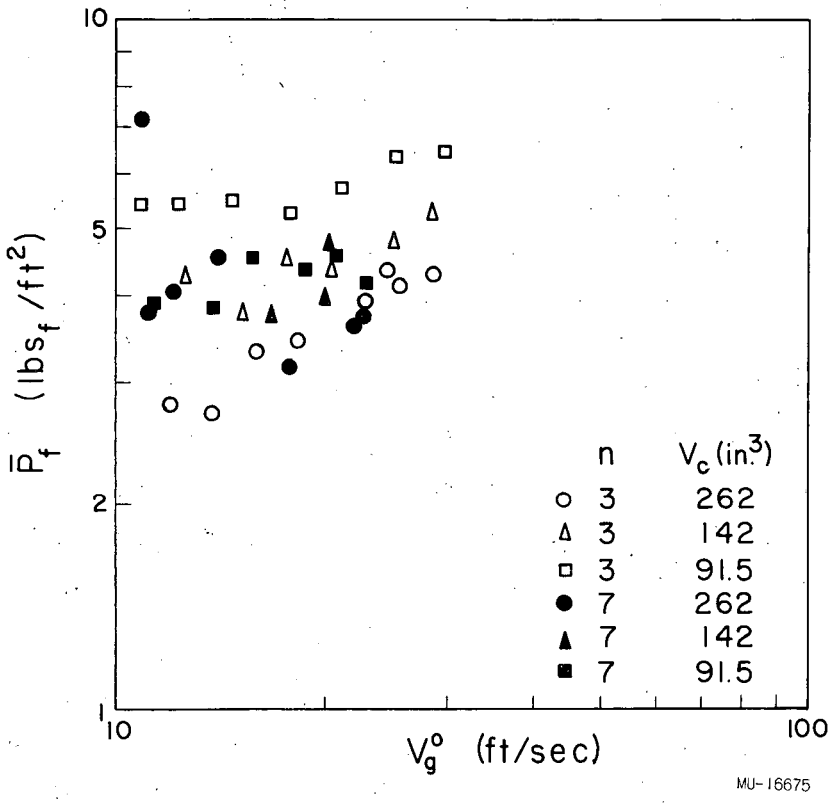

Fig. 18. Effect of chamber volume and number of holes on average amplitude of pressure fluctuations. (Air-water system, D_o = 0.25 in., D = 1.0 in., h_L = 2.0 in.)

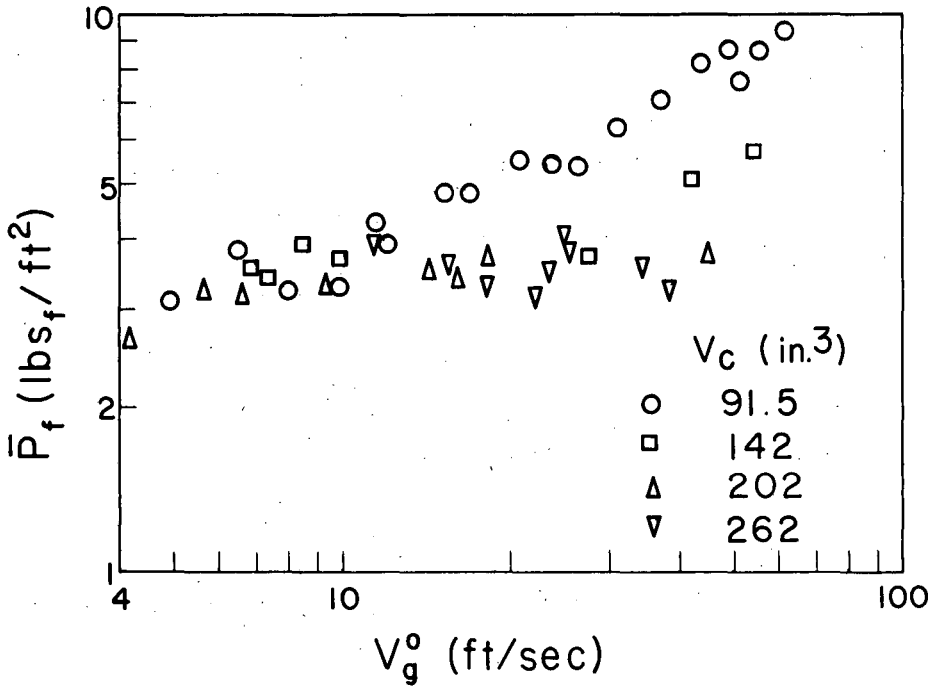

Fig. 19. Single hole data – Effect of chamber volume on average amplitude of pressure fluctuations. (Air-water system, D_o = 0.25 in., h_L = 2.0 in.)

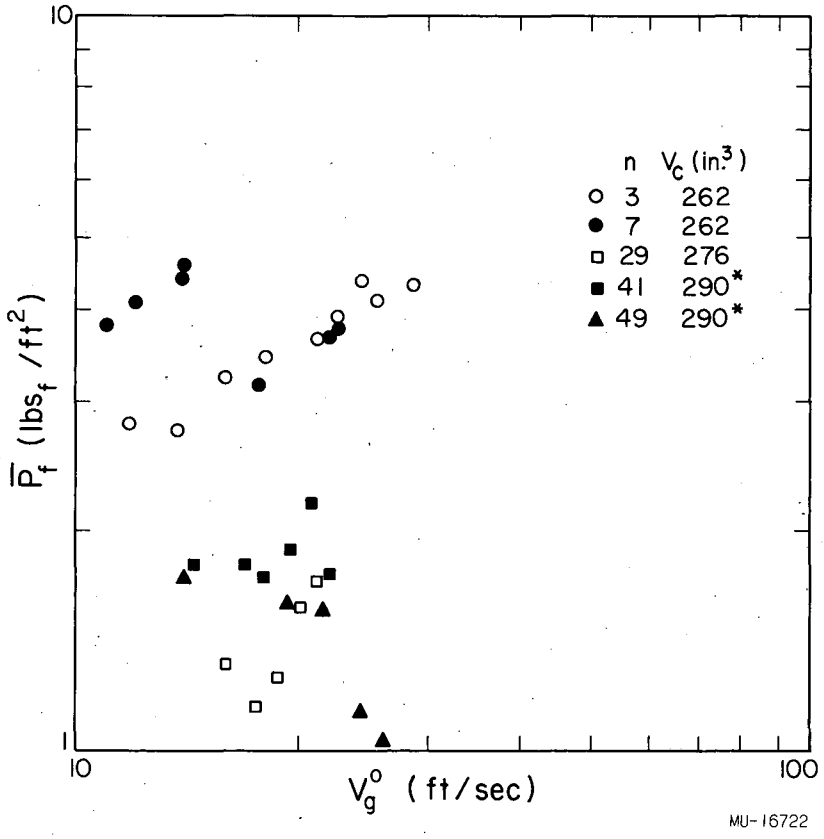

Fig. 20. Multihole data – Effect of number of holes on average amplitude of pressure fluctuations. (Air-water system, D_o = 0.25 in., D = 1.0 in., h_L = 2.0 in., *D = 0.75 in.)

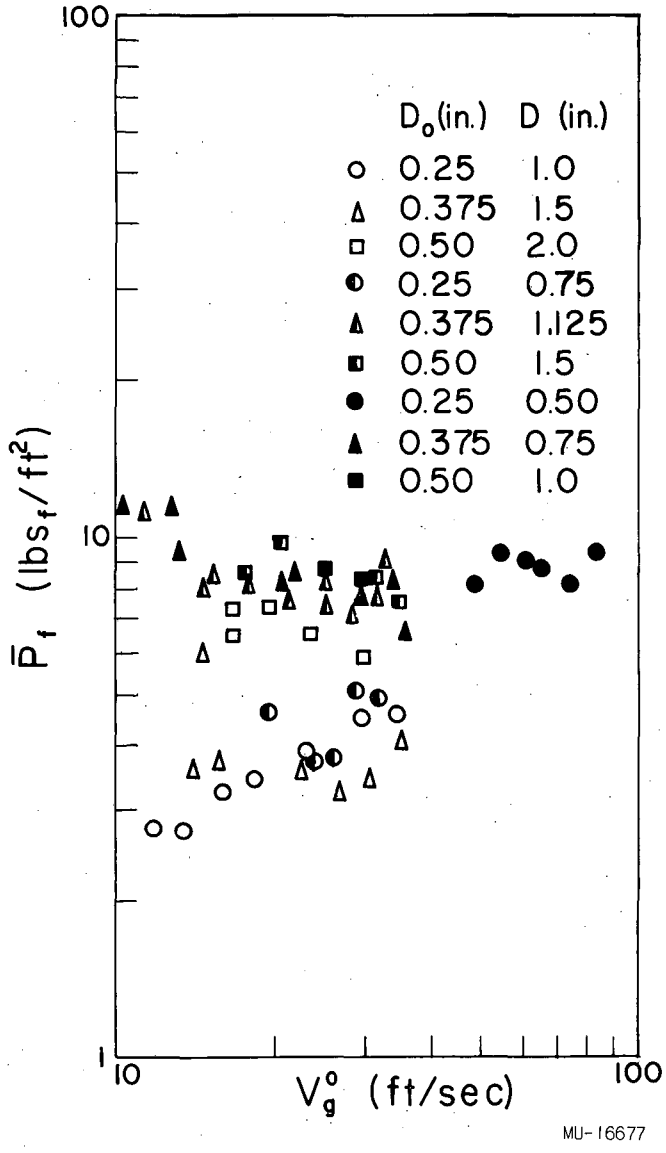

Fig. 21. Effect of hole diameter and spacing on average amplitude of pressure fluctuations. (Air-water system, V_c = 262 in^3., n = 3, h_L = 2.0 in.)

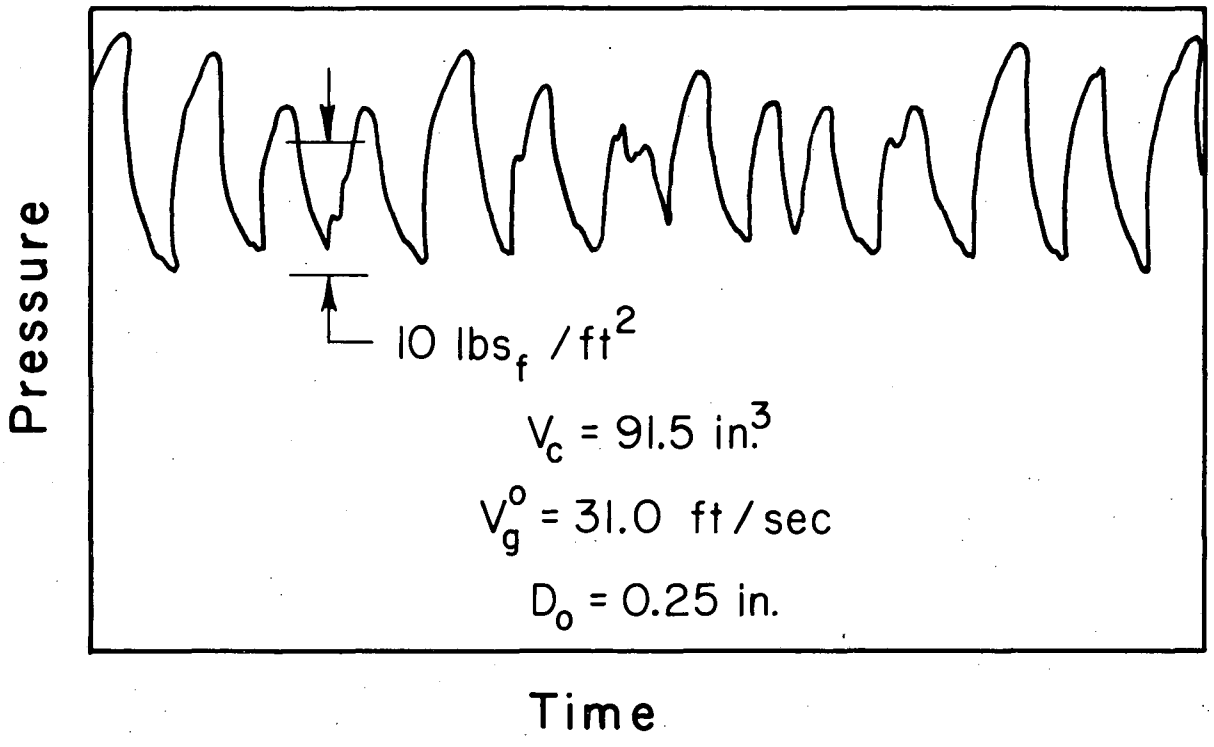

Fig. 22. Single-hole chamber pressure trace for varying amplitude. (V_c = 91.5 in^3., V_g^o = 31.0 ft/sec, D_o = 0.25 in.)

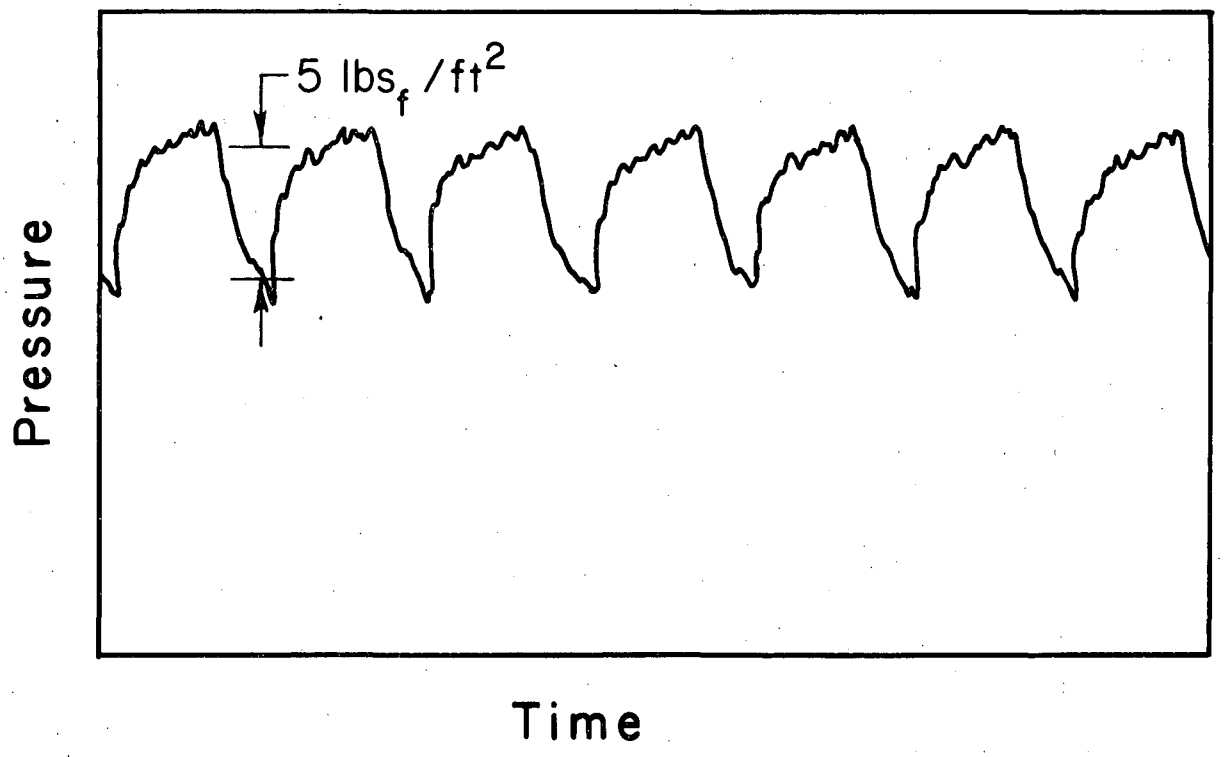

Fig. 23. Single-hole chamber pressure trace for constant amplitude. (V_c = 142 in^3., V_g^o = 6.45 ft/sec, D_o = 0.25 in.)

From the data shown in Fig. 22, the cumulative frequency distribution was determined. The results of this calculation show a linear relationship on probability coordinates (Fig. 24). Thus, it appears that these variations are normally distributed about the average. Therefore, the standard deviation of the amplitude can be used to characterize these variations.

Figure 25 shows a typical pressure trace that was obtained when a multihole plate was used. As in the single-hole case, these amplitudes are not constant but fluctuate during the run. Since the variations in the single-hole amplitudes follow the normal probability distribution, the cumulative frequency distribution was calculated for these multihole data. The results give a straight line on probability coordinates as Fig. 26 shows. Several other checks were made and all showed good linearity on probability paper. Therefore, the assumption of normality is valid for the multihole data, also.

Hence, the standard deviation of each amplitude was calculated. The results of some of these calculations are shown in Figs. 27 through 30. Comparisons of these plots with the similar plots for the amplitudes show the standard deviation to be 20% to 50% of the amplitude. This can be explained in terms of the normality assumption. It seems reasonable to say that most of the minimum points in the pressure wave must be below the time-average pressure. Expressing this mathematically gives the relation:

$$\overline{P}_f - \eta\,\sigma = 0, \tag{9}$$

where σ is the standard deviation and $\overline{P}_f$ is the average amplitude. Then, if the percentage of points below the time average is known, η can be calculated from the normal probability distribution. Table IV shows η as a function of the percentage of points below the time average.

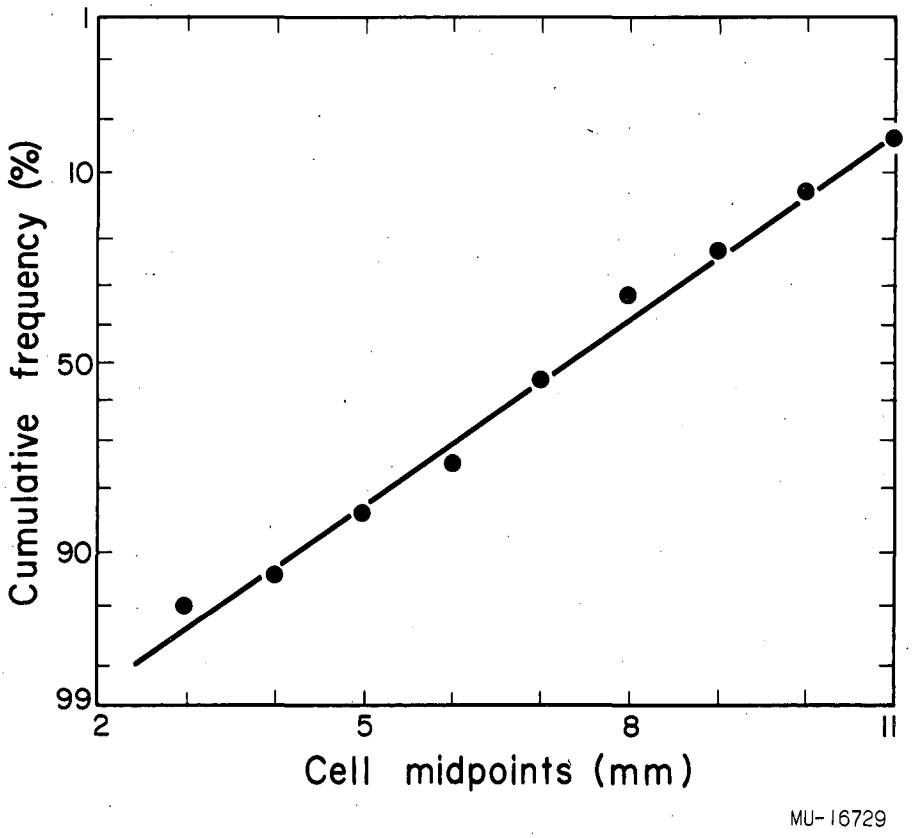

Fig. 24. Test of normality – single-hole plate. (Air-water system, V_c = 91.5 in^3., D_o = 0.25 in., h_L = 2.0 in., V_g^o = 31 ft/sec).

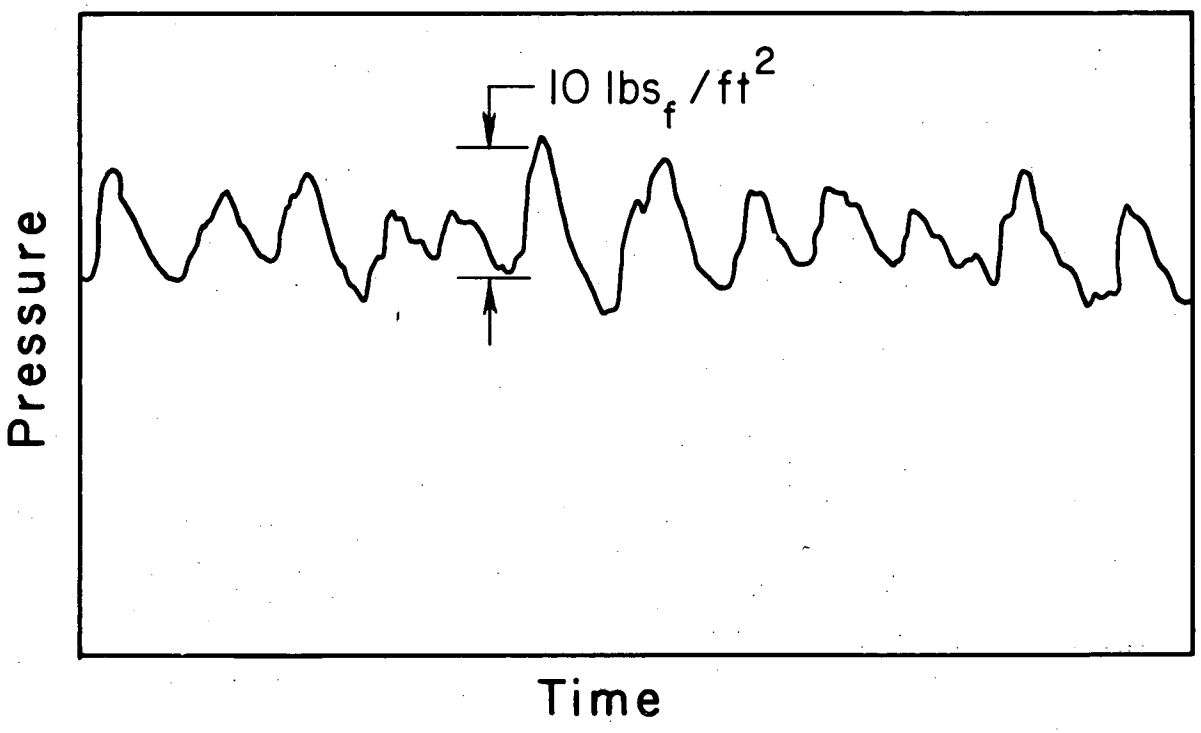

Fig. 25. Multihole chamber pressure trace. (V_c = 262 in^3., h_L = 2.0 in., n = 3, V_g^o = 29.8 ft/sec, D_o = 0.25 in., D = 1.0 in.)

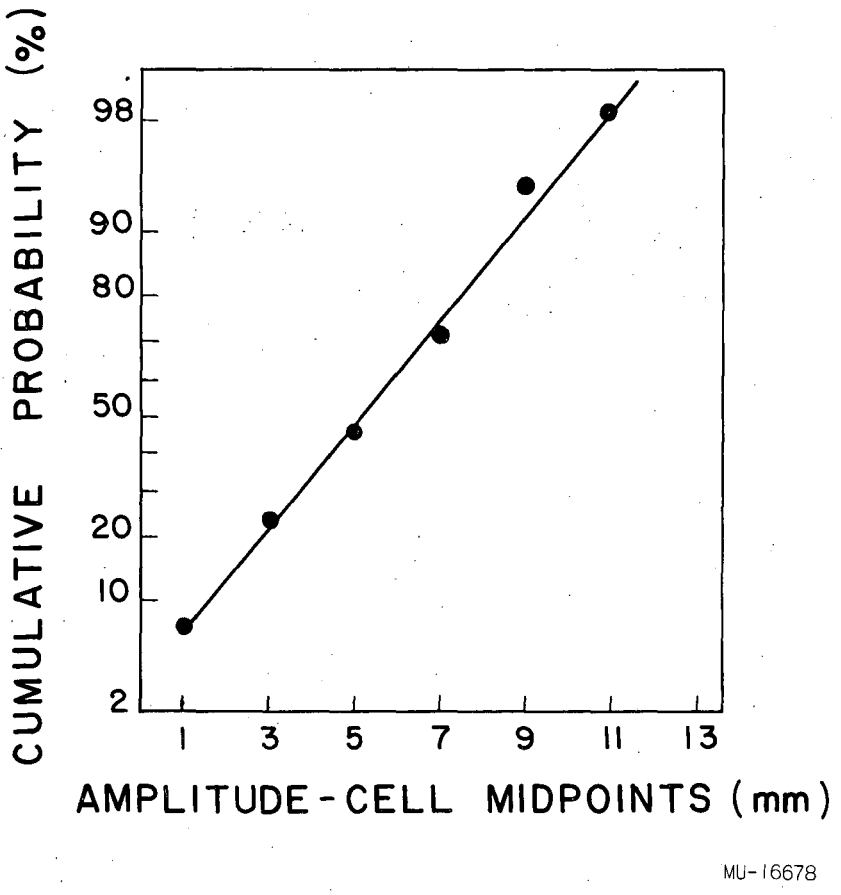

Fig. 26. Test of normality – multihole plate. (Air-water system, V_g^o = 29.8 ft/sec., V_c = 262 in^3., D_o = 0.25 in., D = 1.0 in., n = 3, h_L = 2.0 in.)

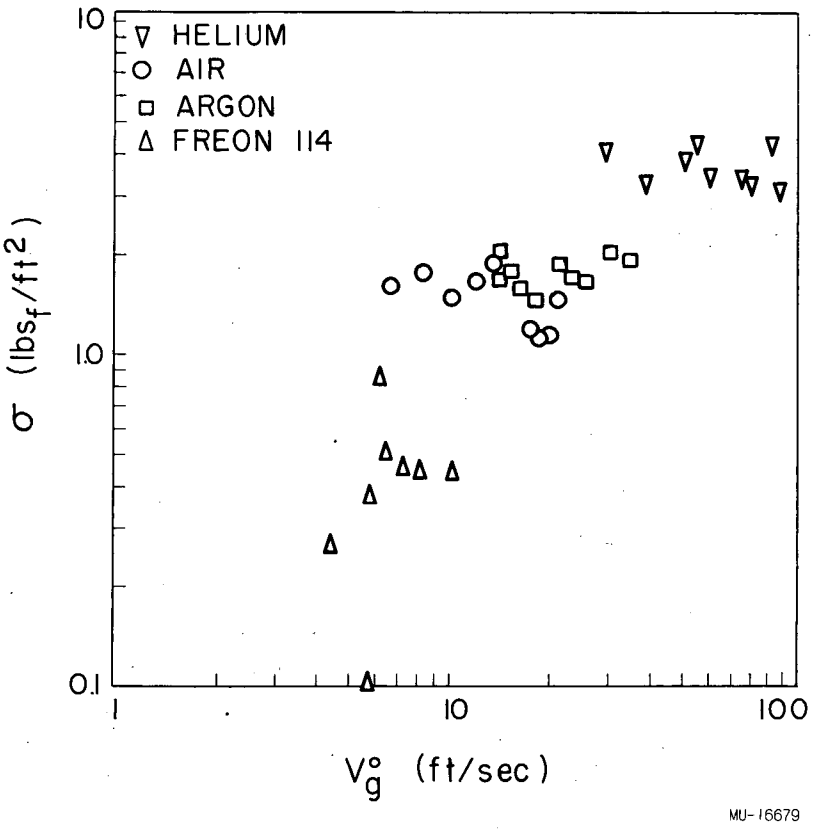

Fig. 27. Effect of gas properties on standard deviation of pressure fluctuations. (Water as liquid, D_o = 0.25 in., D = 1.0 in., V_c = 262 in^3., n = 3, h_L = 2.0 in.)

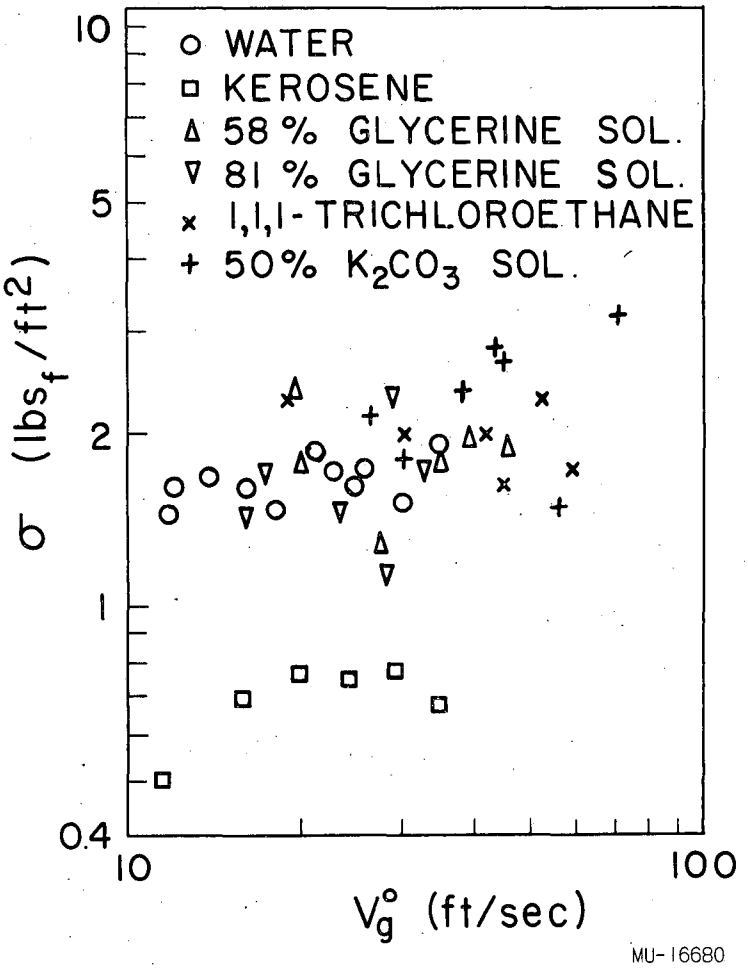

Fig. 28. Effect of liquid properties on standard deviation of pressure fluctuations. (V_c = 262 in^3., D_o = 0.25 in., D = 1.0 in., n = 3, h_L = 2.0 in., air as gas)

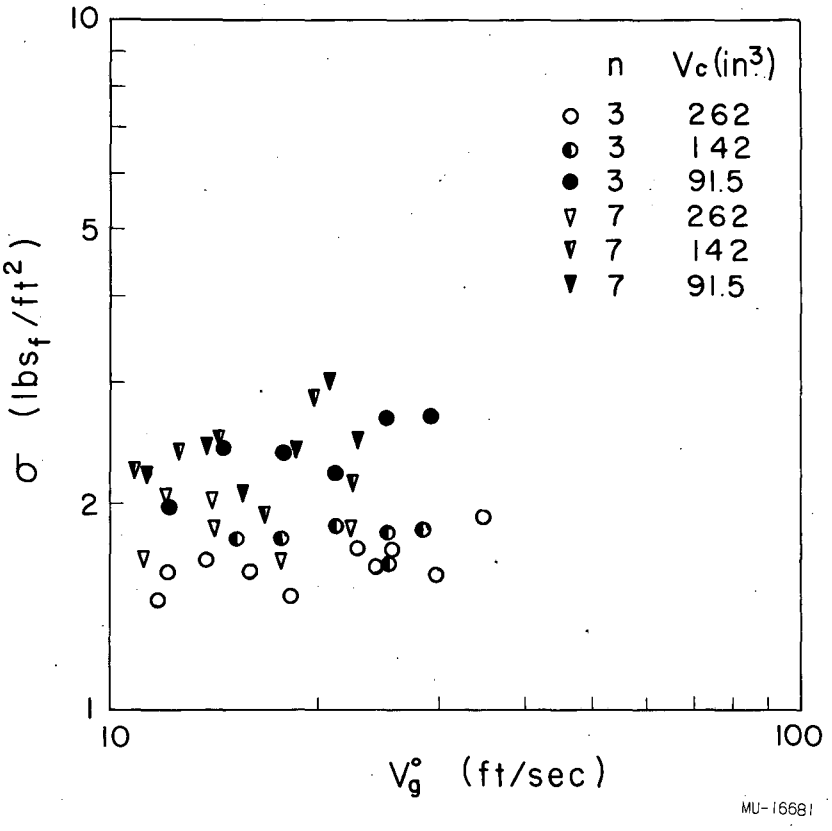

Fig. 29. Effect of chamber volume and number of holes on standard deviation of pressure fluctuations. (Air-water system, D_o = 0.25 in., D = 1.0 in., h_L = 2.0 in.)

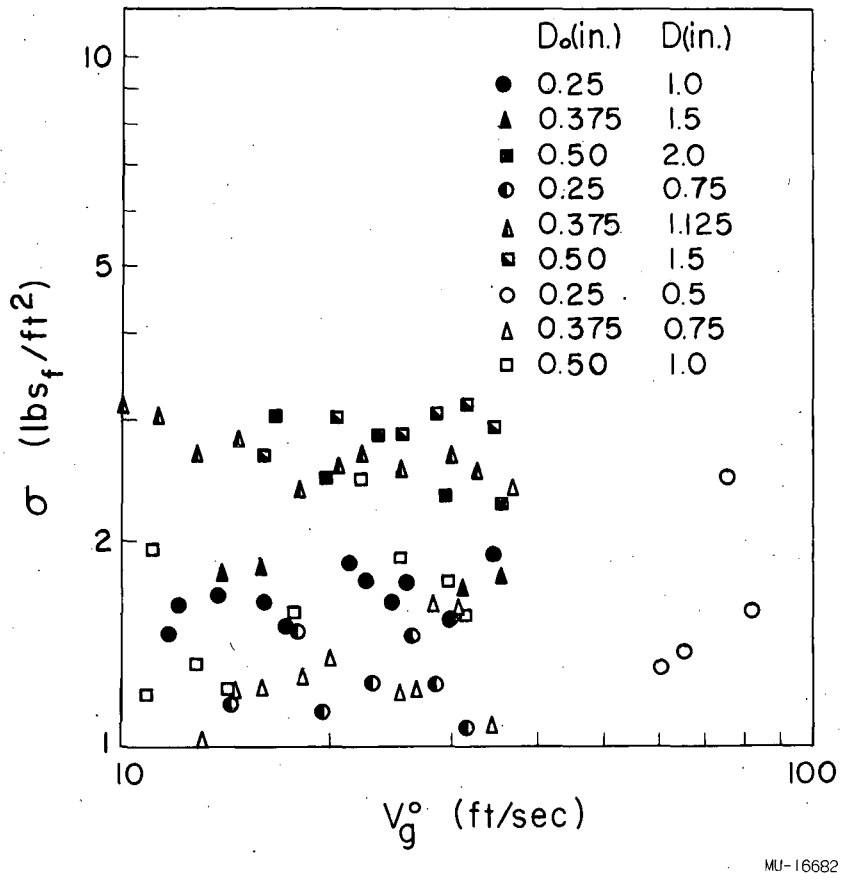

Fig. 30. Effect of hole diameter and spacing of standard deviation of pressure fluctuations. (Air-water system, V_c = 262 in^3., n = 3, h_L = 2.0 in.)

Table IV[19]

Percentage of points below zero vs. η	
Percentage	η
68.3	1
95.4	2
99.7	3
99.99	4

On the basis of this table, it seems reasonable to assume that $2 \leq \eta < 4$. Substituting this range into Eq. (9) and rearranging gives:

$$0.25 < \frac{\sigma}{\overline{P}_f} < 0.50. \qquad (10)$$

The quantity $(\sigma/\overline{P}_f)$ was calculated from the data and, within the accuracy of the data, was found to give fair agreement with Eq. (2). It should be pointed out that this approach breaks down as the tendency for individual, uniform, bubble formation increases. In this region, the standard deviation goes to zero, but the amplitude remains finite. Thus, the quantity $\sigma/\overline{P}_f$ must approach zero as the gas flow is decreased. Hence, if this estimation procedure for the standard deviation is to be used at low gas flows, values of 0.1 or less for $\sigma/\overline{P}_f$ should be used.

One possible approach to the problem of predicting the average amplitude is to write the differential equations and then derive the model laws from these equations. Next, the functional relationships of these dimensionless groups would be determined from the data. At this point, it is apparent from the data that this procedure breaks down. The data indicate that the functions required to properly fit the experimental results are very complicated. With no theoretical framework from which to start and so many variables and interactions between them, this approach becomes too unwieldy and must be discarded.

Another possible attack is a purely empirical approach. Again, because of these complicated functional forms and interactions, a purely empirical attack on the problem is very difficult. Also, one can never be sure just how general a correlation results from this approach. Therefore, this attack was discarded.

Summary of amplitude results. Because of the difficulties that have been pointed out, no correlation for the average amplitude is presented. However, this failure points up the need for more theoretical and experimental investigations on the form of the pressure waves under the plate. Only after more understanding of these waves has been obtained can the problem of predicting the average amplitude of the pressure fluctuations be solved.

PRESSURE DROP THROUGH PERFORATED PLATES

A. Literature Review

No data on the pressure drop across single-hole plates have been reported. However, the pressure drop across plates of industrial size has been one of the chief subjects for study in several recent articles.[1,2,4,5,20] The general approach to this problem has been to first correlate the pressure drop across the plate with no liquid present. Then, pressure drop data for plates with liquid present were obtained.

If we assume that the dry-plate pressure drop is not affected by the presence of liquid on the plate, the expression for the total pressure drop is

$$\Delta P_T = \Delta P_{DP} + \rho_L h_L + \Delta P_R , \qquad (11)$$

where ΔP_{DP} is the dry-plate pressure drop based on the time-average gas velocity through the holes. The ΔP_R term is then calculated from the wet-plate data by the use of Eq. (1). This residual or extra pressure drop is a result of energy losses required to form bubbles and produce additional turbulence in the liquid. However, no successful correlation for ΔP_R has been reported.

Arnold, using only the air-water system, found the residual pressure drop to vary from 1.0 to 3.0 lbs_f/ft^2.[1] His data indicate that ΔP_R is independent of the liquid head and depends only on the average kinetic energy of the gas.

Mayfield took some wet-plate pressure-drop data using water, 50% propylene glycol-water mixture, and absorption oil as liquids and air as the gas.[2] Residual pressure drops from 0.25 to 1.0 lbs_f/ft^2 were found, and some effect of liquid properties noted. However, Mayfield concluded that these differences do not exceed the accuracy of the data and therefore, are negligible.

Hunt et al. made an extensive investigation of the residual pressure drop using water, glycerine-water solutions, kerosene, carbon

tetrachloride, n-hexane and butyl alcohol as liquids.[4] Air, argon, Freon-12, methane, and carbon dioxide were used for the gas phase. Hunt found the residual pressure drop increased with an increase in the kinetic energy of the gas. The surface tension of the liquid, gas molecular weight, and plate geometry were also found to be important variables. No effect of the liquid head was found. Attempts to rationalize this residual pressure drop in terms of bubble-formation theory were unsuccessful. Therefore, no general correlation was presented. However, Hunt recommended using $\Delta P_R = 2.5$ lbs_f/ft^2 for design purposes.

Lee[20] obtained residual pressure drops for eight gas-liquid systems and found an average value of 4.2 lbs_f/ft^2. He also found the residual-pressure drop to be independent of the physical properties of the gas-liquid system and of the geometry of the plate. The head of liquid also had no effect on the residual-pressure drop. No explanation for this drop was presented.

Jones and Pyle reported finding a significant residual pressure drop.[5] However, an extensive investigation of pressure drop was not performed in their study, and no further development of this subject was presented.

Hughmark and O'Connell have proposed a correlation for the wet-plate pressure drop.[15] They have combined the actual clear-liquid height plus the residual pressure drop into one term called the effective head. This effective head is then empirically correlated against the total submergence.

B. Experimental Studies

Theoretical Interpretation

Consideration of Eq. (11) reveals that it is exact only if the gas flow through the plate is constant and not a function of time. If this were true, then the residual pressure drop would have some meaning in terms of bubble-formation energy losses. However, as Hughes has pointed out,[13] the gas flow is definitely not constant over the bubbling cycle.

Therefore, the dry-plate pressure drop based on the time-average gas flow has no real meaning when the wet-plate pressure drop is considered. Hence, the residual pressure-drop data in the literature are meaningless in terms of the actual operation of the bubbling system. It is no wonder that no correlation of this parameter could be obtained.

Hughes and co-workers[13] have considered this problem from a more realistic point of view, and the following analysis is based primarily on their work.

Consider the force balance on the bubble at any arbitrary point in the bubble growth cycle. The force balance becomes

$$\underset{\text{buoyancy}}{\text{net}} + \underset{\text{pressure}}{\text{excess}} - \underset{\text{tension}}{\text{surface}} - \text{drag} = \frac{d(\text{momentum})}{g_c\, dt} . \qquad (12)$$

The excess pressure term accounts for the fact that the gas pressure inside the bubble exceeds the equilibrium pressure difference across the interface. The drag force considers the effect of liquid being dragged along with the growing bubble. The drag force also considers the fact that some liquid is moved away as the bubble grows and therefore, there is an additional acceleration effect.

Expressing this mathematically, we have

$$\frac{P_g V_B}{A_f g_c}\frac{d^2 D_b}{dt^2} = \frac{\Delta\rho g V_B}{g_c A_f} + (P_t - P_p) - \frac{4\gamma}{D_b} - \frac{C_D \rho_L}{2 g_c}\left(\frac{d D_b}{dt}\right)^2 - \frac{b}{A_f g_c}\frac{d^2 D_b}{dt^2} , \qquad (13)$$

where A_f is the frictional surface, P_t is the pressure inside gas bubble, P_p is the pressure in the liquid outside the bubble, D_b is the bubble diameter, b is the mass of liquid being dragged with the bubble, C_D is the drag coefficient, g is the acceleration of gravity, $\Delta\rho$ is $\rho_L - \rho_g$, and t is the time. The terms in Eq. (13) are listed in the same order as they appear in Eq. (12.)

From Fig. 31 we obtain

$$P_p = P_o + \rho_L h_L \quad , \tag{14}$$

$$P_T = P_c - \frac{C \rho_g (V_g^o)^2}{2 g_c} \quad , \tag{15}$$

$$P_c - P_o = \Delta P_T' \quad , \tag{16}$$

where C is an orifice coefficient and h_L is the liquid head on the plate.

Combining Eq. (13), (14), (15), and (16) results in the expression

$$\frac{\rho_g V_B}{g_c A_f} \frac{d^2 D_b}{dt^2} = \frac{\Delta\rho g V_B}{g_c A_f} + (\Delta P_T - \rho_L h_L)^1 - \frac{C \rho_g (V_g)^2}{2 g_c}$$

$$- \frac{4\gamma}{D_b} - \frac{C_D \rho_L}{2 g_c} \left(\frac{d D_b}{dt}\right)^2 - \frac{\rho_L V_B}{A_f g_c} \frac{d^2 D_b}{dt^2} \quad . \tag{17}$$

Hughes combined Eq. (17) with the electrical analogue equations and an integral equation for the bubble volume as a function of time.[13] By introducing certain linearizing assumptions, he was then able to solve these equations in closed form. However at higher flows, the concepts of separate bubbles and laminar flow through the plate is not valid. Also Hughes' solution[13] is extremely complicated to evaluate, and therefore the more empirical approach of using model laws for the process will be developed.

Before deriving the model laws from Eq. (17), it is necessary to decide upon the characteristic velocity, dimension, and time for this system. It seems reasonable to assume that the characteristic time is the reciprocal of the frequency, since this is the period for one complete cycle. The characteristic velocity is the time average gas velocity through the holes, because this quantity governs the over-all speed of the process. Since Fig. 29 shows very little effect of hole-spacing, the only reasonable characteristic dimension is the hole diameter.

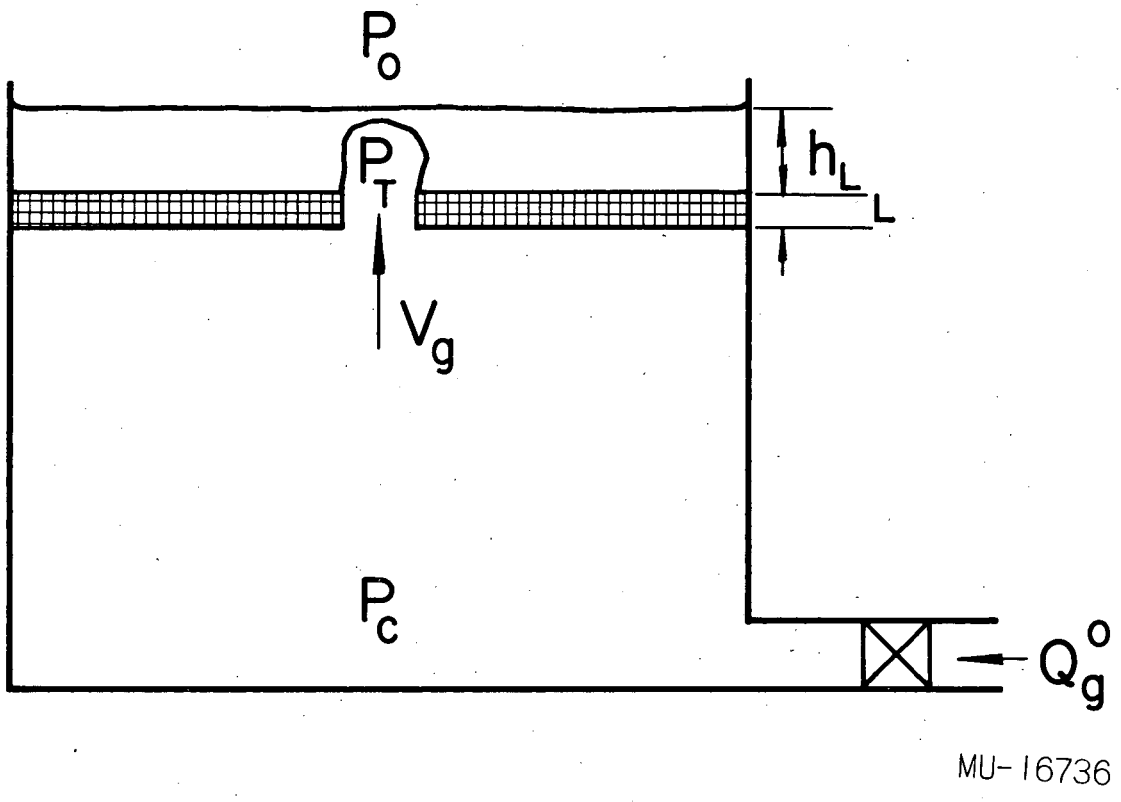

Fig. 31. Schematic diagram of single-hole bubbling.

Now, to form the model laws from Eq. (17), divide each of the terms by the inertia term $\rho_g V_g^2 / 2g_c$. This results in the expression

$$\frac{(\Delta P_T - \rho_L h_L)}{\rho_g (V_g)^2/2g_c} = f \left\{ \left[\frac{\Delta\rho \, V_B \, g}{\rho_g \, V_g^2 \, A_f} \right], \left[\frac{4\gamma}{D_b \, \rho_g \, V_g^2/2g_c} \right], [c], \right.$$

$$\left. \left[\frac{C_D \, \rho_L \left(\frac{d \, D_b}{dt} \right)^2}{\rho_g \, V_g^2} \right], \left[\frac{\rho_L \, V_B}{\rho_g \, V_g^2 \, A_f} \left(\frac{d^2 \, D_b}{dt^2} \right) \right], \left[\frac{V_B \, \frac{d^2 D_b}{dt^2}}{A_f \, V_g^2} \right] \right\} . \qquad (18)$$

Consideration of the term $(dh/dt)^2$ reveals that the substitution

$$\left(\frac{d \, D_b}{dt} \right)^2 \propto V_g^2 \qquad (19)$$

can be made. Also, the substitution

$$\frac{d^2 \, D_b}{dt^2} = \frac{d}{dt} \left(\frac{d \, D_b}{dt} \right) \propto V_g \, F \qquad (20)$$

helps to simplify Eq. (18). Next, the substitution

$$\frac{V_B}{A_f} \propto D_o \qquad (21)$$

can be made in Eq. (18). Thus, combining Eqs. (18) through (21) gives

$$\frac{\Delta P_T - \rho_L h_L}{\rho_g (V_g^o)^2/2g_c} = f \left\{ \left[\frac{\Delta\rho \, D_o \, g}{\rho_g (V_g^o)^2} \right], \left[\frac{4\gamma}{D_o \rho_g (V_g^o)^2/2g_c} \right], [c], \right.$$

$$\left. \left[\frac{C_D \, \rho_L \, (V_g^o)^2}{\rho_g \, (V_g^o)^2} \right], \left[\frac{\rho_L \, D_o F \, V_g^o}{\rho_g \, (V_g^o)^2} \right], \left[\frac{D_o F \, V_g^o}{(V_g^o)^2} \right] \right\} . \qquad (22)$$

Note that the time-average values for the pressure drop and gas velocity have been substituted in Eq. (22) for the instantaneous values in Eq. (18).

The gas velocity through the hole fluctuates between zero and some maximum which is in the turbulent flow region and thus, it seems logical to let the orifice coefficient be a function of Reynold's number based on the gas properties. By the same reasoning, the drag coefficient is a function of the Reynold's number based on the liquid properties, $\rho_L V_g^o D_o/\mu_L$, where μ_L is the viscosity of the liquid.

Also, let
$$Eu = (\Delta P_T - \rho_L h_L) / \frac{\rho_g (V_g^o)^2}{2g_c} \tag{23}$$

$$We = \gamma / \frac{D_o \rho_g (V_g^o)^2}{2g_c} \tag{24}$$

$$FR = D_o g/(V_g^o)^2 \tag{25}$$

$$\Delta\rho = \rho_L - \rho_g \approx \rho_L \tag{26}$$

Combining Eqs. (22) through (26) and in view of the above considerations on the Reynold's numbers results in the equation

$$Eu = f\left[\left(\frac{\rho_L}{\rho_g}\right), \left(\frac{\mu_L}{\mu_L}\right), We, FR, Re_g, \left(\frac{D_o F}{V_g^o}\right)\right] \tag{27}$$

This equation shows the functional groups required to correlate the Euler number. However, the proper functional relationship must be determined from the data.

Correlation of Pressure-Drop Data

In addition to pressure-fluctuation data on the 6-in.-square column, pressure-drop data were also taken. The results, are shown in Figs. 32 through 35.

Figure 32 shows the results obtained for different hole diameters and hole spacings. The data for plates with 0.25-in.- diam. holes are definitely higher than for 0.375-in. and 0.50-in.-diam. holes. It is also of interest to note the changing exponent on the gas velocity. At the higher velocities (greater than 60 ft/sec), the slope on log-log coordinates is two, but as the velocity decreases, the slope decreases to one. It is also interesting to notice the effect of the hole diameter on the slope. This suggests that the Reynold's number based on the gas properties is a significant parameter.

The results of changing the number of holes and chamber volume are shown in Fig. 33. It can be concluded from this plot that these are significant parameters. This suggests that the term $\Delta P_T - \rho_L h_L$ is related to the frequency of the pressure fluctutations. This is perfectly reasonable when one considers the transient nature of the gas flow through the holes.

The use of different liquids resulted in the data shown in Fig. 34. From this plot, it is clear that no one particular physical property stands out as the controlling factor. Rather, the data indicate that the density, surface tension, and perhaps the viscosity are all significant parameters.

Figure 35 shows the data that were obtained using different gases with water. It is interesting to note that the data for argon fall directly in line with the air data. Since argon has a higher viscosity and a higher molecular weight, this suggests a gas Reynolds number effect.

In order to develop a correlation for the pressure-drop term, $\Delta P_T - \rho_L h_L$, thought must be given to the functional relationship of the dimensionless groups in Eq. (27). In particular, the Reynolds number term needs consideration. The Reynolds number is a measure of the ratio of the inertia forces to the viscous forces. At higher Reynolds numbers

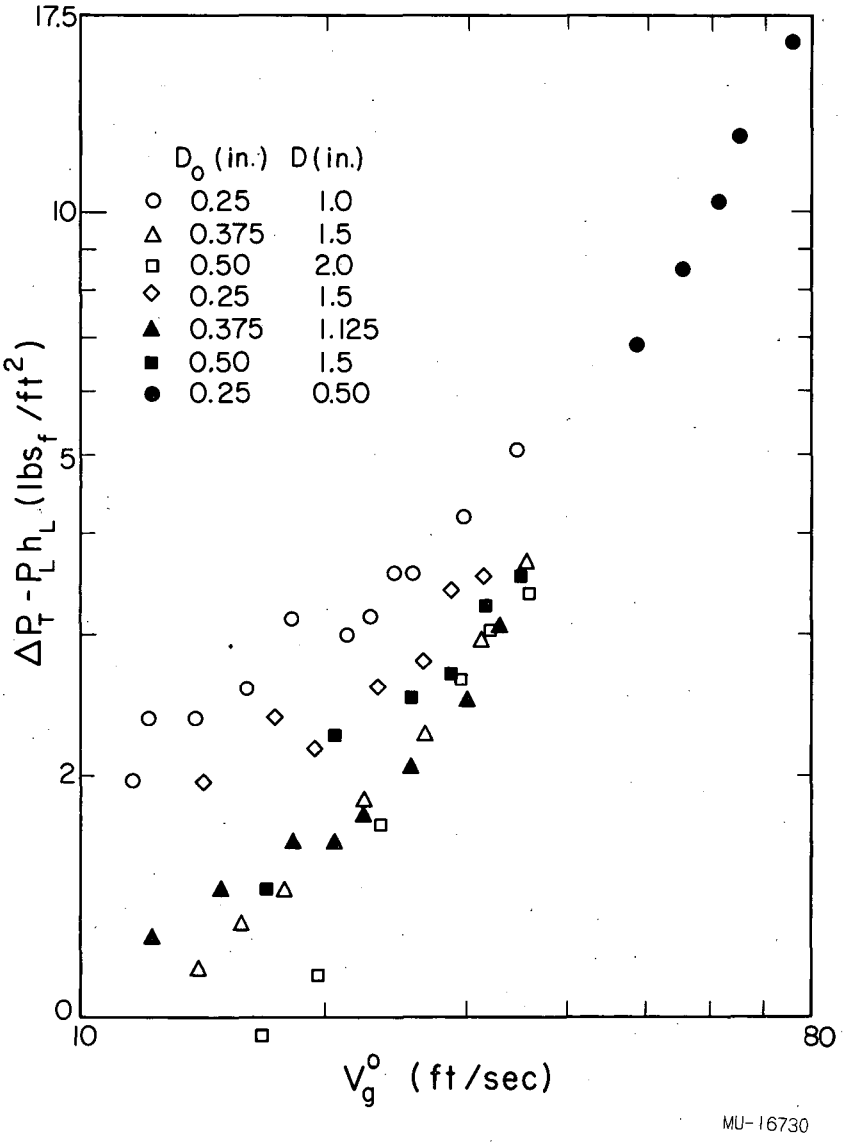

Fig. 32. Effect of hole diameter and spacing on pressure drop. (Air-water system, V_c = 262 in^3., n = 3, h_L = 2.0 in.)

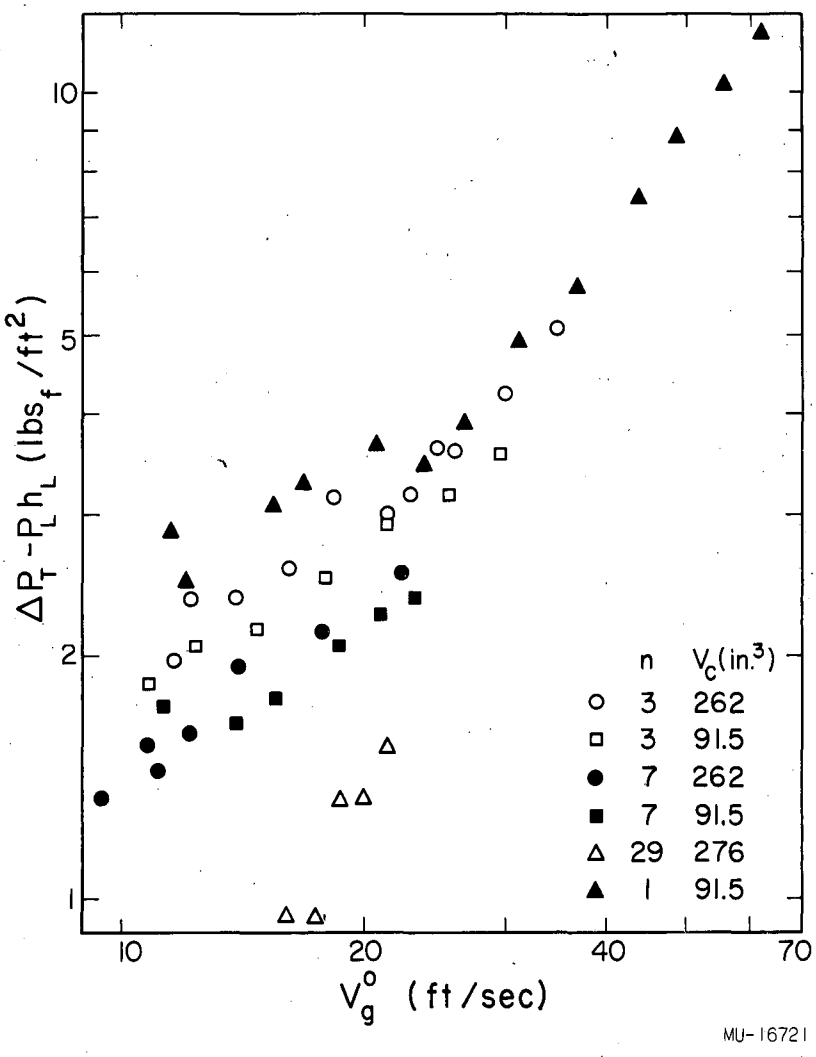

Fig. 33. Effect of chamber volume on pressure drop. (Air-water system, D_o = 0.25 in., D = 1.0 in., h_L = 2.0 in.)

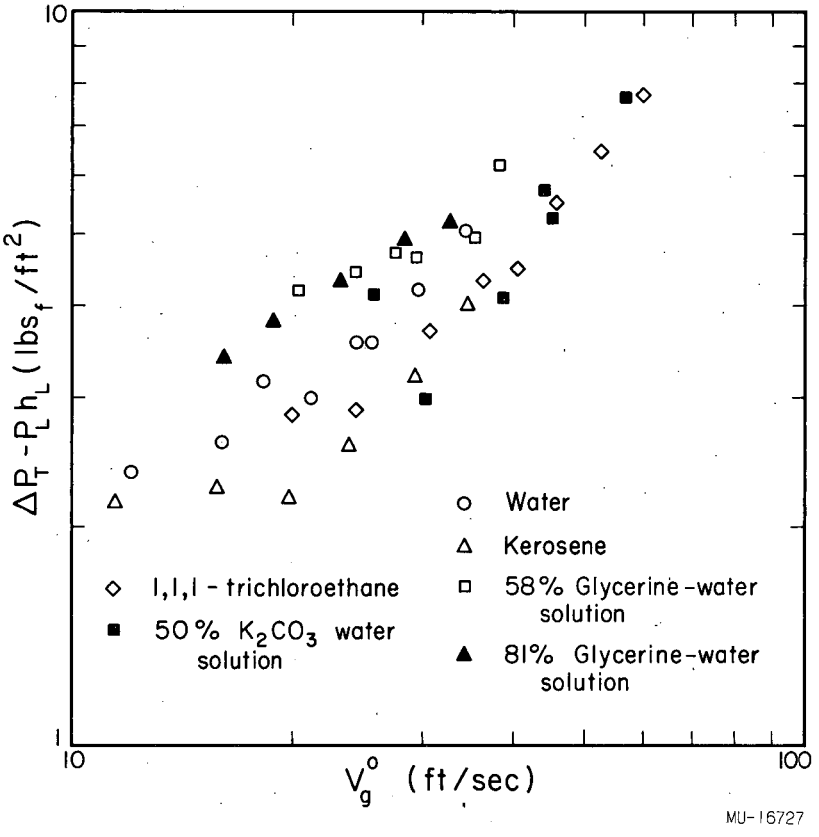

Fig. 34. Effect of liquid properties on pressure drop. (Air as gas, V_c = 262 in^3., D_o = 0.25 in., D = 1.0 in., n = 3, h_L = 2.0 in.)

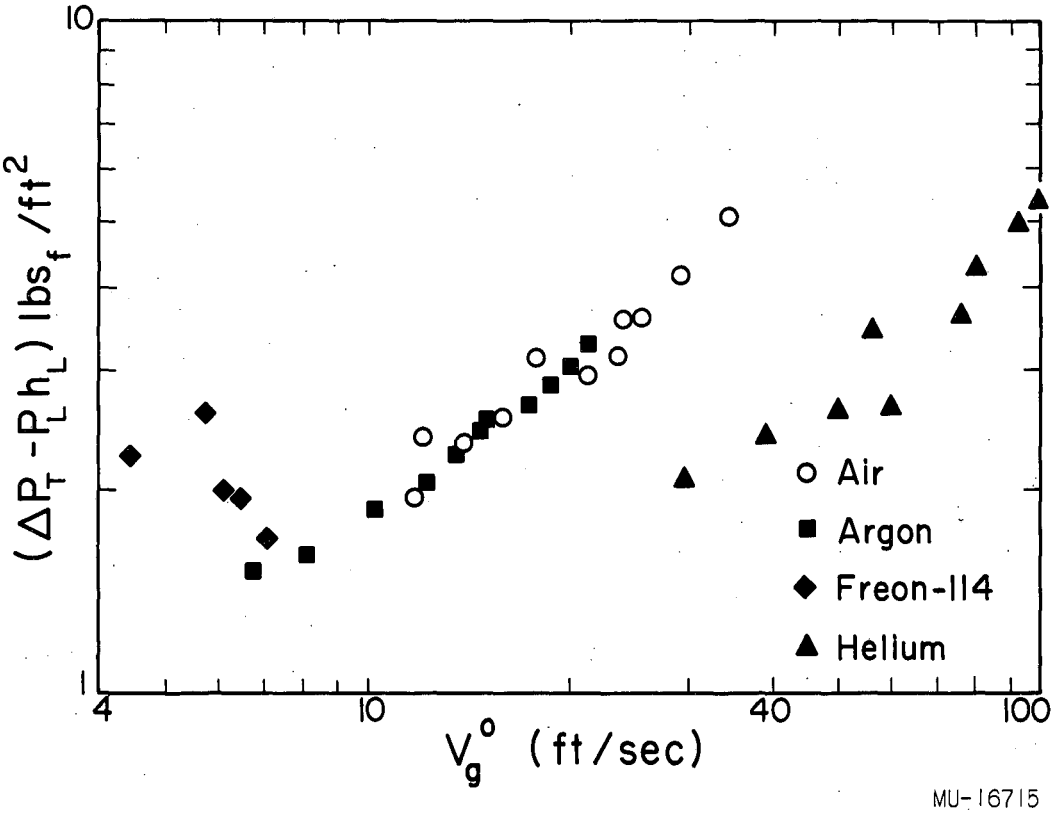

Fig. 35. Effect of gas properties on pressure drop. (Water as liquid, V_c = 262 in^3., D_o = 0.25 in., D = 1.0 in., n = 3, h_L = 2.0 in.)

(higher velocities), the viscous forces become negligible and thus the Reynolds number effect can be ignored. This decreasing importance of the Reynolds number can be expressed as

$$Eu \propto \left(1 + \frac{a}{Re_g}\right)^b \quad . \tag{28}$$

The other parameters are assumed to be exponentially related to the Euler number. This results in the equation

$$Eu = A\left(1 + \frac{a}{Re_g}\right)^b \left(\frac{\rho_L}{\rho_g}\right)^c \left(\frac{\mu_L}{\mu_g}\right)^d (FR)^e (We)^f \left(\frac{D_o F}{V_g^o}\right)^g \quad . \tag{29}$$

The method of least squares was then used to evaluate the constants in Eq. (29). Actually, the procedure was to apply the linear regression theory to the logarithmic form of Eq. (29) using various values of the constant "a".

Substituting the set of constants which gave the best correlation coefficient gives the equation

$$Eu = 9.29\left(1 + \frac{10{,}000}{Re_g}\right)^{0.87} (We)^{0.11} \left(\frac{\mu_L}{\mu_g}\right)^{0.08} \left(\frac{\rho_L}{\rho_g}\right)^{-0.32} \left(\frac{D_o F}{V_g^o}\right)^{-0.36} FR^{0.24} . \tag{30}$$

Discussion of the Correlation

By the use of Eq. (30), a comparison of the calculated vs. the experimental Euler number is obtained, as shown in Figs. 36 through 39. Further analysis of this comparative calculation shows that Eq. (30) accounts for 81% of the total variation of the Euler number. The other 19% is due to experimental error, unconsidered variables, or both. This calculation also shows that the average deviation is ±19%.

At first glance, the figures mentioned above sound high. However, the expected accuracy of the pressure drop is ±0.5 lbs_f/ft^2. Since the average velocity head is on the order of 0.5 lbs_f/ft^2, the expected accuracy of the Euler number is ±1. With the average Euler number

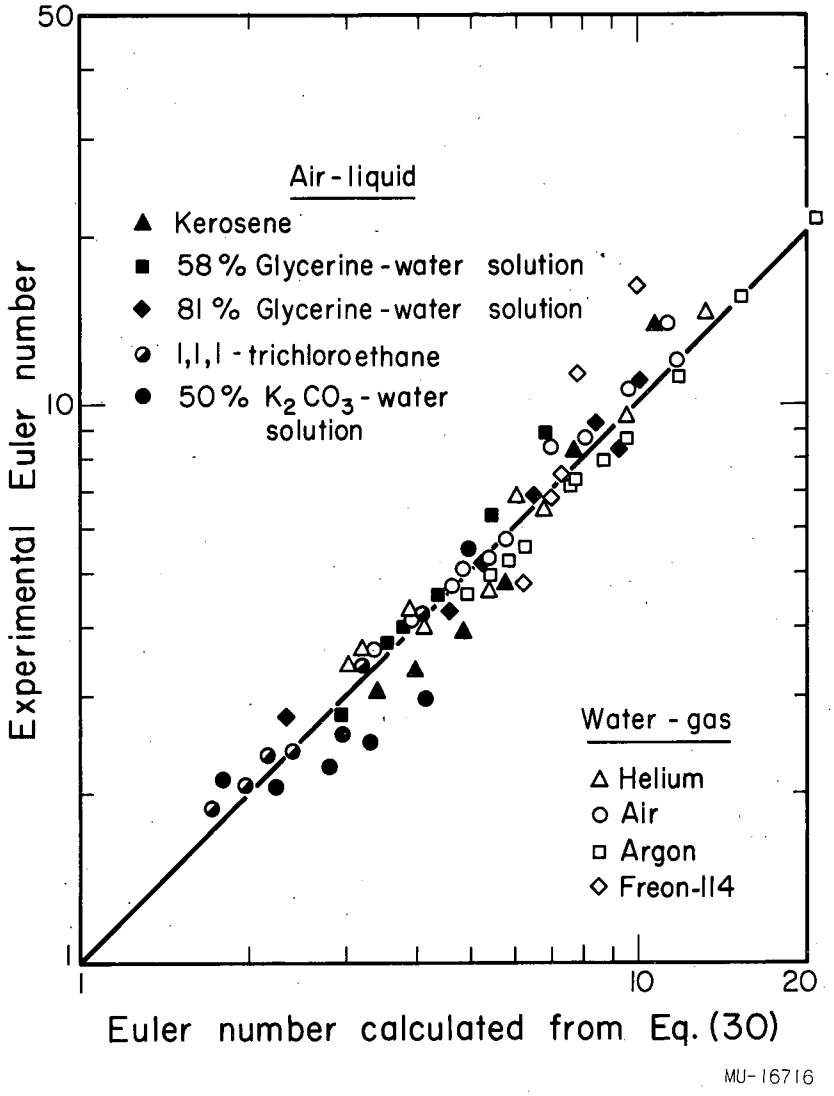

Fig. 36. Correlation of effects of gas and liquid properties on pressure drop. (V_c = 262 in^3., D_o = 0.25 in., D = 1.0 in., n = 3, h_L = 2.0 in.)

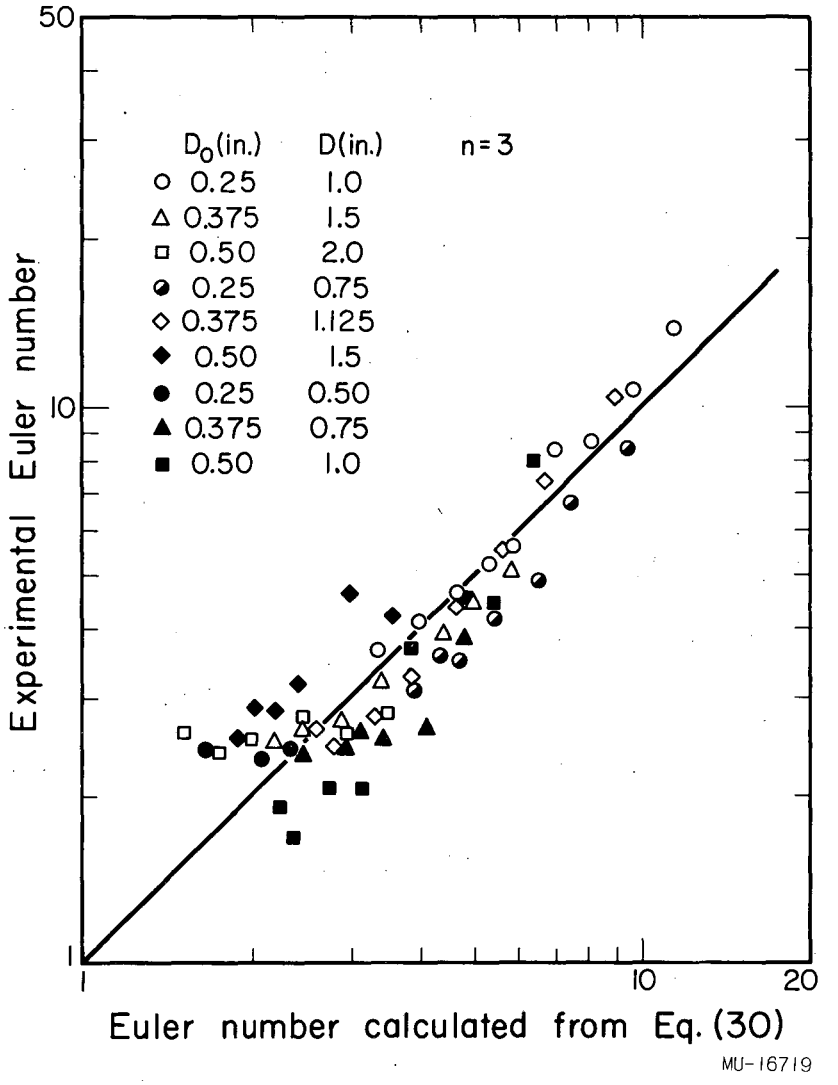

Fig. 37. Correlation of effect of hole diameter and spacing on pressure drop. (Air-water system, V_c = 262 in^3., n = 3, h_L = 2.0 in.)

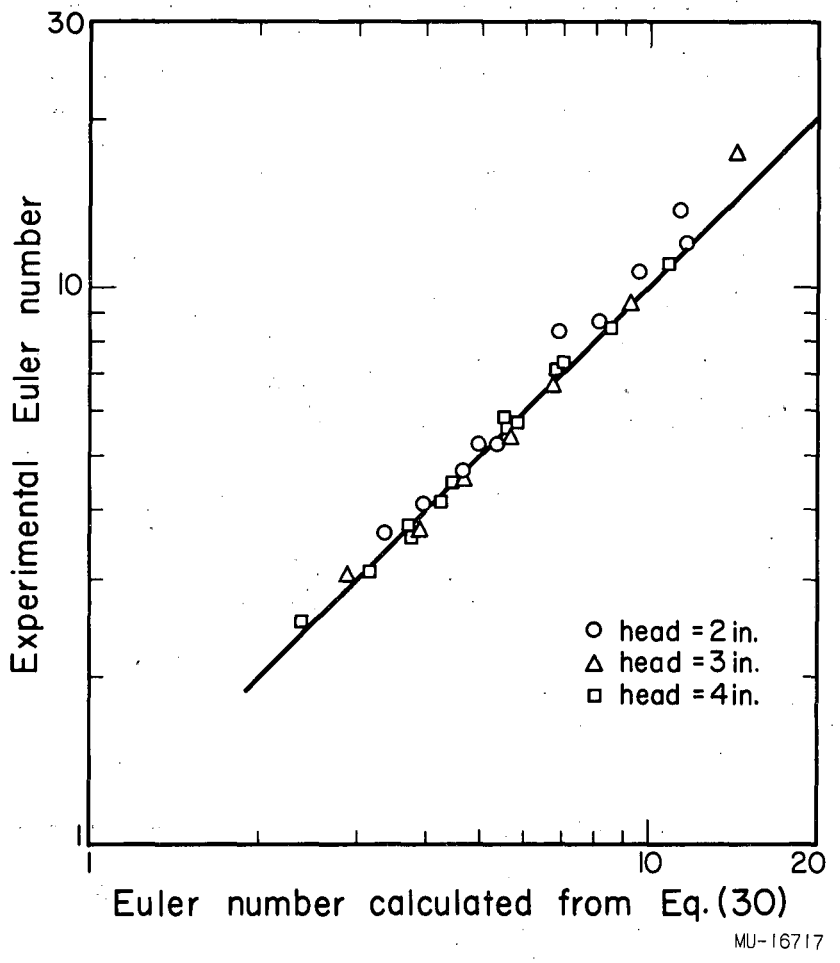

Fig. 38. Effect of liquid head on Euler Number. (Air-water system, V_c = 262 in^3., D_o = 0.25 in., D = 1.0 in., n = 3.)

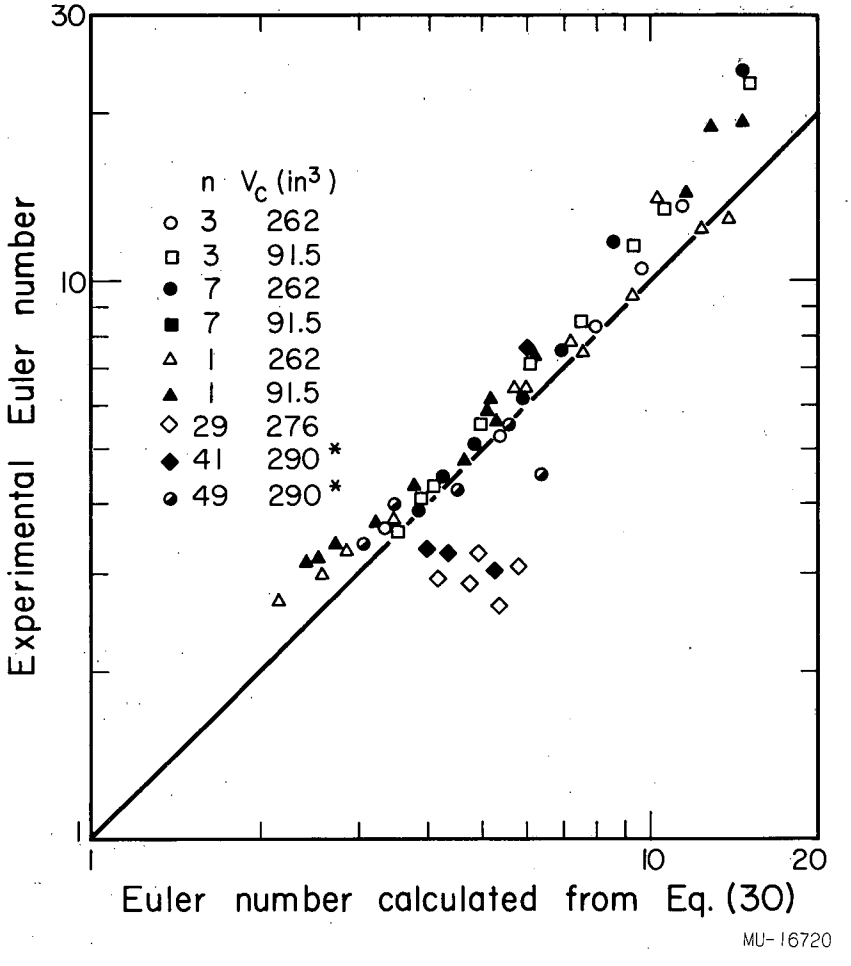

Fig. 39. Correlation of effect of chamber volume on pressure drop. (Air-water system, D_o = 0.25 in., D = 1.0 in., h_L = 2.0 in., *D = 0.75 in.

approximately equal to 5, this means that an average deviation of ±20% is not unreasonable.

There is no theoretical justification for using the exponential form for the dimensionless groups. The possibility of obtaining a better correlation with other forms was considered. However, improvements in Eq. (30) would be marginal, if they could be obtained at all, because of limitations in experimental accuracy. Therefore, Eq. (30) is the final form of the correlation.

Figure 36 shows the calculated vs. experimental Euler number for the various gas-liquid systems used. The agreement is good over the entire range of variables covered with the possible exception of the Freon 114-water data at high Euler numbers. However, this is the region of low-pressure drops, and therefore the accuracy of the data is lower in this region. Thus, the scatter is attributed to experimental error.

By the use of the data obtained on plates with different hole diameters and hole spacings, a comparison of Euler number was made; this is shown in Fig. 37. The scatter is high in the low Euler number region. No explanation for the scatter can be found.

Figure 38 shows that there is no effect of liquid head on the pressure drop $\Delta P_T - \rho_L h_L$. This is in complete agreement with the findings of Hunt[4] and Lee.[20]

Figure 39 shows the calculated vs. experimental Euler numbers using the data for different chamber volumes, different number of holes, and different free-area ratios. The data for the 29-hole and 41-hole plates show considerable deviation from the correlation. However, the 49-hole data are in good agreement with the correlation. Thus, there is no apparent trend in this deviation.

However, this does bring up the subject of the effect of free-area ratio on the orifice coefficient. Hunt[4] and Lee[20] used free-area ratios from 0.04 to 0.20 and found that the orifice coefficient (as used in Eq. (15)) decreased by 40%. In this study, however, free-area ratios from approximately 0.001 to 0.07 were used. Under these conditions, Hunt[4] and Lee[20] predict only a 10% change. Thus, sufficient data are not available to justify including the free-area ratio in the correlation.

One factor which has been ignored in this analysis is the fraction of the holes which are not passing gas during the dumping portion of the cycle. During the other portion of the cycle, all the holes pass gas, and therefore this effect must be considered only during part of the cycle. Because this factor was not measured experimentally, there is no way to include this effect in the correlation. However, it seems reasonable that this fraction is a function of the average gas flow and therefore has already been included in the correlation. It is also possible that this factor causes part of the deviations between the calculated and experimental Euler numbers.

Conclusions about Pressure Drop

Equation (30) predicts the pressure drop term $\Delta P_T - \rho_L h_L$ in the dumping region to within ±20%. More data should be obtained to investigate the effect of free-area ratio. Also, data at higher gas flows should be obtained to check the validity of Eq. (30) in the more useful operating ranges.

LIQUID DUMPING THROUGH PERFORATED PLATES

A. Literature Review

The publication of the papers by Arnold[1] and Mayfield[2] in 1952 were the first recent studies aimed at defining in a reasonably accurate manner the operating characteristics of perforated plate trays. Both studies considered, among other things, the problem of dumping and the minimum gas velocity for stable operation.

Arnold and co-workers,[1] using the air-water system, studied the effect of hole diameter, ratio of total hole area to column cross-sectional area (free-area ratio), weir height, and liquid flow rates on the minimum vapor velocity. This minimum velocity was determined in two ways. The first method was to visually observe the point where dumping first begins. The second method was to note breaks in the curve of pressure drop versus gas velocity. Arnold found that increased liquid heads require increased vapor flows. The free area ratio also affects the minimum velocity but the effect of hole diameter cannot be determined from the data. No attempt was made to present a generalized correlation.

Mayfield et al.[2] used essentially the same approach as Arnold.[1] The effects of free-area ratio, liquid flow rate across the tray, and outlet weir-height on the minimum gas velocity were determined for the air-water system. Plates with 3/16-in.-diam. holes were used. The minimum gas velocity was defined as the minimum flow required to prevent any liquid back-flow through the holes and was determined visually. The results show that the minimum velocity is a function of the free area, liquid flow, and weir height. The data indicate that the dry-plate pressure drop at the minimum vapor flow is a function of the calculated clear liquid head on the plate. Therefore, a plot of this type is presented. Although the data scatter, there is a definite correlation between the two parameters.

Kamei and co-workers in Japan have attacked the problem from a different angle.[21] The approach taken was to determine the relationship between the vapor velocity and the total pressure drop across the plate

when all the holes are passing gas. Then, for a plate with only a fraction of the holes passing gas, a second relation between the pressure drop and gas velocity was determined. This second relation was then extrapolated to the point where all the holes are passing gas. At this point, the pressure drop given by the two expressions can be equated. This results in an equation for the gas velocity at this equivalence point. This velocity is defined as the minimum vapor velocity for stable operation. Experimental work was done using the air-water system and hole diameters of 1, 2, and 3 mm. The liquid head, liquid flow, weir height, and plate geometry were varied. The results of five tests are presented and the proposed correlation predicts the minimum vapor velocity to within ±10%.

Zenz[3] proposed the development of a series of design charts. Each chart would show the operating characteristics of a given tray and liquid on the tray. He suggests plotting the quantity $F_g = V_g^o \sqrt{\rho_g}$ versus the liquid head, where V_g^o is the gas velocity and ρ_g the gas density. Lines of constant froth height and lines of constant weeping rates would be plotted. Several of these charts are presented in the paper. Data on the air-water and the air-methanol systems are presented. However, no information on the actual dumping rates is reported. Zenz gives some general thoughts on the effects of various parameters, but no generalized correlation using these parameters is presented.[3]

Hunt et al. have taken a different approach to the minimum vapor velocity problem.[4] They measured the dumping rate as a function of gas velocity, liquid head, liquid and gas properties, and plate geometry. As the gas rate was decreased, the dumping rate increased slowly at first, then more and more rapidly, giving curves with more or less sharp breaks. The vapor velocity at the break point was defined as the minimum vapor velocity. A table of these minimum velocities for the various gas-liquid systems and plate geometries used is presented. However, no generalized correlation of the results is shown.

Hughmark and O'Connell have also considered the minimum vapor-velocity problem.[20] Their correlation for the minimum velocity is a plot of the F_g factor versus the wet-plate pressure drop, both quantities

being measured at the minimum velocity. The minimum velocity is defined as the velocity at which the holes first begin to dump liquid. Two lines are shown. One applies to hole diameters of 0.375 in. and less when high surface tension liquids are used. The other line applies to holes of 0.25-in. diam. and larger with free-area ratio of 0.18 and larger. This second line also applies to holes with diameters less than 0.125 in. when used with liquids having low surface tension. A comparison of the available data in the literature with this correlation shows that 90% of the points are within ±30% of the proposed correlation. It should be noted that data for the air-water and air-methanol systems are the only data used.

Leibson et al. have also presented a paper on general design procedures.[22] Their correlation for the minimum vapor velocity is a modification of Mayfield's approach.[2] Leibson[22] plots the dry-plate pressure drop versus the measured clear-liquid head instead of the calculated head as Mayfield suggests. This results in a plot with less scatter. No new data are presented, however.

Foss and Gerster in their study of tray efficiency have presented some information on the effects of free-area ratio on the minimum vapor velocity.[23] However, this part of their work was of secondary interest only, and so no general correlation of the data was presented.

Lee has proposed a slightly different approach to the problem.[20] He proposes plotting the dry-plate pressure drop at the minimum velocity versus the liquid head on the plate minus the head required to overcome the surface-tension force. However, the proposal has not been checked experimentally.

Hwang and Hodson have also presented a summary of recommended design methods.[24] For the minimum velocity, they propose using Mayfield's[2] correlation. However, they point out that a better approach to this problem would be to determine an optimum dumping rate in much the same way as an optimum entrainment rate has been derived by Colburn.[25] Because sufficient data were not available, this approach was not carried further.

In view of the remarks of Hwang and Hodson,[24] a search of the literature on tray efficiency was made. Only three papers that discuss the effect of dumping on efficiency has been presented.

Umholtz and Van Winkle[26,27] have measured the over-all average tray efficiency as a function of vapor velocity and column geometry. Their results indicate that the efficiency drops markedly as the dumping rate increases.

Lee[20] has derived an expression for the actual over-all Murphree efficiency in the dumping region in terms of the fraction of the total liquid flow dumping through the holes and the efficiency to be expected if there were no dumping.[30] However, this relation has not been tested because of the lack of experimental data.

B. Experimental Studies

Single-Hole Plates

Theoretical development. On the basis of the general discussion of the bubbling process, one can say that dumping must occur in the period between the release of one bubble and the start of the formation of the next bubble. Therefore, a closer examination of this portion of the bubbling process seems necessary.

There are three possible mechanisms for liquid flow through the plate. The first considers the possibility of liquid running down the side of the hole and gas passing simultaneously up through the center of the hole. This mode of flow would be governed by the nature of the surface of the hole's side and by the surface tension and wetting properties of the liquid. However, from the visual observation of the dumping phenomenon, it can be seen that the holes are completely full of liquid while dumping, except at low dumping rates. Accordingly, this mechanism could not apply except in the region of low dumping rates and correspondingly high gas flows.

The second and third possible mechanisms for liquid flow involve a consideration of the pressures on the liquid. Consider the schematic representation shown in Fig. 40. The nomenclature is as follows:

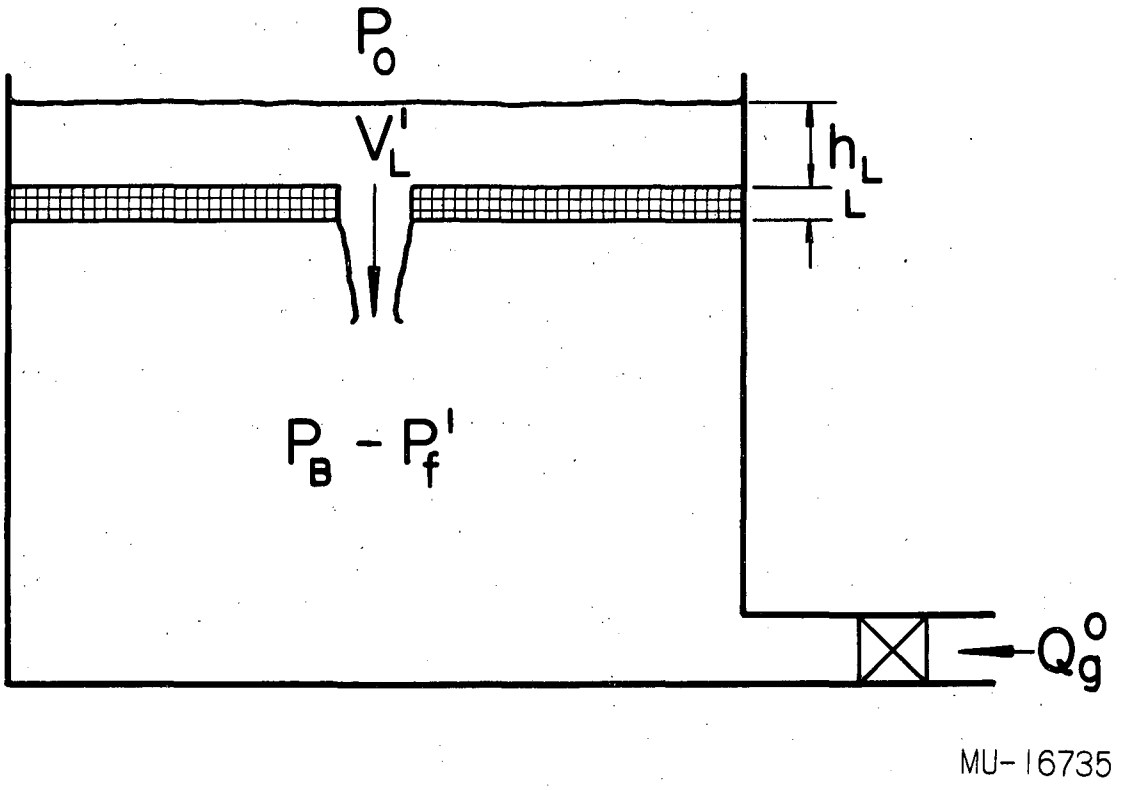

Fig. 40. Schematic diagram of single-hole dumping.

P_o -- pressure in the gas chamber above the liquid

h_L -- head of liquid on the plate

L -- plate thickness

P_B -- time average pressure in the chamber under the plate

P'_f -- instantaneous fluctuating component of pressure in the chamber. P'_f has a time average value of zero.

The downward pressures acting on the liquid in the hole are

$$P_o + \rho_L (h_L + L), \tag{31}$$

where ρ_L is the density of the liquid.

The upward pressures are given by the expression

$$P_B + P'_f . \tag{32}$$

Subtracting Eq. (32) from Eq. (31) gives the net downward pressure, h_D, that would cause liquid flow through the hole. Thus we have

$$h_D = P_o + \rho_L (h_L + L) - P_B - P'_f. \tag{33}$$

Recalling that the time-average total pressure drop across the plate, ΔP_T, is given by the expression

$$\Delta P_T = P_B - P_o, \tag{34}$$

we can simplify Eq. (33) to

$$h_D = -P'_f - [\Delta P_T - \rho_L (h_L + L)] . \tag{35}$$

Thus if we have

$$-P'_f > [\Delta P_T - \rho_L (h_L + L)], \tag{36}$$

there is a potential for liquid flow through the plate.

Now in the second model for dumping, Newton's Second Law is applied and h_D equated to a mass-times-acceleration term. However, if the mass being accelerated is approximately equal to the mass of liquid required to fill the hole, the accelerating mass is small. In other words, assume that only the liquid in the immediate vicinity of the hole experiences

the effects of the acceleration. Also, the liquid velocities are small, and so probably the acceleration-times-mass term is small, and this model is not adequate to describe the process.

The third model for dumping is to assume that the liquid flow is governed by the orifice equation. This amounts to equating

$$h_D = C_o \rho_L (V_L')^2 / 2g_c, \tag{37}$$

where

$$C_o = 1/(C')^2 \tag{38}$$

and C' is the orifice coefficient defined by the equation

$$V = C' \sqrt{2g_c \frac{\Delta P}{\rho}} . \tag{39}$$

Thus, the equation for the instantaneous dumping rate is obtained by combining Eqs. (35) and (37) to yield

$$V_L' = \left(\frac{2g_c}{C_o \rho_L} \right)^{1/2} \left[- P_f' - \Delta P_T + \rho_L (h_L + L) \right]^{1/2} . \tag{40}$$

Now during the dumping portion of the cycle, the hole is completely full of liquid, and therefore, no gas can escape from the chamber. However, the gas feed rate to the chamber remains unchanged, and so the pressure in the chamber must rise. Hughes and co-workers[13] have shown that the expression for the pressure build-up rate in the acoustical capacitance (the chamber) is

$$\frac{d P_f'}{dt} = \frac{\bar{\rho}_g c^2}{g_c V_c} Q_g^o . \tag{41}$$

where c is the sonic velocity of the gas, Q_g^o is the volumetric gas feed rate to the chamber, V_c is the volume of the chamber, and $\bar{\rho}_g$ is the density of the gas at the average chamber pressure.

Equation (41) can be integrated by the use of the boundary condition that, at t = 0,

$$P_f' = P_f, \tag{42}$$

where P_f is the amplitude of the pressure fluctuation.

Equation (41) then integrates to

$$- P'_f = - P_f + \left[\frac{\bar{\rho}_g \, c^2 \, Q^o_g}{g_c \, V_c} \right] t. \qquad (43)$$

If it is assumed that the bubble breaks off at the minimum point in the pressure wave, and that there are no acceleration effects on the liquid, Eq. (43) can be substituted into Eq. (10), resulting in the expression

$$V'_L = \left(\frac{2g_c}{C_o \rho_L} \right)^{1/2} \left[-P_f - \Delta P_T + \rho_L (h_L + L) - \left(\frac{\bar{\rho}_g \, c^2 \, Q^o_g}{g_c \, V_c} \right) t \right]^{1/2} . \qquad (44)$$

The first assumption really says that the gas flow does not decrease appreciably as the bubble breaks off. The traces of the pressure fluctuations show the minimum points in the pressure waves to be very sharply pointed and not rounded. Also, the maximum rate of pressure increase appears to occur in the first stages of the rising pressure period. In view of these facts, the first assumption is justified.

The second assumption states that the liquid reaches the maximum rate of dumping right at the start of weeping. From visual observations of the dumping, it appeared that the liquid attained the maximum rate of dumping almost instantaneously. As the cycle progressed, the rate of flow decreased slowly to zero. In view of these observations, the second assumption is justified.

The time-average dumping rate, V_L, is given by the equation

$$V_L = F \int_0^{t_o} V'_L \, dt \, , \qquad (45)$$

where F is the frequency of the pressure pulses and t_o is the time when $V'_L = 0$.

Substituting Eq. (44) into Eq. (45) and performing the integration yields the equation

$$\frac{3\,V_L}{2F} = \left(\frac{2g_c}{C_o\,\rho_L}\right)^{1/2}\left(\frac{g_c\,V_c}{\overline{\rho}_g\,c^2\,Q_g^o}\right)\left[-P_f - \Delta P_T + \rho_L(h_L + L)\right]^{3/2} \quad .(46)$$

In evaluating Eq. (46), a value for the orifice coefficient must be chosen. Examination of the flow patterns in the liquid reveals that there can be little effect of viscous forces within the liquid. Therefore, the liquid can be considered as an ideal fluid. Streeter[28] has shown theoretically that $C_o = 2.68$ for these conditions.

It should perhaps be pointed out at this point that Eq. (46) predicts the dumping rate to be independent of the liquid head on the plate. Hunt[4] has shown that

$$\Delta P_T = \Delta P_{DP} + \rho_L h_L + \Delta P_R, \qquad (47)$$

where ΔP_{DP} is the pressure drop through the plate with all holes running full of gas and no liquid on the plate, and ΔP_R is the residual pressure drop. Substituting Eq. (47) into Eq. (46) gives

$$\frac{3\,V_L}{2F} = \left(\frac{2g_c}{C_o\,\rho_L}\right)^{1/2}\left(\frac{g_c\,V_c}{\overline{\rho}_g\,c^2\,Q_g^o}\right)\left[-P_f - \Delta P_{DP} - \Delta P_R + \rho_L\,L\right]^{3/2}, \qquad (48)$$

which shows V_L to be independent of h_L if ΔP_R is independent of h_L. Hunt has shown this to be true.[4]

However, Eq. (46) is the preferred form, since it contains all easily measurable quantities.

Correlation of results. Because of the variation in the amplitude of the pressure fluctuations, Eq. (46) must be modified to account for this fact. In order to do this, the fact that these variations follow the normal probability distribution can be used. This distribution is expressed by the equation

$$P_r\left\{P_f - dP_f < P_f < P_f + dP_f\right\} = \frac{1}{\sigma\sqrt{2\pi}}\,e^{-Z^2/2}, \qquad (49)$$

where Z is the $(P_f - \overline{P}_f)/\sigma$, $\overline{P}_f$ is the average amplitude, and σ is the standard deviation.

Also, let

$$Z_o = \left[\left(\Delta P_T - \rho_L (h_L + L) - \bar{P}_f \right] \right] / \sigma \quad . \tag{50}$$

Then combining Eqs. (46), (49), and (50) and rearranging terms gives

$$\frac{3 V_L}{2F} \left(\frac{C_o \rho_L}{2 g_c} \right)^{1/2} \frac{\bar{p}_g \bar{c}^2 Q_g^o}{g_c V_c} = \frac{\sigma^{3/2}}{\sqrt{2\pi}} \int_{Z_o}^{\infty} (Z - Z_o)^{3/2} e^{-Z^2/2} \, dZ . \tag{51}$$

The lower limit of Z_o on the integral can be determined by an examination of Eq. (46). This equation says that, for V_L to have a meaningful value, $- P_f'$ must be greater than $\Delta P_T - \rho_L (h_L + L)$. This in turn means that Z must be greater than Z_o and, hence, a lower limit of Z_o.

Equation (51) cannot be evaluated analytically, and thus recourse to numerical methods is required. In fact, this integration was programmed for the IBM-650 computer. The upper limit of the integration was chosen to be 4. The probability of $Z > 4$ is 0.0032%. Thus, terms where $Z > 4$ have a negligible contribution to the numerical value of the integral.

In some cases, as has been mentioned, the amplitude of the pressure fluctuations is constant, which means $\sigma = 0$. Since Eq. (51) cannot be evaluated under this condition, the program was arranged to use Eq. (46) to calculate the dumping rate whenever $\sigma = 0$.

A plot of the results of these calculations is shown in Fig. 41. The calculated dumping rate is the value obtained by evaluating Eq. (46) or (51), whichever applies. This plot shows an apparent change in the flow mechanism in the low dumping region. The dumping in this region is probably controlled by the nature of the side of the hole and the wetting characteristics of the liquid. Since this region is of secondary interest for column-design purposes, and because a theoretical treatment is extremely difficult, no further analysis of this region will be attempted.

The accuracy of these calculations is inherently low. The total pressure drop and head are each based on two manometer readings. The

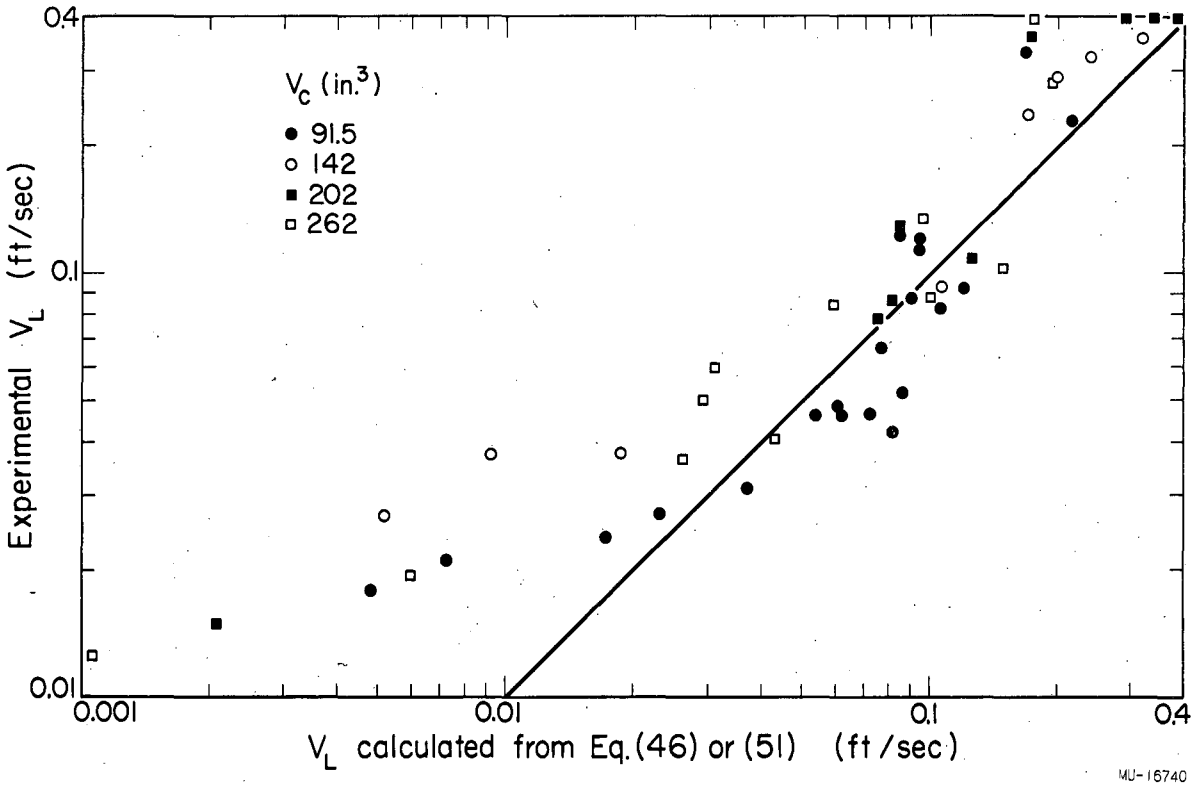

Fig. 41. Single-hole dumping correlation.

manometer readings are each within ±0.025 in. of water or ±0.13 lbs_f/ft^2. This means that the term $\Delta P_T - \rho_L(h_L + L)$ has a possible error of ±0.5 lbs_f/ft^2. The accuracy of the mean pressure fluctuation is approximately ±0.5 lbs_f/ft^2. The problem here is to determine the time-average pressure line on the traces (i.e., Fig. 22 and 23). The variance has essentially no error since its calculation is based only on the values of the minimum points in the pressure wave. The point of reference one chooses on which to base the numbers is immaterial. The term $-P_f - P_T + \rho_L(h_L + L)$ takes on typical values of 1 to 5 lbs_f/ft^2 and has an expected accuracy of ±1.0 lbs_f/ft^2. Thus, the high scatter in Fig. 41 is to be expected.

In preparing Fig. 41, the value of the orifice coefficient was taken to be 2.68. However, it apperas that if a value of 1.68 were used, a better correlation would be obtained. In view of the low accuracy of the calculations and the theoretical basis for using $C_o = 2.68$, this change is not justified.

Dumping Through Multihole Plates

Theoretical interpretation. In contrast to single-hole plates, multihole plates can operate in two different ways. The first is for all the holes to act in complete unision, that is, completely in phase with each other. In this type of operation, all the holes dump together and therefore no gas can flow out of the chamber during the dumping portion of the cycle. Hence, the equations developed for single-hole plates apply with equal validity to multihole plates operating in this fashion.

In the second type of operation, some of the holes dump liquid and the rest simultaneously pass gas. This type of operation is shown schematically in Fig. 42. Following the same analysis used in the single-hole development for a hole dumping liquid, it can be shown that if

$$-P_f' \geq \Delta P_T - \rho_L h_L - \rho_L L, \tag{52}$$

then the pressure above this hole is greater than the pressure below. Thus, there is a driving force for dumping under these conditions.

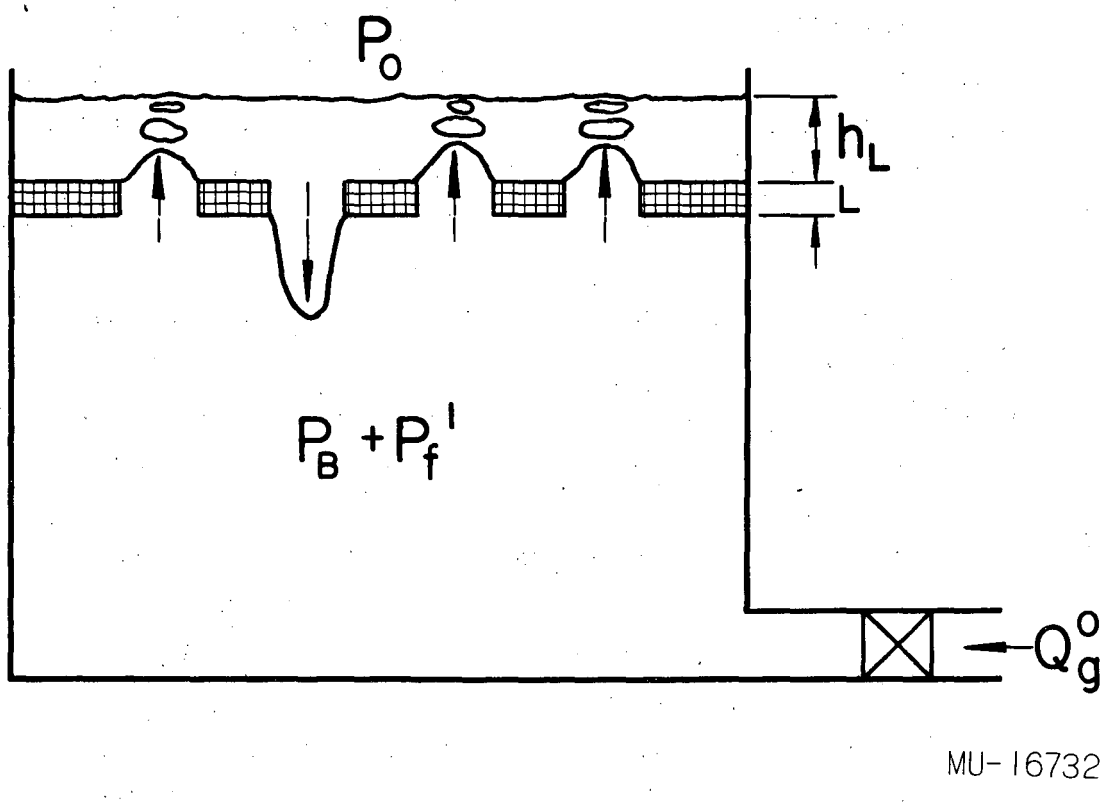

Fig. 42. Schematic diagram of type-2 multihole dumping.

However, during this portion of the cycle where Eq. (52) applies, gas is flowing upwards. Thus, it appears that gas is flowing from a low-pressure region to a high-pressure region. A possible explanation for this can be found in an examination of the rising bubbles. As these bubbles rise rapidly, liquid is dragged along. Because of the liquid motion, the effective head at the plate surface is reduced. Also, the plate thickness term is negligible because gas is flowing through the hole. From Eq. (52) it is apparent that higher amplitudes are required if the head term is reduced and the thickness term drops out. Therefore, these effects can account for the gas flowing upwards while liquid is dumping from different holes at the same time.

From this discussion, a model for the dumping from multihole plates can be developed. The characteristic of this second type of operation is that the holes do not operate in unison. Therefore, if hole A is just starting to bubble, the rapidly expanding bubble from hole B can force liquid to cover and fill hole A. Equation (52) then applies to hole A, but hole B sees the reduced head and no thickness term and therefore does not dump. The chamber pressure then builds up to the point where the dumping stops. The liquid is ejected from the hole, and the cycle then repeats itself.

Thus, in addition to the effects that were considered in the single-hole development, the effect of reduced liquid head and the phase difference in bubbling from neighboring holes must be brought into the analysis. Since there is no way to get at these quantities theoretically, an exact treatment of the data is not possible. Therefore, an examination of the data is required to check the possibility of an empirical correlation.

Correlation of data. Figure 43 shows the data obtained for different gases. The large effect of the gas density can be explained from the behavior of the amplitude, frequency, and pressure drop. The frequency and pressure drop are not greatly affected by the gas properties, but Fig. 15 shows high amplitudes for helium and low amplitudes for Freon 114. Thus, on the basis of Eq. (46), the higher dumping rates for helium and the lower rates for Freon 114 are to be expected.

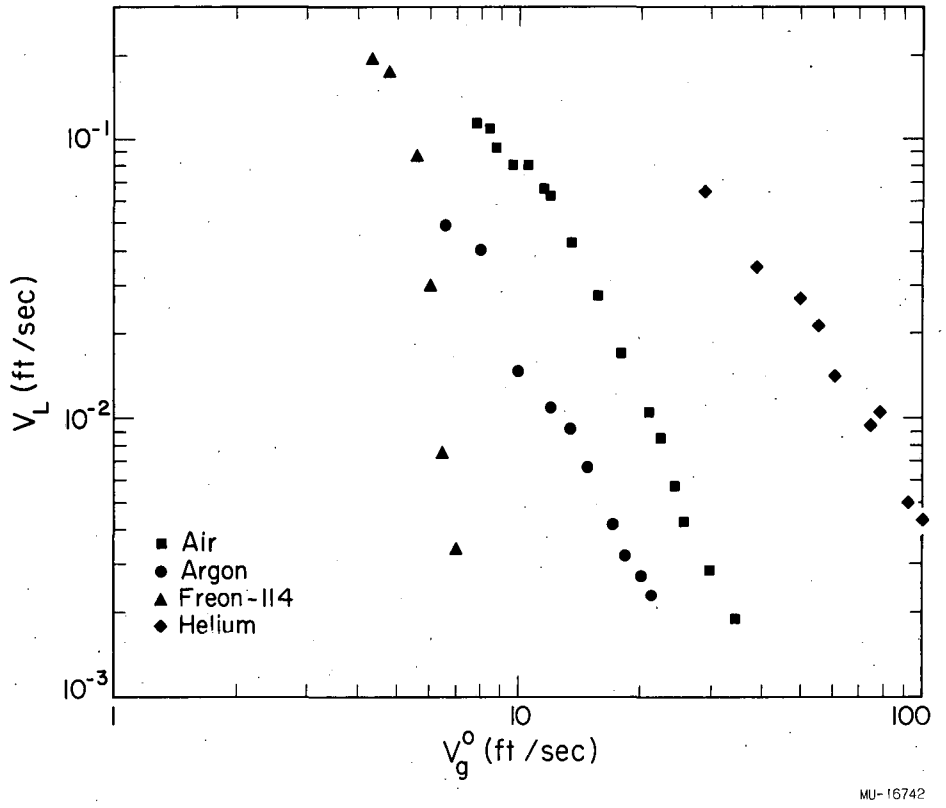

Fig. 43. Effect of gas properties on multihole dumping rates. (Water as liquid, V_c = 262 in^3., D_o = 0.25 in., D = 1.0 in., n = 3, h_L = 2.0 in.)

Of course, Eq. (46) does not apply to multihole plates. However, it seems reasonable to say that the multihole equation must reduce to the single-hole equation. Therefore, the trends predicted by Eq. (46) can be used to explain the effect of certain variables on the dumping rate.

The data obtained when different liquids were used are shown in Fig. 44. Again, the amplitude, frequency, and pressure-drop measurements explain the behavior shown on this plot. For example, high liquid densities (i.e. 50% K_2CO_3-water solution) give higher amplitudes, lower pressure drops, but only slightly lower frequencies. Therefore, the results shown in Fig. 44 can be expected from the trends predicted by Eq. (46).

The liquid viscosity is also important in determining the dumping rate. This is apparent from the change in dumping with the different concentrations of glycerine in water. The effect of the surface tension is not apparent because it is hidden by the density and viscosity effects. A least-squares approach is the only way to determine the surface-tension effect if there is one.

The data obtained by the use of different hole diameters and spacings are shown in Fig. 45. Two facts stand out. The first is that the data for $3D_o$ and $4D_o$ spacings are essentially independent of the spacing and depend only on the diameter. The second fact is that for $2D_o$ spacings, there is a large spacing diameter interaction.

The effects of hole diameter and spacing on the dumping rate are not easy to interpret in terms of the amplitude, frequency, and pressure drop. The frequency is a function of the spacing and the pressure drop depends primarily on the diameter. As Fig. 21 shows, the amplitude is a complicated function of both the diameter and spacing. When these three parameters are combined in Eq. (16), it becomes very difficult to follow the effect of diameter and spacing through and see their effect on the dumping. However, it seems reasonable that these two variables do affect the dumping through the amplitude, frequency, and pressure drop. Also, the plate thickness probably enters in some complicated manner as discussed in the section on multihole theory.

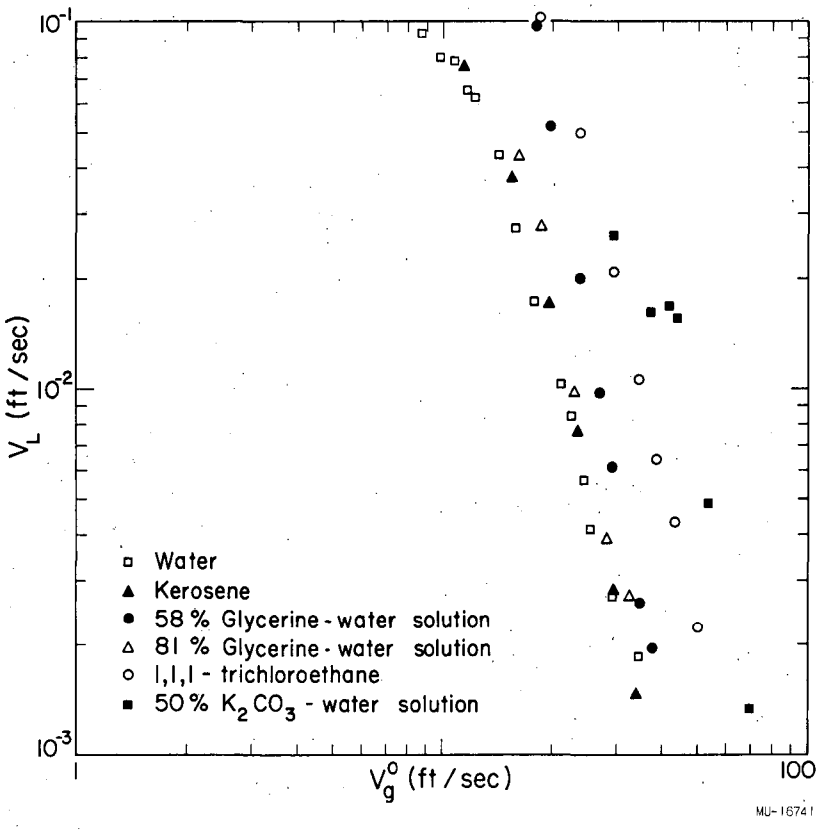

Fig. 44. Effect of liquid properties on multihole dumping rates. (Air as gas, V_c = 262 in^3., D_o = 0.25 in., D = 1.0 in., n = 3, h_L = 2.0 in.)

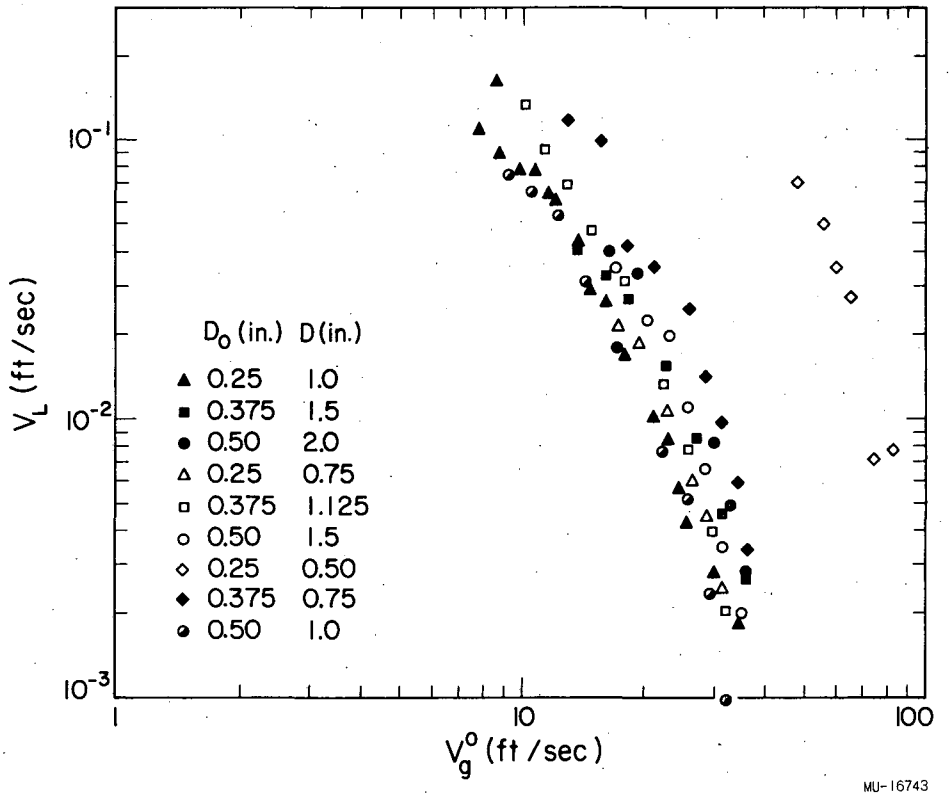

Fig. 45. Effect of hole diameter and spacing on multihole dumping rates. (Air-water system, V_c = 262 in^3., n = 3, h_L = 2.0 in.)

It is interesting to compare these data with the data for plates with large numbers of holes reported by Hunt.[6] He reports high dumping rates for 0.25-in.-diam. holes on $2D_o$ centers indicating a spacing rather than free-area effect. However, comparing the data for 0.50-in.-diam. holes on $2D_o$ centers results in exactly the opposite conclusion. Hunt's data show high dumping rates under these conditions,[6] but Fig. 45 shows comparatively low dumping. Hence, it appears that the effect of free area depends on the hole diameter. There may also have been a wall effect which influenced Hunt's results differently in the two cases.

It seems reasonable to say that plates with small hole spacings and therefore high free-area ratios are poorly designed from a stability standpoint. This view is also held by Hughmark and O'Connell.[15] Therefore, the $2D_o$ spacing data will not be considered in the correlation.

Figure 46 shows that the dumping rate is independent of the head of liquid for these three-hole plates. This is in direct contrast to the results reported by Hunt,[6] Mayfield,[2] and Arnold.[1] These authors all report increased dumping rates with increased heads. Since their data were obtained on plates with large numbers of holes, it is apparent that the effect of head depends on the number of holes.

The fact that the dumping rate is independent of the liquid head can also be explained by an examination of the frequency, pressure drop, and amplitude. All these parameters are independent of the head, and hence there is no reason for the dumping rate to be a function of the head.

The data obtained when different chamber volumes and different numbers of holes were used are shown in Fig. 47. It is obvious from this plot that the volume-per-hole is not the correct parameter as would be predicted by the single-hole theory. At the lower flows, dumping tends to be influenced by the volume-per-hole parameter. This is to be expected since more uniform bubbling occurs at the lower flows, and hence the single-hole type of action is being approached.

At the higher flows, the effect appears to be one of restricted flow to the dumping hole or holes. One-hole plate can draw liquid from

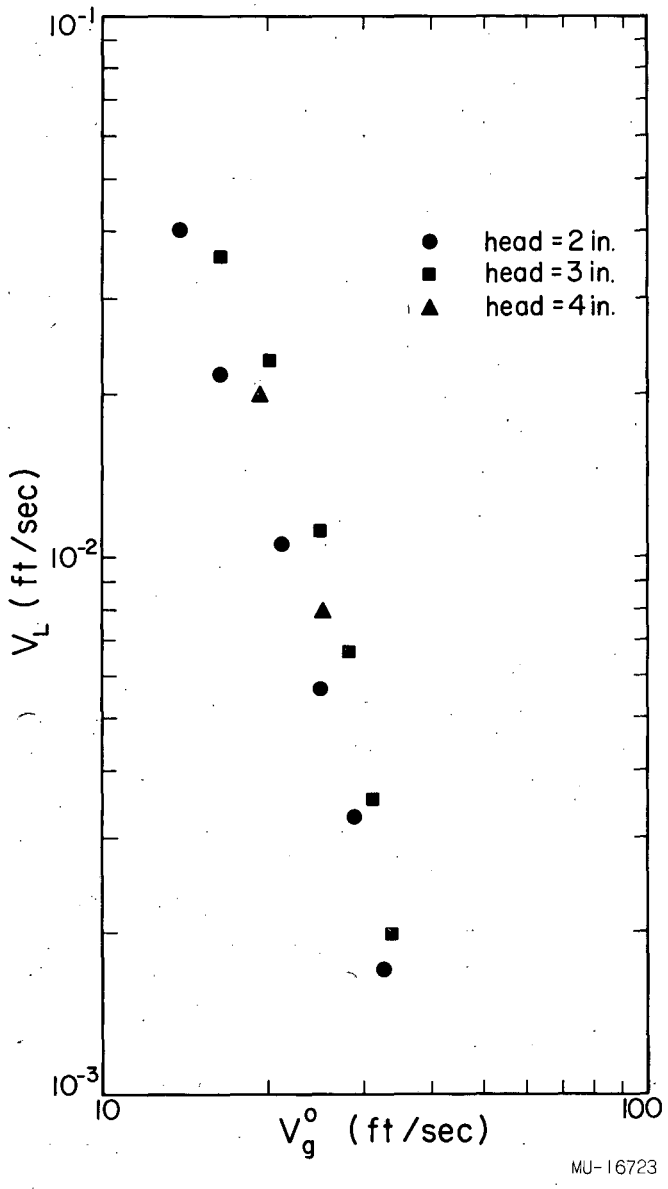

Fig. 46. Effect of head on multihole dumping rates. (Air-water system, V_c = 262 in^3., D_o = 0.25 in., D = 1.0 in., n = 3.)

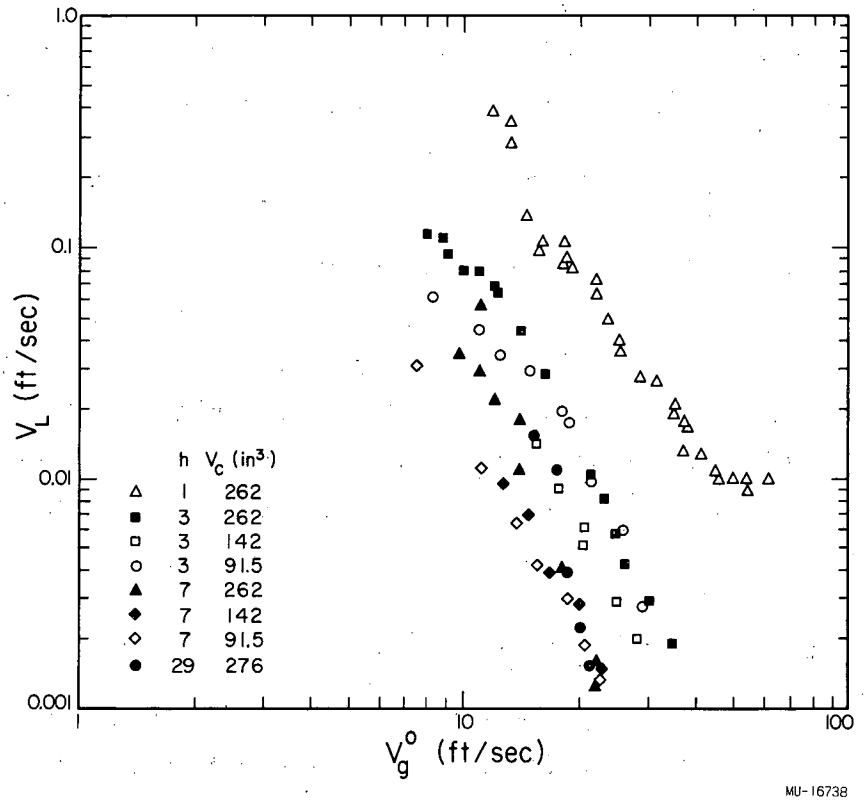

Fig. 47. Effect of chamber volume and number of holes on multihole dumping rates. (Air-water system, D_o = 0.25 in., D = 1.0 in., h_L = 2.0 in.)

all directions. With only one-hole dumping in a three-hole plate, the other holes partially block the liquid flow with the column of rising gas. This is also true to a greater extent with a seven-hole plate and is carried to the limit with the 29-hole plate. Figure 47 shows that this blocking effect levels out and eventually becomes independent of the number of holes, which seems intuitively correct.

An examination of Figs. 43 through 47 indicates that the dumping might be expressed as a function of the variables shown in the equation:

$$V_L = f\,[\,V_g^o,\ D_o,\ \rho_L,\ \rho_g,\ \mu_L,\ \mu_g,\ \gamma,\ \epsilon\,], \tag{53}$$

where ϵ is a factor that accounts for the blocking of liquid flow to a hole.

The single-hole appraoch has shown that the pressure-drop term, $\Delta P_T - \rho_L h_L$, and the frequency are important variables in determining the dumping rate. Therefore, it seems reasonable to also include these variables in the development of a correlation for multihole plates. Thus, Eq. (53) becomes

$$V_L = f\,[\,V_g^o,\ D_o,\ F,\ (\Delta P_T - \rho_L h_L),\ \rho_L,\ \rho_g,\ \mu_L,\ \mu_g,\ \gamma,\ \epsilon\,]. \tag{54}$$

Since the effects of all the variables except ϵ were investigated on three-hole plates, ϵ is constant under these conditions. Therefore, consideration of this effect will be postponed until the effects of the other variables have been considered.

From Figs. 43 through 47, it appears that the most reasonable functional form for Eq. (2) is

$$V_L = A(\Delta P_T - \rho_L h_L)^a\,(F)^b\,(V_g^o)^c\,(D_o)^d\,(\rho_L)^e\,(\rho_g)^f\,(\mu_L)^g\,(\mu_g)^h\,(\gamma)^j. \tag{55}$$

It is apparent from the data that the exponential dependence of the dumping rate on the gas velocity breaks down in the high dumping region. Since this region is small and of lesser interest in design problems, the error made by assuming the exponential form is small and unimportant.

The constants in Eq. (55) were determined by the method of least squares using only the three-hole data. Substituting these constants into Eq. (55) gives

$$V_L = 15.35 \times 10^{-16} (\Delta P_T - \rho_L h_L)^{-0.48} F^{-0.74} (V_g^o)^{-2.25} \rho_L^{2.8} \rho_g^{-1.63} \mu_g^{-2.25} \gamma^{-0.78} D_o^{0.61} \quad (56)$$

where V_L and V_g^o are in ft/sec, F is in hr^{-1}, $(\Delta P_T - \rho_L h_L)$ in lbs_f/ft^2, ρ_L and ρ_g are in lbs/ft^3, γ is in lbs_f/ft, μ_g is in lbs_f/ft sec, and D_o is in inches.

The least-squares analysis showed that the exponent on the liquid viscosity was not significant at the 95% confidence level. Hence, this term has been dropped from the correlation. However, the liquid viscosity is significant in determining the pressure drop and therefore is really a hidden variable in the dumping correlation. The correlation coefficient calculated from this analysis is 81%. The average deviation is ±55% if Eq. (8) is used to estimate the frequency and Eq. (30) is used to estimate the pressure drop.

Now, the ϵ effect can be included in this analysis by modifying the constant in Eq. (55) for plates with different numbers of holes. Thus, Fig. 47 indicates that a good value for the constant for the seven- or 29-hole plates is 5.6×10^{-16}.

The next step in the development of a correlation is to rearrange Eq. (56) into dimensionless groups. However, this approach does not work. A gas-velocity term and a gas-density term remain after all the other variables are combined into groups. Therefore, the dumping process cannot be described by such a simple combination of effects. Thus, no general correlation in dimensionless form is presented.

Comparison with other investigations. It is interesting to compare the results of this work with some of the correlations that have been proposed by other investigators. From these comparisons, it is possible to obtain some idea of the dumping rates that are found at the minimum velocity as calculated from these correlations. Thus, an evaluation of

these correlations can be made. For these comparisons, consider a system comprising a plate with 0.25-in.-diam. holes on 1.0-in. triangular centers, a 2-in. head of water on the plate, and air as the gas.

Under these conditions, Mayfield et al.[2] predict the dry plate pressure drop at the minimum flow to be 2 lbs_f/ft^2. If Hunt's equation[4] is used for the dry plate pressure drop, the minimum gas velocity is 32 ft/sec. From Fig. 47, the dumping rate is only 0.0022 ft/sec or 0.058 lbs. liquid per lb. gas. However, Mayfield's correlation[2] fails to account for the effects of different liquid and gas properties and for different geometries. Also, higher dumping rates have been found at 32 ft/sec when different systems were used. Therefore, this correlation should be used with caution when untested systems are used.

Hunt et al.[4] report the minimum velocity to be 30 ft/sec through the holes under these conditions. This figure is in good agreement with the 32 ft/sec calculated from Mayfield's correlation.[2] Hunt considers the effect of the system's physical properties which is an improvement over Mayfield's proposal. However, extrapolation of Hunt's results to other systems is difficult because no general correlation is presented.

The correlation of Hughmark and O'Connell[15] predicts a minimum gas velocity of 45 ft/sec under the conditions stated above. This is conservative in comparison to the results of Hunt's work,[4] and Mayfield's correlation.[2] Hughmark's correlation is also relatively insensitive to the system's physical properties. Since it gives a higher minimum velocity, this proposal is recommended over Hunt's or Mayfield's method for design purposes when untested systems are being considered.

Leibson et al.,[22] Lee,[20] Zenz,[3] and Hwang and Hodson[24] all use Mayfield's approach or some slight modification of it as their recommended method of predicting the minimum gas velocity. Therefore, no really new information can be obtained by an examination of these proposals. The correlation of Kamei and co-workers[21] was developed for very small diameter holes. Surface-tension effects become very important under these conditions and therefore their correlation is not applicable for 0.25-in.-diam. holes.

Conclusions about multihole dumping. Because of theoretical and empirical difficulties that have been pointed out, no general correlation of the dumping data is presented. However, this analysis shows the need for more theoretical and experimental investigations of the decreased effective head because of the liquid being dragged upwards by the rising gas.

Equation (56) may be of some limited use in estimating the minimum velocity for design purposes.

Large-Column Investigations

Since one of the objectives of this study is to develope a method of predicting dumping rates in industrial-size columns, a column of this type was constructed. This equipment is shown schematically in Fig. 48.

Apparatus and procedure. The dural test section had a rectangular cross section which measured 2 ft by 2.5 ft and was 10 ft high. The rectangular cross section was used to eliminate the effect of expansion and contraction of the liquid as it moved across circular towers. The plates were 2 ft on a side and also made of dural. All the holes were drilled and reamed to size to assure square edges and no burrs.

The dumping rate was determined by collecting in a calibrated tank the liquid that dumped through the holes. The level change over a known period of time was noted, and from the known tank area the time-average dumping rate was calculated. The collection tank was made in two sections. One section was 2 by 2 by 1 ft and the other was 3 ft long and 6 in. in diam. This arrangement made it possible to obtain reasonable level changes in reasonable times and still maintain good accuracy.

Gas was pumped to the column by a Sutorbilt blower, model 1436, and the blower was driven by a U.S. Electrical Motors 20-hp. motor. Thus, by adjusting the speed of the blower and the setting of the by-pass valve, good control of the gas flow was achieved.

From the blower, the gas passed through a water cooler to remove the heat of compression and the heat supplied by the steam heater. The gas then entered the test section and passed up through the plate. Since the gas circulated in a closed system, it soon became saturated with liquid.

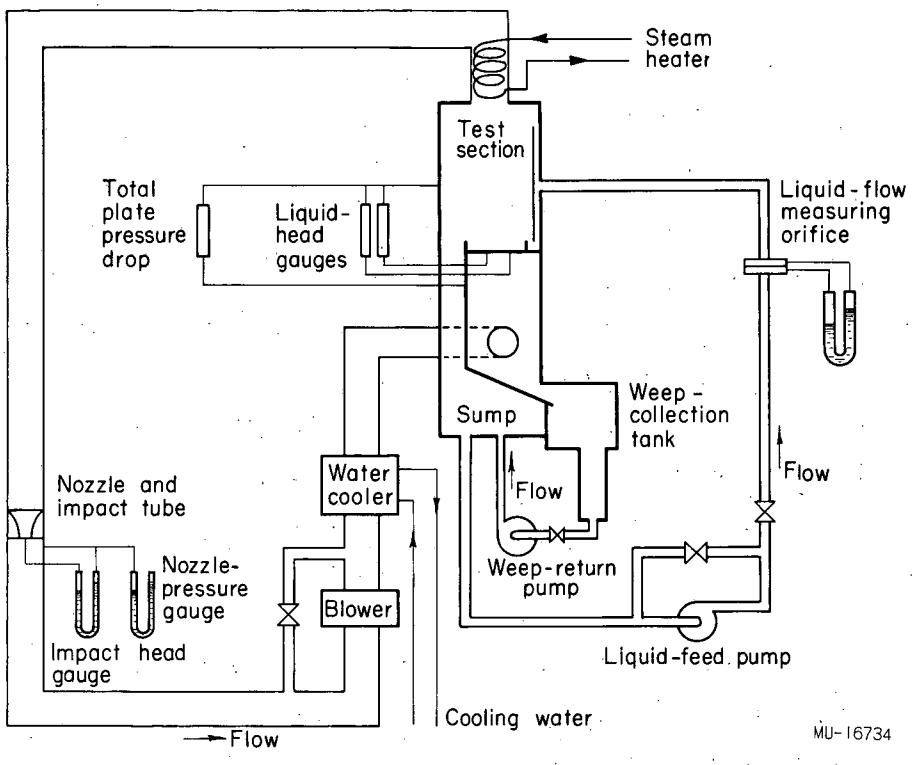

Fig. 48. Schematic diagram of 2-ft. column.

At the exit of the test section, the gas was heated to approximately 100°F. This heating prevented the liquid from condensing in the return line and, thus, from reaching the blower, where rust formation would cause contact between the rotating lobes and the fixed case. In other words, this heater was designed to protect the close tolerances of the blower.

The gas flow was determined by placing an impact tube at the center of a nozzle throat. Bean et al. have shown that the velocity is essentially uniform over the entire cross-section.[29] Thus, the velocity determined from the impact-tube reading times the cross-sectional area of the nozzle gave the volumetric flow of gas through the test section. The impact tube was used since its alignment in the direction of gas flow is not as critical as the alignment of a pitot tube. The nozzle used in this equipment had the dimensions of Bean's C-2 nozzle.[29]

The temperature of the gas was measured with copper-constantan thermocouples connected to a Leeds and Northrup student-type potentiometer. These thermocouples were located in the gas chambers above and below the plate, at the nozzle, and at the blower intake.

The liquid was pumped from the sump in the bottom of the test section through a standard ASME flow-measuring orifice to the test section. After passing through a distributor, the liquid hit the baffle and flowed down to the plate, across it, and back to the sump.

The head of liquid on the plate was measured at six points. Two taps were located just downstream of the inlet weir, one in the center of the plate, one three-quarters of the way across the plate, and one just upstream of the outlet weir. All of these taps were on the center line parallel to the direction of flow. The sixth tap was located on the center line perpendicular to the liquid flow and 6 inches from one of the tower sides.

The head manometers were arranged in such a way that the lines could be flushed out to remove any gas bubbles and thus insure accurate readings. These gauges could be read to ±0.03 in. The liquid-orifice manometer was arranged so that its lines could also be flushed out. The readings on this manometer were within ±0.05 in. of the true value.

An over-all picture of this apparatus is shown in Fig. 49. The test section can barely be seen near the top of the picture to the right of center. The windows (the top one is very bright because of a light directly behind it) were located above and below the plate so that visual observations of the bubbling and dumping could be made. The blower can be plainly seen in the foreground.

A close-up of the test section is shown in Fig. 50. The liquid entered the test section from the left, and the outlet weir and downcomer were on the right. The window in the foreground was large enough so that the plates could be removed through it.

For a given series of runs, the desired weir and plate were placed in the column and the windows bolted down. The blower, cooling water, steam, and then the liquid pump were started. The gas flow was adjusted to the desired value and then the liquid flow was adjusted to give the desired head. The apparatus was then run for 10 minutes, after which the weep-collection tank was emptied and the run started. The run lasted from four to six minutes, but data were taken every two minutes to be sure steady state had been reached. After the run, the weep-collection tank was emptied and the gas flow changed to the next point. The liquid flow was then changed to maintain a constant head of liquid. After four minutes, the data at this second point were obtained.

By the use of this procedure, a series of six to ten points covering a reasonable portion of the dumping region was obtained. Upon completion of a series, the apparatus was shut down, the necessary changes in weir height and plate geometry were made, and the above procedure was repeated for these new conditions.

Before any dumping data were taken, the gas velocity at various points on the plate was measured. No effect of position was found and thus it can be concluded that the velocity profile below the plate was flat. Therefore, no areas of the plate dumped because of a poor velocity distribution.

By the use of the procedure described above, the effect of the following variables was studied:

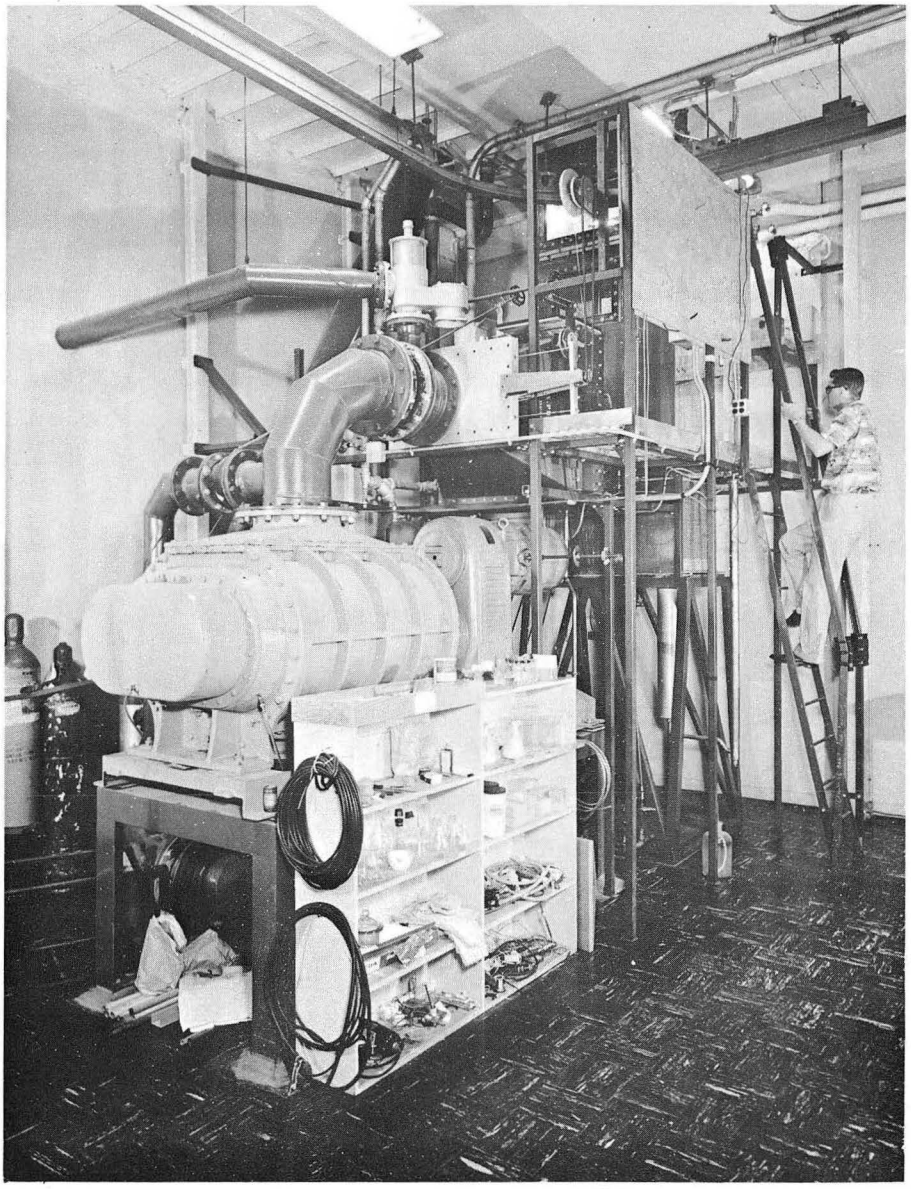

ZN-2116

Fig. 49. Over-all view of 2-ft. column.

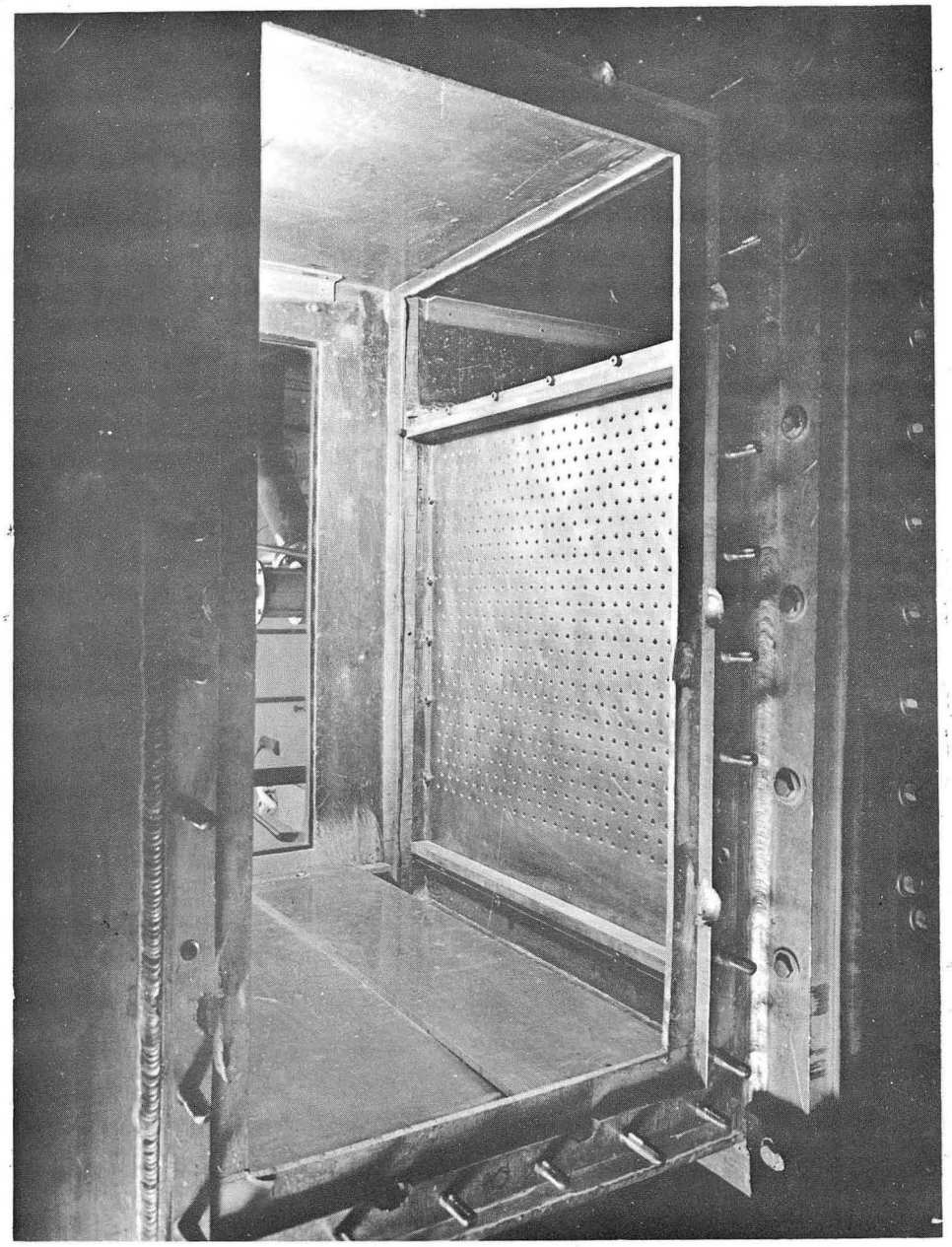

ZN-2117

Fig. 50. View of plate in 2-ft. column.

1. Time-average gas velocity from 10 ft/sec to 60 ft/sec.
2. Liquid head from 1.0 in. to 4.5 in.
3. Weir heights from 1.0 in. to 5.0 in.

Only the air-water system was used in this equipment. The only plate used has 450 holes of 0.25 in. diam. on 1 in. triangular centers. The free area ratio was 0.0418.

Correlation of data. A limited amount of data was obtained on the large column. These data are shown in Figs. 51 and 52. Figure 51 shows the data obtained when the equivalent clear liquid head on the plate was greater than the weir height, and Fig. 52 shows the data when the liquid head was equal to or less than the weir height. Comparison of these two plots shows that the dumping rate depends on the weir height as well as the liquid head. This fact has not been reported by other investigators.[1,2,4]

Figures 51 and 52 also show the effect of gas velocity depends on the relation between the weir height and the liquid head. It seems that the dumping is a function of the gas flow rate, liquid head, and weir height. These three variables interact to give the resultant effect shown on these two plots. An explanation for these interactions becomes apparent from the correlation of the data, and therefore further discussions on this point will be postponed to the next section.

Unfortunately, this apparatus was constructed and the data obtained before the importance of the pressure fluctuations was discovered. Prior to this discovery, it had been thought that the pulsations put out by the positive displacement blower were small and unimportant. After the importance of the pulsations was realized, the diaphragm was attached to the chamber below the plate and measurements taken at a constant gas flow and varying blower speeds. The blower frequency was measured with a "Strobotac". The following table shows the results of these measurements.

Table V

Comparison of blower and chamber frequencies

	Run 1	Run 2	Run 3
Blower frequency (sec^{-1})	5.65	10.2	14.1
Pressure frequency (sec^{-1})	5.7	10.1	13.8

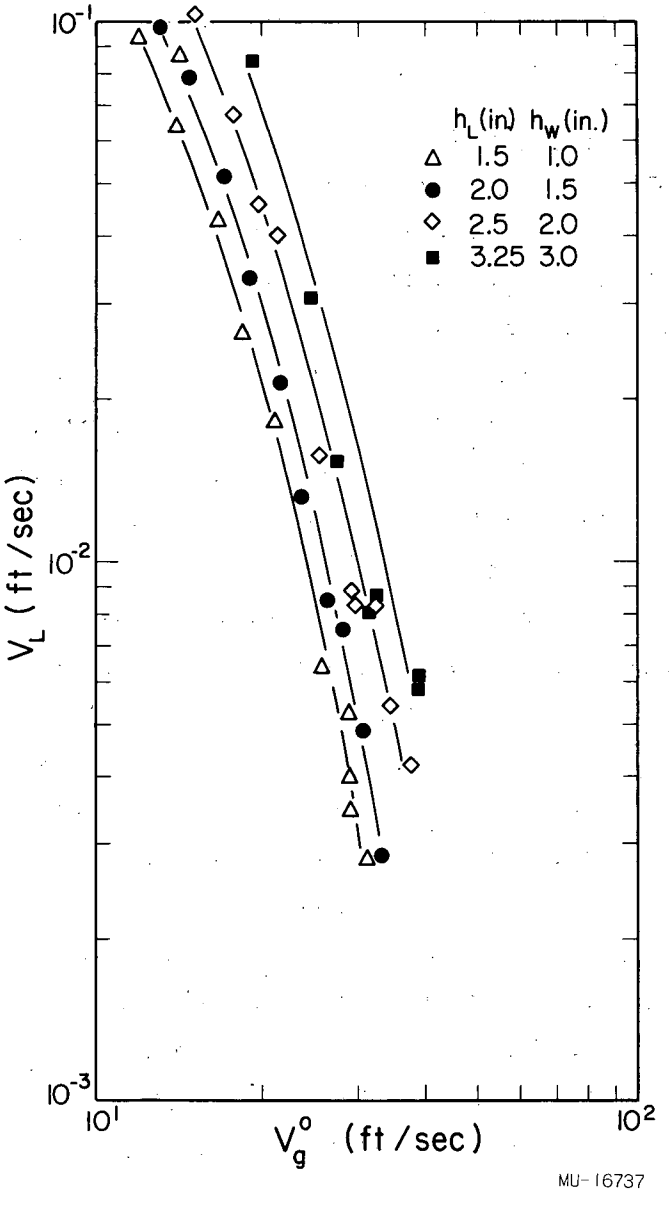

Fig. 51. Dumping data for 2-ft. column. (Air-water system, $h_L > h_w$).

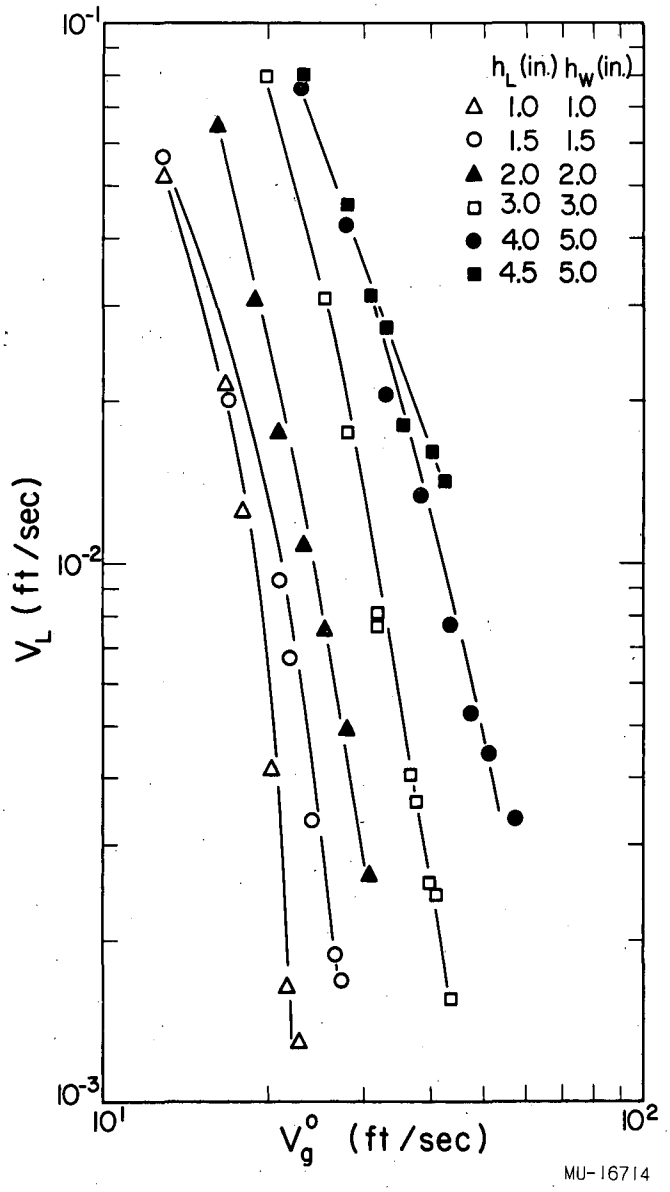

Fig. 52. Dumping data for 2-ft. column. (Air-water system, $h_L \leq h_w$).

This table shows the frequency of the pressure fluctuations is completely controlled by the blower speed. Therefore, these data do not necessarily model the operation of an industrial tower. However, a correlation for these data was obtained which explains some of the interactions previously mentioned. Also, the form of the correlation suggests a possible form for correlating industrial-column data.

Correlation of Data

Consider Eq. (46) which was developed for single-hole plates and neglect the plate thickness term. Now, on the basis of the small column-fluctuation measurements for plates with large numbers of holes, Fig. 53 shows it is reasonable to assume a linear relation between the amplitude and the pressure drop term $\Delta P_T - \rho_L h_L$. On this basis, then, Eq. (46) predicts that the dumping rate is proportional to the pressure-drop term, $\Delta P_T - \rho_L h_L$, raised to the 1.5 power. Since the dumping rate is also a function of the gas velocity and the liquid head, a least-squares analysis of the equation

$$V_L = A \left(\Delta P_T - \rho_L h_L \right)^{1.5} (V_g^o)^x (h_L)^y \qquad (57)$$

was made. The exponential form for the velocity and head dependence was chosen purely on the basis of the data. Figures 51 and 52 indicate that these forms are the most reasonable to use.

Substituting the least-squares constants into Eq. (57) gives the final correlating equation

$$V_L = 2.64 \times 10^4 (\Delta P_T - \rho_L h_L)^{1.5} (V_g^o)^{-5.6} (h_L)^{2.5}. \qquad (58)$$

Discussion of correlation. Figure 54 shows the experimental dumping rate plotted against the parameter $(\Delta P_T - \rho_L h_L)^{1.5} (V_g^o)^{-5.6} (h_L)^{2.5}$ which is essentially the calculated dumping rate. An analysis of this plot shows that 96.8% of the total variation in the dumping rate has been accounted for by Eq. (58). The other 3.2% was caused by errors and effects that were not considered.

This plot shows that the correlation is in good agreement with the data for all conditions except for the 1.0-in.-head data. However, for

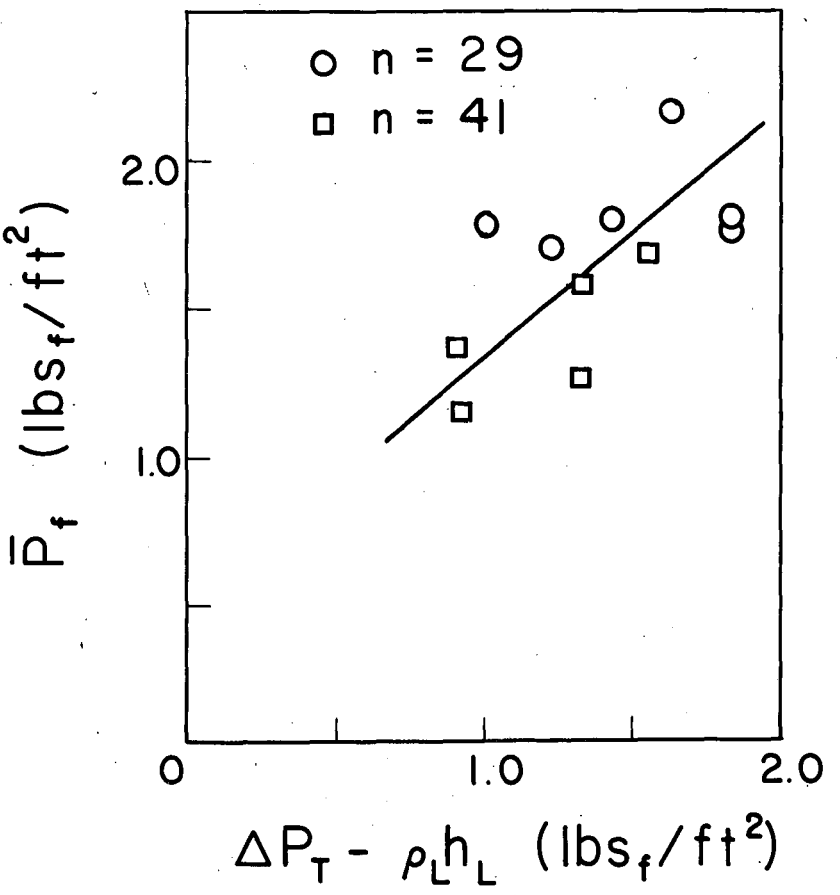

Fig. 53. Comparison of average amplitude and pressure drop in six-in. column for plates with large numbers of holes. (Air-water system, V_c = 276 in^3., h_L = 2.0 in.)

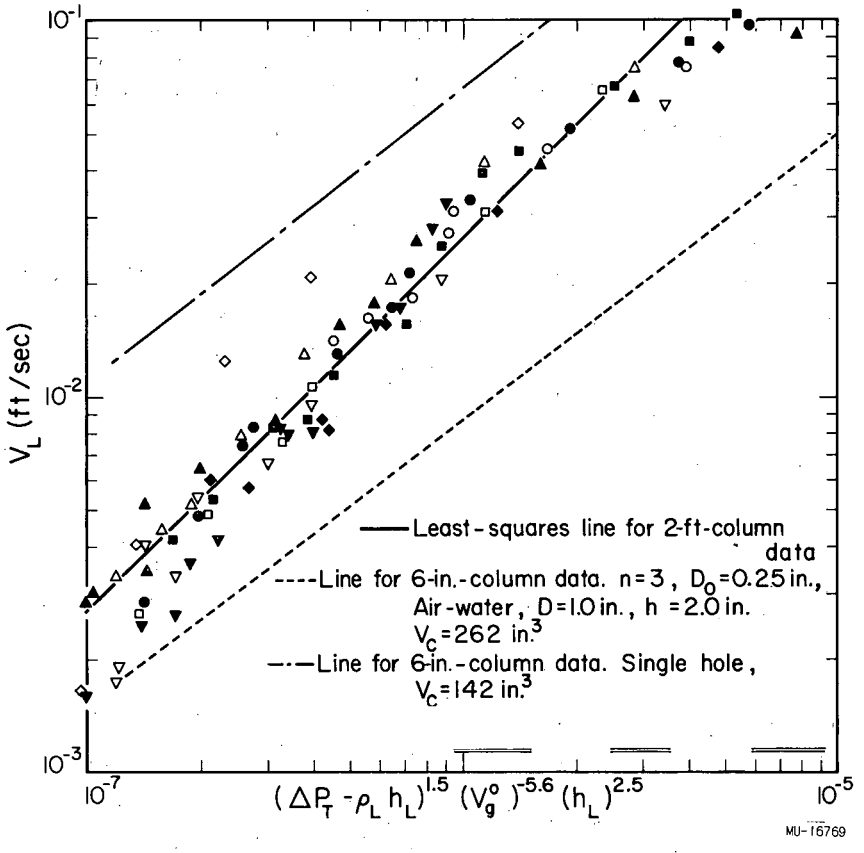

Fig. 54. Proposed correlation for 2-ft-column dumping data. ($\Delta P_t - p_L h_L$ in lb/ft^2, V_g^o in ft/sec, h_L in inches of water.)

- ▲ h_L = 1.5, h_w = 1.0
- ◇ h_L = 1.0, h_w = 1.0
- ● h_L = 2.0, h_w = 1.5
- ▽ h_L = 1.5, h_w = 1.5
- ■ h_L = 2.5, h_w = 2.0
- □ h_L = 2.0, h_w = 2.0
- ◆ h_L = 3.25, h_w = 3.0
- △ h_L = 4.0, h_w = 5.0
- ▼ h_L = 3.0, h_w = 3.0
- ○ h_L = 4.5, h_w = 5.0

such low heads, peculiarities in the bubbling process might occur which would affect the dumping rate. Therefore, these deviations are not too surprising.

The deviations from the curve at the higher dumping rates are also to be expected. Equation (58) predicts that the dumping rate goes to infinity as the gas flow goes to zero. Of course, the dumping rate cannot go to infinity but is limited by the head of liquid on the plate. Therefore, deviations from the equation are to be expected at the higher dumping rates.

It is also interesting to note that the use of the pressure-drop term, $\Delta P_T - \rho_L h_L$ in the correlation removed the interaction effects noted in Figs. 51 and 52. Therefore, Fig. 55, which shows the pressure-drop term as a function of the time-average gas velocity, was prepared. This plot shows that the pressure drop is a function of the parameter $(h_L - h_w)/h_w$. This factor is a measure of the height of the foam over the weir. Thus it seems reasonable that this parameter $(h_L - h_w)/h_w$ is then a measure of the turbulence in the liquid. The higher this turbulence, the higher the pressure drop across the plate, which agrees with the results shown in Fig. 55.

One possible explanation for this might be a liquid-flow effect. This possibility was checked, and it was found that, for the data where $h_L > h_w$, the liquid flow required to maintain a constant head is a function of the gas flow and independent of the weir height. Thus this possibility is ruled out. Therefore, if this really is a turbulence effect, it is related to the foam height over the weir.

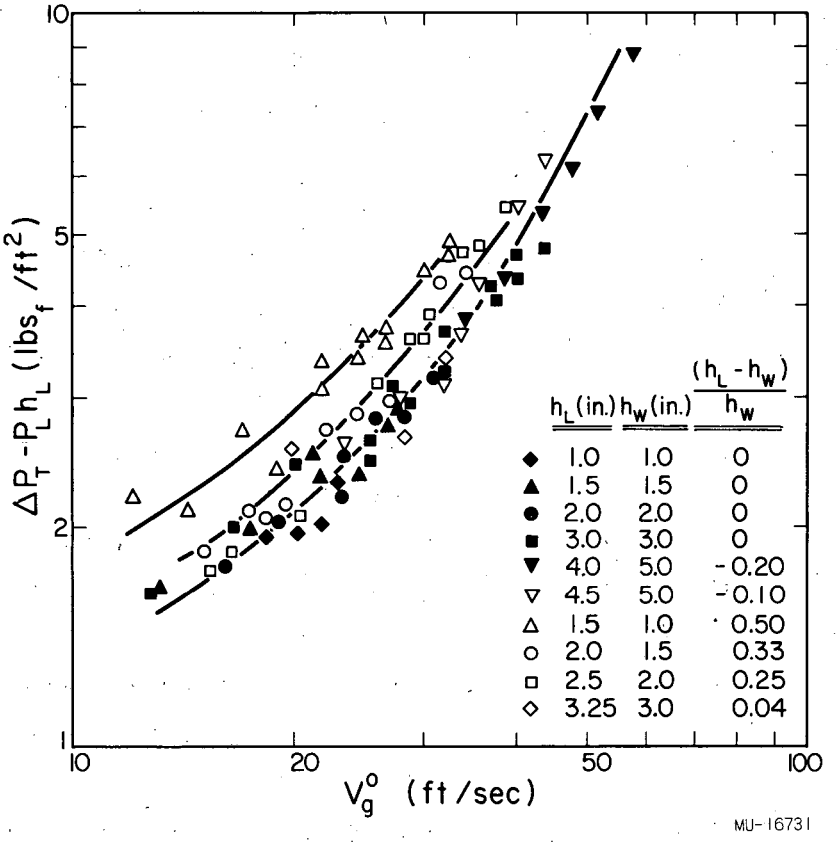

Fig. 55. Pressure-drop data for two-ft-column.

GENERAL CONCLUSIONS

From the results of this work, an increased understanding of the bubbling process has been obtained. A correlation for the frequency of the pressure fluctuations under multihole plates has been developed. The force-balance equation for a growing bubble has been used to explain the previously reported residual pressure-drop data and also used as a basis for a correlation of the pressure-drop data obtained in this study. The amplitude of the pressure fluctuations under the plate was measured, but no theoretical or empirical correlation for these data was obtained.

An equation that predicts the dumping rate from single-hole plates was derived and shown to be in good agreement with the experimental data. A model for the dumping from multihole plates was proposed, but the fluid dynamics involved are too complicated to be expressed in mathematical terms. An empirical correlation of the data was attempted, but the resulting equation does not reduce to a dimensionless form.

A limited amount of data was obtained on a column of industrial proportions, and a possible method of correlation proposed. However, pulsations in the gas flow produced by the positive-displacement blower dominated the bubbling.

ACKNOWLEDGEMENTS

I wish to express my gratitude to Professors Donald N. Hanson and Charles R. Wilke for their guidance and assistance, and to Professor Leonard Farbar for his critical review of this text.

The help of Mr. Eugene J. Fenech in the use of the computer and preparing the tables of data is greatly appreciated.

Thanks are extended to Mrs. June Brown for her encouragement throughout this work and for typing the rough draft of this report.

The continued help of the Accelerator Technicians in the construction of the equipment is greatly appreciated.

I thank the Dow Chemical Company for their financial assistance during the academic year 1954-1955.

This work was performed under the auspices of the United States Atomic Energy Commission.

APPENDICES

Appendix I. Calibrations of Small Column Components

Diaphragm Calibration

The diaphragm used to determine the pressure fluctuations in the gas chamber below the plate was calibrated with the equipment shown diagrammatically in Fig. 56. The diaphragm, and its holder, B, were placed inside the large cylinder A of known cross-sectional area a known distance from the closed end. The small piston C was moved by turning the wheel D to the position of maximum volume. Valve F was opened to allow the chamber to come to atmospheric pressure, then closed, and the motor was started. The sinusoidal output from the Wheatstone bridge was recorded on the Brush recorder.

If ideal gas behavior is assumed, the pressure change in the enclosed chamber is given by the relation,

$$\Delta P = \frac{P_a}{V_c} \Delta V. \qquad (59)$$

Since the area and stroke length of the piston C are known, the maximum volume displaced by the piston is known. From this volume, the maximum pressure change in the chamber can be calculated by the use of Eq. (59). This pressure change corresponds to twice the amplitude of the bridge output. Thus, by the use of various diaphragm positions, a plot of pressure vs. output voltage can be obtained.

The frequency of these pressure pulses could be changed by rearranging the gears connecting the motor to the wheel D. Frequencies from 1 to 9 cps were used but had no effect on the bridge output. The results, which are shown in Fig. 57, show a slight curvature when plotted as the bridge output voltage vs. pressure change. Since the average pressure in the chamber was approximately 4 in. of water, the slope at that pressure was used as the conversion factor.

The calibration was repeated several times during the life of the batteries, and no effect of time was observed provided the surface charge on the batteries had been drained off.

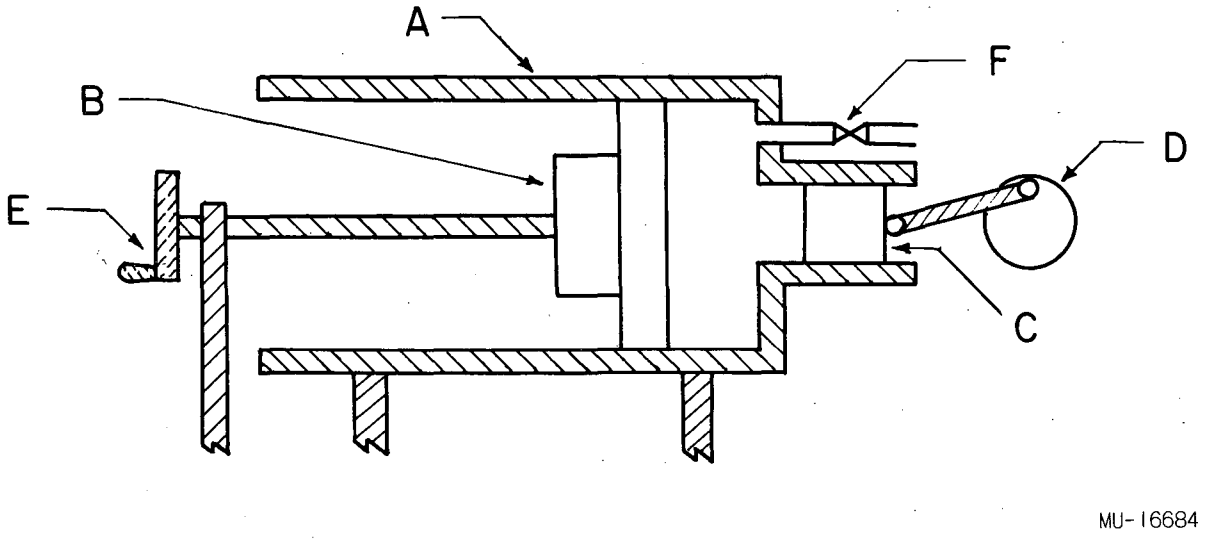

Fig. 56. Schematic diagram of strain-gauge calibration apparatus.

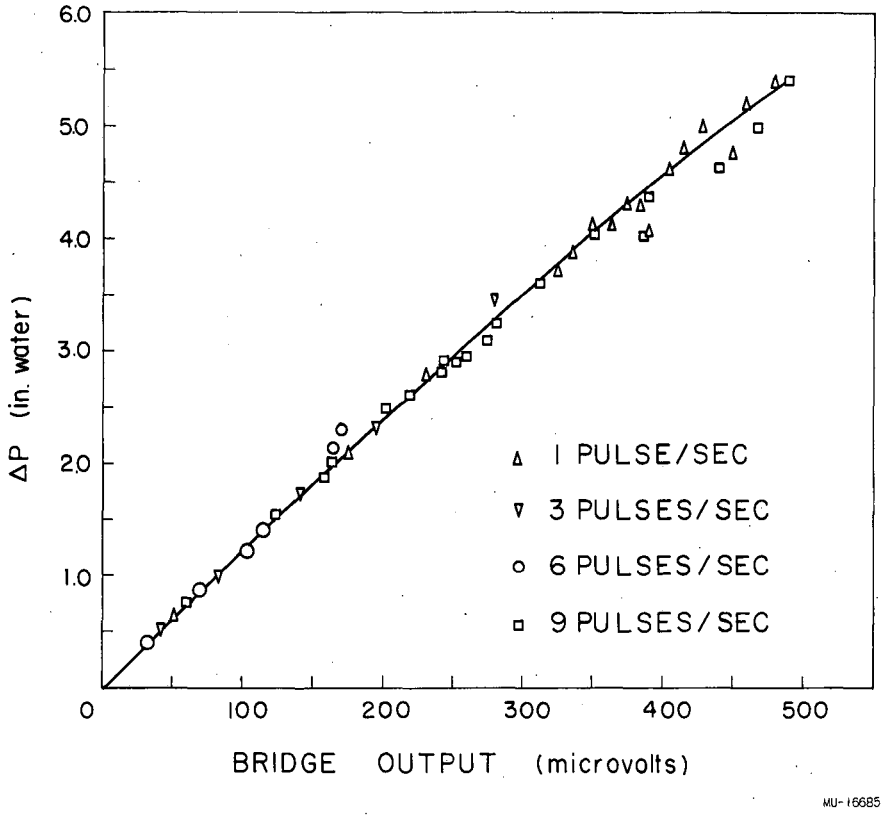

Fig. 57. Strain-gauge diaphragm calibration.

Figure 58 shows an over-all picture of the equipment. The piece to the left is the diaphragm holder. The main cylinder is in the center, and the piston C and gear D are shown on the left. Figure 59 shows a close-up of the motor, gear train, and eccentric wheel.

Gas-Orifice Calibration

The four orifices used in this equipment were calibrated against a 50 ft^3/hr Precision wet-test meter (Model 3118) for the low-flow ranges. For air velocities greater than 50 ft^3/hr, the orifice flows were measured by a calibrated Brooks dual-float rotameter (Type 1111).

Weep-Collection Tanks

The four weep-collection tanks were calibrated by simply adding a known volume of water to the tank and noting the level change. The tanks were filled in small increments and an average area obtained.

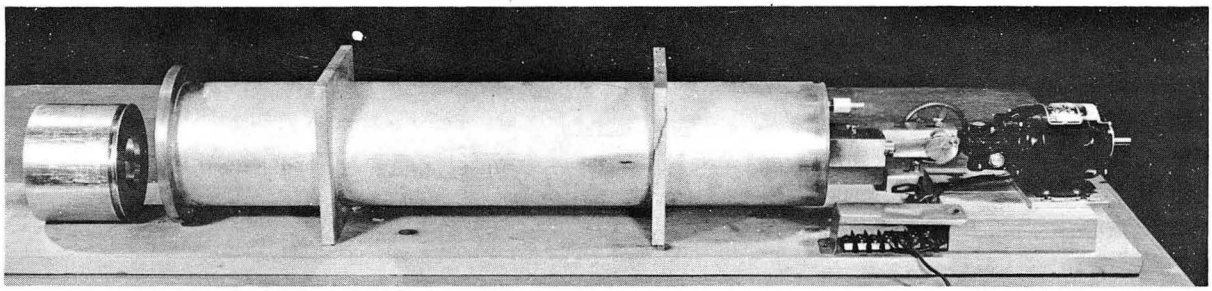

ZN-2112

Fig. 58. Over-all view of strain-gauge calibration apparatus.

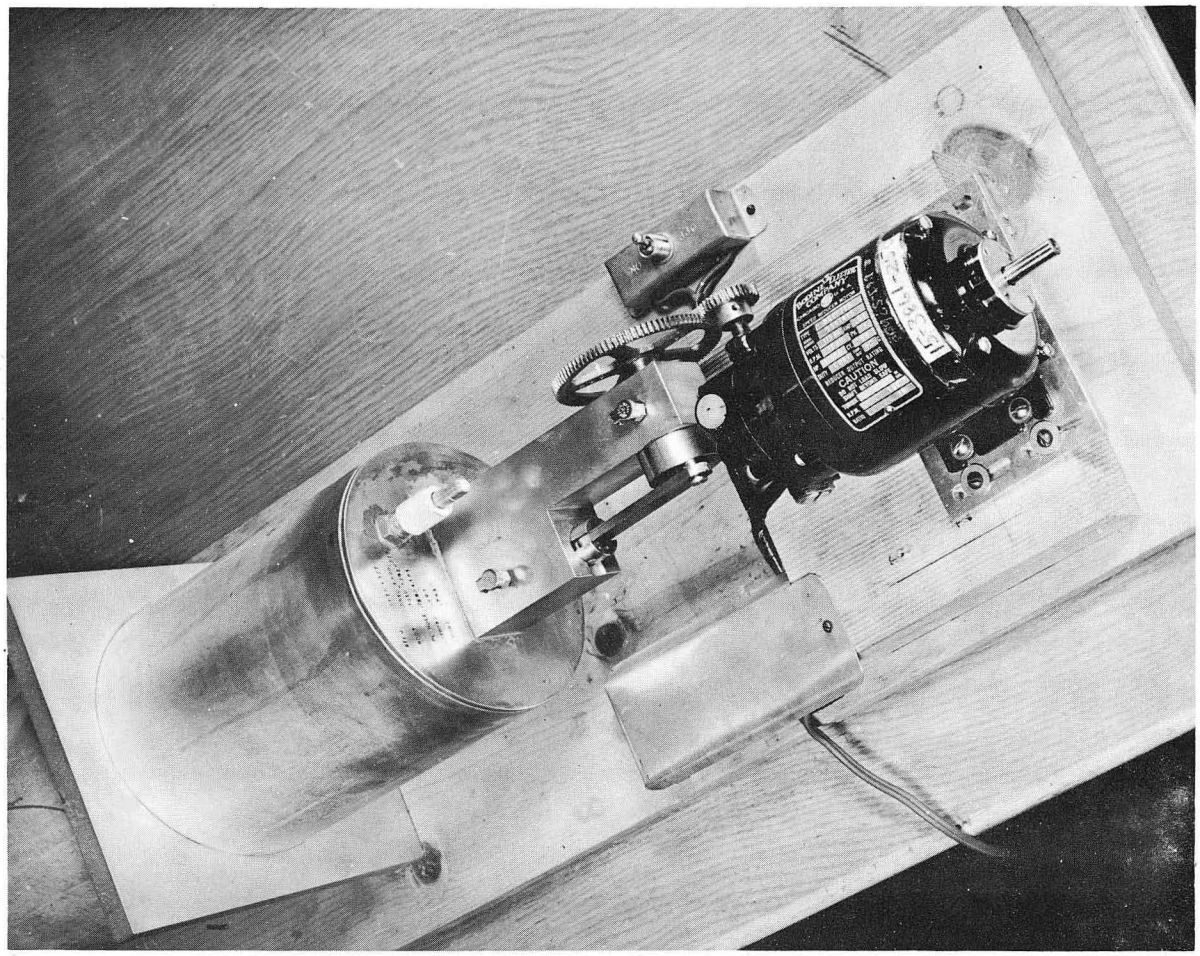

ZN-2113

Fig. 59. Close-up of pulsing piston on diaphragm calibration apparatus.

Six-In. Column Data

Air-Water System

D_o = 0.250 in. D = 1.00 in. L = 0.250 in. n = 3 V_c = 262 in^3.

Run No.	V_g^o (ft/sec)	V_L (ft/sec)	F (sec^{-1})	$\Delta P - \rho_L h_L$ (lbs_f/ft^2)	$\bar{P}_f$ (lbs_f/ft^2)	σ (lbs_f/ft^2)	h_L (in. liq.)
811	13.8	0.0431	8.8	2.4	2.7	1.7	2.0
807	22.8	0.0084	10.6	3.2	3.9	1.7	2.0
808	34.7	0.0019	12.3	5.1	4.6	1.9	2.0
806	29.8	0.0028	11.7	4.2	4.5	1.5	2.0
803	18.1	0.0172	9.8	3.2	3.4	1.5	2.0
801	16.0	0.0272	9.3	2.6	3.2	1.6	2.0
802	12.1	0.0633	8.2	2.4	3.8	1.6	2.0
804	21.3	0.0103	10.4	3.0	3.7	1.9	2.0
805	25.7	0.0042	11.1	3.6	4.2	1.7	2.0
809	24.6	0.0056	11.0	3.6	4.4	1.6	2.0
814	11.8	0.0650	8.1	1.9	2.8	1.5	2.0

Helium-Water System

D_o = 0.250 in. D = 1.00 in. L = 0.250 in. n = 3 V_c = 262 in^3.

Run No.	V_g^o (ft/sec)	V_L (ft/sec)	F (sec^{-1})	$\Delta P - \rho_L h_L$ (lbs_f/ft^2)	$\bar{P}_f$ (lbs_f/ft^2)	σ (lbs_f/ft^2)	h_L (in. liq.)
961	60.1	0.0148	11.8	2.7	6.0	3.5	2.0
962	50.3	0.0273	11.3	2.7	10.1	3.6	2.0
963	39.1	0.0345	10.0	2.4	10.7	3.4	2.0
964	74.9	0.0098	12.8	3.6	7.1	3.4	2.0
965	29.5	0.0636	9.5	2.1	7.2	4.1	2.0
966	56.2	0.0216	11.3	3.5	11.1	4.4	2.0
971	79.8	0.0106	12.5	4.3	8.3	3.2	2.0
972	92.0	0.0051	13.5	5.0	12.0	4.4	2.0
973	99.4	0.0044	13.3	5.4	13.5	3.1	2.0

Argon-Water System

D_o = 0.250 in. D = 1.00 in. L = 0.250 in. n = 3 V_c = 262 in^3.

Run No.	V_g^o (ft/sec)	V_L (ft/sec)	F (sec^{-1})	$\Delta P - \rho_L h_L$ (lbs_f/ft^2)	$\bar{P}_f$ (lbs_f/ft^2)	σ (lbs_f/ft^2)	h_L (in. liq.)
991	12.3	0.0147	11.5	2.1	3.3	1.7	2.0
992	15.0	0.0092	12.0	2.5	3.5	1.8	2.0
995	10.2	0.0262	10.5	1.8	3.8	1.5	2.0
996	8.1	0.0398	10.5	1.6	3.4	1.8	2.0
997	6.6	0.0484	8.5	1.5	4.0	1.7	2.0
081	14.8	0.0066	11.8	2.5	2.2	2.1	2.0
082	17.5	0.0040	12.8	2.7	2.3	1.2	2.0
083	21.3	0.0022	14.3	3.3	3.6	1.5	2.0
084	20.0	0.0027	13.5	3.1	2.4	1.2	2.0
085	18.6	0.0032	13.3	2.9	2.7	1.1	2.0
086	13.4	0.0106	11.5	2.3	3.7	1.9	2.0

Freon 114-Water System

D_o = 0.250 in. D = 1.00 in. L = 0.250 in. n = 3 V_c = 262 in^3

Run No.	V_g^o (ft/sec)	V_L (ft/sec)	F (sec^{-1})	$\Delta P - \rho_L h_L$ (lbs_f/ft^2)	$\bar{P}_f$ (lbs_f/ft^2)	σ (lbs_f/ft^2)	h_L (in. liq.)
061	6.5	0.0074	10.0	1.9	1.8	0.5	2.0
062	6.1	0.0295	9.8	2.0	2.4	0.9	2.0
063	7.0	0.0033	11.3	1.6	0.9	0.5	2.0
064	5.7	0.0895	9.5	2.7	3.0	0.4	2.0
069	4.4	0.2050	8.8	2.3	1.4	0.3	2.0

Air-Kerosene System

D_o = 0.250 in. D = 1.00 in. L = 0.250 in. n = 3 V_c = 262 in^3

Run No.	V_g^o (ft/sec)	V_L (ft/sec)	F (sec^{-1})	$\Delta P - \rho_L h_L$ (lbs_f/ft^2)	$\bar{P}_f$ (lbs_f/ft^2)	σ (lbs_f/ft^2)	h_L (in. liq.)
381	19.9	0.0169	13.0	2.2	2.1	0.8	1.9
382	23.9	0.0077	12.8	2.6	1.7	0.8	2.0
383	29.0	0.0029	13.0	3.2	2.3	0.8	1.9
384	34.5	0.0015	13.0	4.0	1.9	0.7	1.9
385	15.6	0.0378	12.3	2.3	2.0	0.7	1.9
386	11.5	0.0762	11.5	2.2	2.6	0.5	1.9

Air-58% Glycerine System

D_o = 0.250 in. D = 1.00 in. L = 0.250 in. n = 3 V_c = 262 in^3

Run No.	V_g^o (ft/sec)	V_L (ft/sec)	F (sec^{-1})	$\Delta P - \rho_L h_L$ (lbs_f/ft^2)	$\bar{P}_f$ (lbs_f/ft^2)	σ (lbs_f/ft^2)	h_L (in. liq.)
391	29.2	0.0061	12.0	4.6	4.5	1.6	2.0
392	35.0	0.0026	11.8	5.0	4.7	1.8	2.0
393	24.4	0.0197	11.5	4.5	4.2	1.6	1.9
394	20.0	0.0517	10.5	4.2	3.9	1.8	2.0
395	38.0	0.0020	12.0	6.3	4.7	2.0	2.0
396	27.5	0.0096	10.8	4.8	4.2	1.3	1.9
397	46.1	0.0025	11.3	6.7	6.2	1.9	3.8
398	19.9	0.0328	10.8	4.3	3.8	2.5	3.8

Air-81% Glycerine System

D_o = 0.250 in. D = 1.00 in. L = 0.250 in. n = 3 V_c = 262 in^3

Run No.	V_g^o (ft/sec)	V_l (ft/sec)	F (sec^{-1})	$\Delta P - \rho_L h_L$ (lbs_f/ft^2)	$\bar{P}_f$ (lbs_f/ft^2)	σ (lbs_f/ft^2)	h_L (in. liq.)
401	28.2	0.0039	11.3	4.9	5.5	1.2	1.9
402	23.3	0.0098	11.0	4.4	4.7	1.5	1.9
403	18.9	0.0278	10.0	3.8	4.4	1.5	1.8
404	32.6	0.0027	11.3	5.1	4.6	2.7	2.1
405	16.1	0.0424	9.8	3.4	3.6	1.4	1.8
406	28.6	0.0086	11.5	4.0	4.2	2.4	4.4
407	17.4	0.0245	9.5	2.8	4.3	1.7	4.2

Air-81% Glycerine System

D_o = 0.500 in. D = 1.50 in. L = 0.500 in. n = 3 V_c = 276 in.^{3}

Run No.	V_g^o (ft/sec)	V_L (ft/sec)	F (sec^{-1})	$\Delta P - \rho_L h_L$ (lbs_f/ft^2)	$\bar{P}_f$ (lbs_f/ft^2)	σ (lbs_f/ft^2)	h_L (in. liq.)
411	39.2	0.0015	11.3	5.0	11.3	2.4	2.0

Air-1, 1, 1-Trichloroethane System

D_o = 0.250 in. D = 1.00 in. L = 0.250 in. n = 3 V_c = 262 in.^{3}

Run No.	V_g^o (ft/sec)	V_L (ft/sec)	F (sec^{-1})	$\Delta P - \rho_L h_L$ (lbs_f/ft^2)	$\bar{P}_f$ (lbs_f/ft^2)	σ (lbs_f/ft^2)	h_L (in. liq.)
431	30.6	0.0204	11.5	3.7	5.2	2.0	2.0
433	40.6	0.0064	12.0	4.5	5.0	1.9	2.0
434	52.1	0.0022	11.3	6.6	3.9	2.3	2.0
435	45.5	0.0043	12.3	5.5	4.7	1.6	2.0
436	59.4	0.0006	12.3	7.8	5.0	1.8	2.0
437	24.4	0.0497	10.8	2.9	4.8	1.0	2.0
438	18.9	0.0948	10.3	2.9	4.4	2.3	2.0

Air-50% K_2CO_3 System

D_o = 0.250 in. D = 1.00 in. L = 0.250 in. n = 3 V_c = 262 in.^{3}

Run No.	V_g^o (ft/sec)	V_L (ft/sec)	F (sec^{-1})	$\Delta P - \rho_L h_L$ (lbs_f/ft^2)	$\bar{P}_f$ (lbs_f/ft^2)	σ (lbs_f/ft^2)	h_L (in. liq.)
441	30.1	0.0258	8.0	3.0	9.0	1.8	2.1
442	38.0	0.0161	8.8	4.1	9.7	2.4	2.2
443	45.0	0.0156	9.0	5.2	11.5	2.7	2.1
444	56.9	0.0048	9.3	7.7	14.7	1.5	2.1
445	70.9	0.0013	10.3	12.3	13.0	3.2	2.1
446	43.9	0.0168	8.8	5.7	17.3	2.8	2.1
447	25.9	0.0656	7.8	4.2	10.7	2.2	2.1

Air-Water System

D_o = 0.250 in. D = 0.00 in. L = 0.250 in. n = 1 V_c = 091 $in.^3$

Run No.	V_g^o (ft/sec)	V_L (ft/sec)	F (sec^{-1})	$\Delta P - \rho_L h_L$ (lbs_f/ft^2)	$\bar{P}_f$ (lbs_f/ft^2)	σ (lbs_f/ft^2)	h_L (in. liq.)
721	23.8	0.0425	10.5	3.5	5.5	0.9	2.0
722	31.0	0.0497	12.3	4.9	6.4	1.5	2.0
723	36.7	0.0462	12.3	5.7	7.0	2.0	2.0
724	26.5	0.0466	11.0	3.9	5.4	2.2	2.0
725	20.9	0.0524	9.5	3.7	5.7	1.3	2.0
726	43.5	0.0309	13.0	7.4	8.2	2.0	2.0
727	48.9	0.0241	13.5	8.8	8.7	1.4	2.0
728	55.2	0.0181	14.0	10.2	8.6	1.6	2.0
731	61.6	0.0184	14.0	12.5	9.4	1.2	2.0
732	50.8	0.0213	14.3	9.0	7.5	1.8	2.0
733	24.0	0.0463	11.0	4.1	5.4	1.2	2.0
734	16.7	0.0676	8.8	3.3	4.8	0.0	2.0
735	15.2	0.0875	8.5	3.1	4.8	0.0	2.0
736	11.5	0.1230	8.0	2.9	4.3	0.0	2.0
737	15.6	0.0815	8.8	3.1	5.1	0.7	2.0
738	12.1	0.1150	8.0	2.5	4.0	0.0	2.0
739	45.7	0.0278	13.5	7.8	8.1	1.4	2.0
761	10.0	0.1190	7.8	2.3	3.2	0.9	2.0
762	8.0	0.0915	8.0	2.1	3.3	0.0	2.0
763	6.4	0.2290	6.0	1.2	3.8	0.0	2.0
764	4.9	0.3340	4.8	1.2	3.1	0.0	2.0

Air-Water System

D_o = 0.250 in. D = 0.00 in. L = 0.250 in. n = 1 V_c = 142 $in.^3$

Run No.	V_g^o (ft/sec)	V_L (ft/sec)	F (sec^{-1})	$\Delta P - \rho_L h_L$ (lbs_f/ft^2)	$\bar{P}_f$ (lbs_f/ft^2)	σ (lbs_f/ft^2)	h_L (in. liq.)
676	31.8	0.0382	11.7	5.4	4.9	2.0	2.0
677	27.4	0.0387	10.4	4.6	3.8	0.6	2.0
678	41.5	0.0275	13.7	6.9	5.1	1.3	2.0
679	53.7	0.0198	13.7	9.7	5.7	1.5	2.0
755	6.9	0.3290	5.5	1.4	3.6	0.0	2.0
756	9.8	0.0930	7.3	2.9	3.7	0.0	2.0
757	7.3	0.2960	5.8	1.6	3.4	0.0	2.0
758	8.4	0.2410	5.8	2.3	4.0	0.0	2.0
759	4.9	0.3620	4.7	0.6	3.0	0.0	2.0

Air-Water System

D_o = 0.250 in. D = 0.00 in. L = 0.250 in. n = 1 V_c = 202 in^3

Run No.	V_g^o (ft/sec)	V_L (ft/sec)	F (sec^{-1})	$\Delta P - \rho_L h_L$ (lbs_f/ft^2)	$\bar{P}_f$ (lbs_f/ft^2)	σ (lbs_f/ft^2)	h_L (in. liq.)
671	18.3	0.0865	7.7	3.0	3.7	0.0	2.0
672	14.2	0.1090	8.0	2.6	3.5	0.5	2.0
673	15.9	0.0795	8.0	3.0	3.3	0.6	2.0
674	44.7	0.0129	13.3	7.5	3.8	1.1	2.0
675	52.8	0.0120	14.3	9.3	5.1	2.2	2.0
751	9.2	0.3670	5.3	1.8	3.3	0.0	2.0
752	6.6	0.4060	5.0	1.2	3.1	0.0	2.0
753	4.1	0.4060	3.3	0.6	2.7	0.0	2.0
754	5.6	0.4000	4.8	1.0	3.3	0.0	2.0

Air-Water System

D_o = 0.250 in. D = 0.00 in. L = 0.250 in. n = 1 V_c = 262 in^3

Run No.	V_g^o (ft/sec)	V_L (ft/sec)	F (sec^{-1})	$\Delta P - \rho_L h_L$ (lbs_f/ft^2)	$\bar{P}_f$ (lbs_f/ft^2)	σ (lbs_f/ft^2)	h_L (in. liq.)
690	23.5	0.0506	8.3	4.0	3.4	0.8	2.0
701	34.7	0.0191	11.3	5.2	3.5	0.9	2.0
702	25.4	0.0379	9.3	4.4	3.8	0.7	2.0
704	17.9	0.0885	8.0	2.8	3.2	0.9	2.0
705	22.0	0.0636	8.3	3.6	3.1	0.7	2.0
706	24.9	0.0409	9.0	4.3	4.1	0.7	2.0
707	37.9	0.0170	12.0	5.9	3.2	0.8	2.0
708	19.1	0.0852	8.0	3.3	3.2	0.8	2.0
709	15.5	0.1010	7.0	2.6	3.6	1.0	2.0
700	14.5	0.1350	6.5	3.4	3.8	0.6	2.0
711	12.8	0.2880	5.8	2.4	3.9	0.9	2.0
712	11.7	0.3900	5.5	2.1	3.4	0.0	2.0
713	45.7	0.0107	13.0	7.3	3.1	0.9	2.0
714	41.0	0.0127	12.7	6.5	2.8	1.5	2.0
715	53.8	0.0103	13.0	9.5	3.1	1.5	2.0
716	54.7	0.0090	14.0	9.4	4.3	1.2	2.0
718	45.0	0.0111	12.5	7.2	3.5	0.9	2.0
719	61.6	0.0100	13.8	10.8	3.6	1.3	2.0

Air-Water System

D_o = 0.250 in. D = 1.00 in. L = 0.250 in. n = 3 V_c = 142 in^3

Run No.	V_g^o (ft/sec)	V_L (ft/sec)	F (sec^{-1})	$\Delta P - \rho_L h_L$ (lbs_f/ft^2)	$\bar{P}_f$ (lbs_f/ft^2)	σ (lbs_f/ft^2)	h_L (in. liq.)
041	20.4	0.0052	12.5	3.0	4.8	2.2	2.0
042	20.9	0.0061	12.8	2.9	4.4	1.6	2.0
043	25.1	0.0027	14.0	3.3	4.7	1.8	2.0
044	28.5	0.0020	14.0	3.7	5.2	1.8	2.0
045	17.6	0.0089	12.0	2.7	4.5	1.8	2.0
046	15.3	0.0151	11.8	2.4	3.7	1.8	2.0

Air-Water System

D_o = 0.250 in. D = 1.00 in. L = 0.250 in. n = 3 V_c = 091 in^3

Run No.	V_g^o (ft/sec)	V_L (ft/sec)	F (sec^{-1})	$\Delta P - \rho_L H_L$ (lbs_f/ft^2)	$\bar{P}_f$ (lbs_f/ft^2)	σ (lbs_f/ft^2)	h_L (in. liq.)
901	17.8	0.0193	15.5	2.6	5.3	2.4	2.0
902	21.2	0.0101	16.3	2.9	5.7	2.2	2.0
903	29.3	0.0028	17.8	3.6	6.5	2.7	2.0
904	25.4	0.0059	17.3	3.2	6.4	2.7	2.0
905	14.6	0.0285	15.0	2.2	5.5	2.4	2.0
906	10.9	0.0451	14.3	1.8	5.5	3.1	2.0
907	12.3	0.0358	14.5	2.1	5.4	2.0	2.0
907	8.1	0.0630	13.3	1.7	5.3	2.0	2.0

Air-Water System

D_o = 0.250 in. D = 1.00 in. L = 0.250 in. n =7 V_c =262 in^3

Run No.	V_g^o (ft/sec)	V_L (ft/sec)	F (sec^{-1})	$\Delta P - \rho_L h_L$ (lbs_f/ft^2)	$\bar{P}_f$ (lbs_f/ft^2)	σ (lbs_f/ft^2)	h_L (in. liq.)
911	12.2	0.0216	12.3	1.6	4.0	2.1	2.0
912	9.7	0.0349	11.8	1.3	4.9	2.2	2.0
913	14.0	0.0108	12.8	2.0	4.4	1.9	2.0
914	17.8	0.0042	13.3	2.2	3.1	1.7	2.0
915	22.2	0.0012	14.0	2.6	3.6	1.8	2.0
916	11.2	0.0276	12.3	1.4	3.8	1.7	2.0
917	14.0	0.0179	12.5	2.0	4.6	2.1	2.0
918	22.4	0.0016	14.0	2.6	3.7	2.2	2.0
919	10.8	0.0511	11.5	1.5	7.2	2.3	2.0

Air-Water System

D_o = 0.250 in. D = 1.00 in. L = 0.250 in. n = 7 V_c = 142 in^3

Run No.	V_g^o (ft/sec)	V_L (ft/sec)	F (sec^{-1})	$\Delta P - \rho_L h_L$ (lbs_f/ft^2)	$\bar{P}_f$ (lbs_f/ft^2)	σ (lbs_f/ft^2)	h_L (in. liq.)
931	16.8	0.0039	18.8	2.1	3.7	1.9	2.0
932	19.9	0.0028	20.3	2.3	3.9	2.9	2.0
933	22.4	0.0015	21.3	2.5	4.3	2.2	2.0
934	12.6	0.0094	18.3	1.8	4.3	2.4	2.0
935	14.5	0.0069	18.7	1.9	3.3	2.5	2.0

Air-Water System

D_o = 0.250 in. D = 1.00in. L = 0.250 in. n = 7 V_c = 091 in^3

Run No.	V_g^o (ft/sec)	V_L (ft/sec)	F (sec^{-1})	$\Delta P - \rho_L h_L$ (lbs_f/ft^2)	$\bar{P}_f$ (lbs_f/ft^2)	σ (lbs_f/ft^2)	h_L (in. liq.)
921	15.6	0.0042	23.8	1.7	4.6	2.1	2.0
922	18.6	0.0029	25.3	2.1	4.4	2.4	2.0
923	13.8	0.0062	22.3	1.6	3.9	2.5	2.0
924	20.9	0.0019	25.8	2.3	4.6	3.1	2.0
925	11.3	0.0111	22.5	1.7	3.9	2.2	2.0
926	22.9	0.0013	26.0	2.4	4.2	2.5	2.0
917	7.4	0.0264	19.3	1.5	4.6	1.9	2.0

Air-Water System

D_o = 0.250 in. D = 1.00 in. L = 0.250 in. n = 29 V_c = 276 in^3

Run No.	V_g^o (ft/sec)	V_L (ft/sec)	F (sec^{-1})	$\Delta P - \rho_L h_L$ (lbs_f/ft^2)	$\bar{P}_f$ (lbs_f/ft^2)	σ (lbs_f/ft^2)	h_L (in. liq.)
271	21.4	0.0016	25.0	1.5	1.7	0.9	2.0
272	17.5	0.0118	23.5	0.9	1.2	0.8	1.9
273	19.8	0.0022	24.0	1.3	1.6	0.7	2.0
274	18.7	0.0038	23.5	1.3	1.3	0.7	2.1
275	16.0	0.0156	23.5	0.9	1.3	0.7	2.1

Air-Water System

D_o =0.250 in. D,=0.75 in. L = 0.250 in. n = 41 V_c =290 in^3

Run No.	V_g^o (ft/sec)	V_L (ft/sec)	F (sec^{-1})	$\Delta P - \rho_L h_L$ (lbs_f/ft^2)	$\bar{P}_f$ (lbs_f/ft^2)	σ (lbs_f/ft^2)	h_L (in. liq.)
453	21.9	0.0021	28.5	1.8	1.8	1.4	2.0
454	19.5	0.0069	28.0	1.4	1.9	0.9	2.0
455	17.9	0.0227	27.5	1.2	1.7	1.2	2.0
456	17.0	0.0261	26.5	1.0	1.8	1.0	2.0
457	14.5	0.0352	26.0	1.8	1.8	1.5	2.0
458	20.7	0.0036	28.0	1.6	2.2	1.1	2.0

Air-Water System

D_o =0.250 in. D = 0.75 in. L = 0.250 in. n = 49 V_c = 290 in^3

Run No.	V_g^o (ft/sec)	V_L (ft/sec)	F (sec^{-1})	$\Delta P - \rho_L h_L$ (lbs_f/ft^2)	$\bar{P}_f$ (lbs_f/ft^2)	σ (lbs_f/ft^2)	h_L (in. liq.)
471	21.4	0.0173	18.6	1.8	1.6	1.3	2.0
472	27.4	0.0088	21.0	2.9	1.3	1.0	2.0
473	33.0	0.0047	25.0	4.1	1.1	1.2	2.0

Air-Water System

D_o = 0.250 in. D = 0.75 in. L = 0.250 in. n = 49 V_c = 290 in^3

Run No.	V_g^o (ft/sec)	V_L (ft/sec)	F (sec^{-1})	$\Delta P - \rho_L h_L$ (lbs_f/ft^2)	$\bar{P}_f$ (lbs_f/ft^2)	σ (lbs_f/ft^2)	h_L (in. liq.)
481	21.6	0.0063	28.0	2.3	1.6	1.2	2.0
482	24.2	0.0030	29.5	2.7	1.1	1.0	2.0
483	26.0	0.0020	32.0	2.7	1.0	0.8	2.0
484	19.4	0.0103	27.5	1.9	1.6	1.3	2.0
485	16.2	0.0204	26.0	1.6	0.8	0.9	2.1
486	13.9	0.0316	24.5	1.0	1.7	1.3	2.0

Air-Water System

D_o = 0.250 in. D = 1.00 in. L = 0.250 in. n = 3 V_c = 262 in^3

Run No.	V_g^o (ft/sec)	V_L (ft/sec)	F (sec^{-1})	$\Delta P - \rho_L h_L$ (lbs_f/ft^2)	$\bar{P}_f$ (lbs_f/ft^2)	σ (lbs_f/ft^2)	h_L (in. liq.)
891	19.4	0.0378	10.7	3.4	6.9	1.4	1.0
892	13.9	0.1050	9.4	2.8	8.6	0.7	1.0
893	25.7	0.0049	11.9	4.2	5.8	1.5	1.0
894	20.7	0.0265	10.9	3.6	6.7	1.1	1.0
895	23.0	0.0123	11.4	3.9	6.2	1.9	1.0
896	26.6	0.0043	12.0	4.3	5.7	2.0	1.0
897	16.1	0.0075	10.0	3.0	7.8	1.5	1.0
898	28.5	0.0027	12.3	4.5	5.4	2.3	1.0
131	17.4	0.0111	14.8	2.5	2.5	1.4	1.0
132	20.7	0.0070	15.7	2.7	2.3	1.3	1.0
133	15.3	0.0179	14.7	2.3	2.0	1.3	1.0
134	13.0	0.0365	12.3	2.1	2.8	1.5	0.9
135	10.7	0.0795	8.0	1.8	4.6	0.5	1.0
136	26.4	0.0048	15.8	3.1	2.3	1.2	1.0
137	29.2	0.0041	18.3	3.7	2.2	1.0	1.0
311	20.9	0.0278	10.3	3.9	4.6	0.9	1.1
312	17.1	0.0696	9.8	3.5	5.0	0.9	1.0
313	14.8	0.1090	9.0	3.1	6.4	1.1	1.1
314	26.0	0.0048	12.0	4.5	3.4	1.2	1.1
315	31.0	0.0016	12.8	4.3	3.4	1.3	1.1

Air-Water System

D_o = 0.250 in. D = 1.00 in. L = 0.250 in. n = 3 V_c = 262 in^3

Run No.	V_g^o (ft/sec)	V_L (ft/sec)	F (sec^{-1})	$\Delta P - \rho_L h_L$ (lbs_f/ft^2)	$\bar{P}_f$ (lbs_f/ft^2)	σ (lbs_f/ft^2)	h_L (in. liq.)
111	17.1	0.0079	10.8	2.1	3.4	1.4	1.5
112	21.2	0.0036	11.5	2.5	3.7	2.3	1.5
113	13.2	0.0318	9.3	2.1	4.6	1.4	1.5
114	14.7	0.0170	9.5	2.1	4.8	2.4	1.5
115	25.6	0.0021	12.5	3.3	4.8	2.0	1.5
116	11.0	0.0484	8.5	1.8	5.8	1.5	1.5
117	19.7	0.0036	11.3	2.5	3.7	1.2	1.5
331	20.5	0.0398	10.0	3.5	5.8	0.8	1.5
332	30.6	0.0017	11.8	4.3	4.3	1.4	1.5
333	24.3	0.0074	10.5	3.9	5.5	1.3	1.5
334	26.1	0.0045	10.5	3.9	4.2	1.9	1.5
335	22.3	0.0210	10.3	3.7	6.0	2.4	1.4

Air-Water System

D_o = 0.250 in. D = 1.00 in. L = 0.250 in. n = 3 V_c = 262 in^3

Run No.	V_g^o (ft/sec)	V_L (ft/sec)	F (sec^{-1})	$\Delta P - \rho_L h_L$ (lbs_f/ft^2)	$\bar{P}_f$ (lbs_f/ft^2)	σ (lbs_f/ft^2)	h_L (in. liq.)
881	17.8	0.0173	10.8	2.5	3.3	1.8	3.0
882	21.2	0.0111	11.6	2.9	3.7	1.7	3.0
883	13.9	0.0375	9.9	2.1	2.9	2.1	3.0
884	30.0	0.0049	13.2	4.0	4.4	2.4	3.0
885	38.4	0.0033	14.6	5.2	5.0	3.0	3.0
886	25.4	0.0069	12.4	3.5	4.0	3.0	3.0
887	9.6	0.0908	8.8	1.9	2.4	3.0	3.0
321	19.6	0.0197	9.0	3.3	4.6	2.0	3.0
322	16.1	0.0297	8.8	2.9	4.7	2.4	3.0
323	25.7	0.0093	9.5	3.9	4.8	2.3	3.0
324	33.1	0.0045	9.8	4.7	5.4	1.4	3.0
325	39.4	0.0026	9.8	5.5	6.6	2.3	3.0
326	43.5	0.0020	10.3	6.1	4.9	1.7	3.0
327	10.7	0.1160	7.8	2.5	5.9	0.7	3.0

Air-Water System

D_o =0.250 in. D =1.00 in. L = 0.250 in. n = 3 V_c = 262 in^3

Run No.	V_g^o (ft/sec)	V_L (ft/sec)	F (sec^{-1})	$\Delta P - \rho_L h_L$ (lbs_f/ft^2)	$\bar{P}_f$ (lbs_f/ft^2)	σ (lbs_f/ft^2)	h_L (in. liq.)
861	17.3	0.0104	11.4	2.5	3.3	2.3	4.0
862	20.9	0.0074	12.2	2.9	3.6	2.2	4.0
863	11.9	0.0231	9.9	1.8	2.7	2.0	4.0
864	25.4	0.0055	13.1	3.3	4.0	2.4	4.0
865	14.6	0.0144	10.8	2.1	3.0	2.2	4.0
866	30.0	0.0045	13.9	3.8	4.4	2.6	4.0
871	17.3	0.0115	11.4	2.5	3.3	1.8	4.0
872	20.7	0.0070	12.1	2.9	3.6	2.0	4.0
873	30.0	0.0042	13.9	3.8	4.4	2.2	4.0
874	26.7	0.0060	13.3	3.4	4.1	1.6	4.0
875	35.0	0.0035	14.8	4.4	4.7	3.2	4.0
876	45.6	0.0025	16.3	6.0	5.4	3.1	4.0
121	18.6	0.0130	11.8	1.6	2.8	1.2	3.9
122	21.0	0.0108	12.5	2.3	2.9	2.0	3.9
123	15.8	0.0135	11.0	1.6	2.8	1.7	3.9
124	10.7	0.0219	9.5	1.4	2.6	1.7	3.9
125	26.2	0.0067	13.0	3.1	3.5	1.2	3.9
302	19.6	0.0133	10.3	2.5	4.1	2.0	3.9
303	13.3	0.0307	8.8	1.0	3.5	1.8	3.9
304	22.0	0.0116	10.0	3.1	4.1	2.1	3.9
305	29.3	0.0067	10.3	3.9	5.3	2.3	3.9
306	35.7	0.0038	10.3	4.7	6.1	2.4	3.9
307	40.1	0.0025	10.3	5.3	5.5	2.1	3.9
308	48.9	0.0018	10.5	6.6	6.7	2.5	3.9

Air-Water System

D_o =0.250 in. D = 0.75 in. L = 0.250 in. n = 3 V_c=262 in.^{3}

Run No.	V_g^o (ft/sec)	V_L (ft/sec)	F (sec^{-1})	$\Delta P - \rho_L h_L$ (lbs_f/ft^2)	$\bar{P}_f$ (lbs_f/ft^2)	σ (lbs_f/ft^2)	h_L (in. liq.)
231	31.9	0.0024	10.5	3.6	4.9	1.1	1.9
232	26.4	0.0070	10.0	2.8	3.8	1.5	1.9
233	19.6	0.0191	9.5	2.2	4.6	1.1	1.9
234	23.1	0.0107	9.8	2.6	3.9	1.3	1.9
235	28.7	0.0045	10.0	3.4	5.1	1.2	1.9
236	17.4	0.0222	9.3	2.4	3.4	1.5	1.9
237	14.3	0.0293	8.3	1.9	2.8	1.2	1.9

Helium-Water System

D_o= 0.250 in. D = 0.50 in. L = 0.250 in. n = 3 V_c = 262 in.^{3}

Run No.	V_g^o (ft/sec)	V_L (ft/sec)	F (sec^{-1})	$\Delta P - \rho_L h_L$ (lbs_f/ft^2)	$\bar{P}_f$ (lbs_f/ft^2)	σ (lbs_f/ft^2)	h_L (in. liq.)
281	48.6	0.0729	10.3	6.9	8.2	0.7	1.9
282	55.1	0.0504	10.3	8.5	9.6	0.9	2.0
283	60.4	0.0365	10.5	10.3	9.1	1.3	1.9
284	65.0	0.0278	11.0	12.4	8.9	1.4	1.9
285	74.2	0.0061	11.5	16.1	8.1	2.5	2.0
286	83.1	0.0077	11.0	18.3	9.4	1.6	2.0

Argon-Water System

D_o = 0.375 in. D = 1.50 in. L = 0.375 in. n = 3 V_c = 262 in.^{3}

Run No.	V_g^o (ft/sec)	V_L (ft/sec)	F (sec^{-1})	$\Delta P - \rho_L h_L$ (lbs_f/ft^2)	$\bar{P}_f$ (lbs_f/ft^2)	σ (lbs_f/ft^2)	h_L (in. liq.)
161	22.4	0.0153	14.5	1.8	3.7	1.7	2.0
162	26.9	0.0085	14.3	2.3	3.1	1.2	2.0
163	31.1	0.0046	15.3	3.0	3.5	1.7	1.9
164	35.5	0.0027	15.3	3.7	4.1	1.8	2.0
165	17.7	0.0274	13.7	1.4	3.5	1.5	2.0
166	15.9	0.0331	13.0	1.3	3.7	1.8	2.0
167	14.0	0.0421	12.5	1.2	3.6	1.8	1.9
371	35.7	0.0025	10.0	3.3	6.6	2.2	3.0
372	27.5	0.0050	10.0	2.5	7.1	2.5	3.0
373	20.2	0.0203	9.5	1.6	6.6	2.1	3.0
374	15.4	0.0430	9.5	1.2	6.2	2.1	3.0
375	34.0	0.0026	10.0	2.5	6.8	3.3	3.9
376	26.4	0.0118	10.5	1.8	7.4	2.3	3.8
377	18.5	0.0410	10.5	0.8	6.9	2.4	3.8

Air-Water System

D_o = 0.375 in. D = 1.12 in. L = 0.375 in. n = 3 V_c = 262 $in.^3$

Run No.	V_g^o (ft/sec)	V_L (ft/sec)	F (sec^{-1})	$\Delta P - \rho_L h_L$ (lbs_f/ft^2)	$\bar{P}_f$ (lbs_f/ft^2)	σ (lbs_f/ft^2)	h_L (in. liq.)
221	25.4	0.0077	11.0	2.1	6.4	2.5	2.0
222	29.8	0.0040	11.5	2.5	7.8	2.7	2.0
223	32.6	0.0021	11.8	3.1	9.3	2.5	2.0
224	22.1	0.0136	11.0	1.8	8.8	2.7	2.0
225	18.1	0.0318	11.0	1.6	8.2	2.4	2.0
226	14.9	0.0492	10.8	1.4	8.0	2.8	2.0
227	20.5	0.0206	11.5	1.6	8.2	2.6	2.0
294	12.8	0.0707	10.5	1.4	11.7	2.6	2.0
295	10.0	0.1420	9.8	1.2	12.0	3.1	2.0
296	11.3	0.0943	10.3	1.2	11.3	3.1	2.0

Air-Water System

D_o = 0.375 in. D = 0.75 in. L = 0.375 in. n = 3 V_c = 262 $in.^3$

Run No.	V_g^o (ft/sec)	V_L (ft/sec)	F (sec^{-1})	$\Delta P - \rho_L h_L$ (lbs_f/ft^2)	$\bar{P}_f$ (lbs_f/ft^2)	σ (lbs_f/ft^2)	h_L (in. liq.)
241	25.3	0.0248	10.0	1.9	7.7	1.2	2.0
242	28.2	0.0147	10.0	2.4	7.1	1.6	2.0
243	31.3	0.0098	9.8	2.8	7.7	1.6	2.0
244	33.9	0.0058	10.3	3.2	8.2	1.1	2.0
245	36.9	0.0033	10.6	3.6	6.4	2.4	2.0
246	21.0	0.0351	9.8	1.3	7.8	1.3	2.0
247	18.2	0.0427	9.5	1.4	7.4	1.3	1.9
248	14.5	0.0610	9.5	0.9	6.0	1.2	2.0
297	13.0	0.1210	8.8	0.8	9.5	1.0	2.1
298	15.9	0.1070	9.0	1.0	8.6	1.2	2.1
341	25.4	0.0406	9.3	2.9	14.1	2.7	3.0
342	34.8	0.0171	9.5	4.1	14.4	2.0	3.0
343	29.8	0.0312	9.8	3.3	12.7	3.2	3.0
344	41.2	0.0081	10.3	4.9	13.6	3.1	2.9
345	44.5	0.0046	10.5	5.5	13.1	3.8	2.9
346	50.3	0.0021	10.5	6.8	14.2	1.9	2.9
351	40.6	0.0049	9.8	2.1	12.1	4.0	3.9
352	44.5	0.0026	9.8	2.3	13.3	5.0	3.9
353	36.2	0.0078	9.3	1.6	15.1	3.5	3.9
354	29.6	0.0195	9.3	1.0	12.9	4.2	3.9
355	25.3	0.0345	9.0	0.2	11.8	3.8	3.9

Air-Water System

D_o = 0.500 in. D = 2.00 in. L = 0.500 in. n = 3 V_c = 276 $in.^3$

Run No.	V_g^o (ft/sec)	V_L (ft/sec)	F (sec^{-1})	$\Delta P - \rho_L h_L$ (lbs_f/ft^2)	$\bar{P}_f$ (lbs_f/ft^2)	σ (lbs_f/ft^2)	h_L (in. liq.)
191	35.1	0.0028	17.5	3.4	6.3	2.3	2.0
192	29.4	0.0083	17.0	2.7	5.8	2.4	1.9
193	23.3	0.0201	16.5	1.7	6.6	2.8	2.0
194	31.9	0.0048	16.5	3.0	6.4	2.7	2.0
195	19.6	0.0332	15.5	1.1	7.5	2.5	1.9
196	16.7	0.0408	15.5	0.9	6.5	3.1	2.0
201	31.3	0.0034	15.0	3.3	8.6	3.2	2.0
202	34.7	0.0020	16.0	3.6	7.6	2.9	2.0
203	28.4	0.0067	14.8	2.7	8.2	3.1	1.9
204	25.7	0.0111	14.3	2.5	9.7	2.8	1.9
205	20.5	0.0231	13.5	2.3	9.9	3.0	1.9
206	17.0	0.0353	13.0	1.4	7.2	2.7	1.9
361	33.1	0.0017	10.5	4.7	9.2	3.4	4.1
362	28.6	0.0033	10.3	3.5	10.7	3.6	4.1
363	25.5	0.0057	9.5	3.3	8.8	3.2	4.1
364	21.3	0.0105	9.8	2.7	9.0	3.1	4.1
365	16.5	0.0218	9.0	2.7	9.7	3.6	4.1
366	13.7	0.0504	10.3	2.3	7.6	3.8	4.1
367	25.9	0.0080	9.8	3.5	9.2	3.6	3.0
368	19.4	0.0196	10.0	3.1	9.2	0.0	3.0
369	27.8	0.0053	10.8	3.7	9.9	3.6	2.9

Air-Water System

D_o = 0.500 in. D = 1.00 in. L = 0.500 in. n = 3 V_c =276 $in.^3$

Run No.	V_g^o (ft/sec)	V_L (ft/sec)	F (sec^{-1})	$\Delta P - \rho_L h_L$ (lbs_f/ft^2)	$\bar{P}_f$ (lbs_f/ft^2)	σ (lbs_f/ft^2)	h_L (in. liq.)
261	25.3	0.0050	10.3	1.5	8.7	1.9	2.0
262	29.2	0.0023	10.5	1.7	8.3	1.7	2.0
263	22.1	0.0076	10.0	1.1	9.2	2.5	2.0
264	17.6	0.0179	9.8	1.3	8.7	1.6	2.0
265	14.5	0.0305	9.8	1.1	8.1	1.2	1.9
266	31.3	0.0010	10.5	2.2	10.3	1.6	1.9
267	11.0	0.0582	9.8	1.1	5.5	2.0	1.9
291	12.7	0.0550	9.5	0.8	9.4	1.3	1.9
292	10.8	0.0665	9.5	1.0	8.1	1.2	1.9
293	9.3	0.0779	9.0	1.2	7.8	1.9	2.0

Air-Water System

D_o= 0.250 in. D = 1.00 in. L = 0.750 in. n = 3 V_c = 262 $in.^3$

Run No.	V_g^o (ft/sec)	V_L (ft/sec)	F (sec^{-1})	$\Delta P - \rho_L h_L$ (lbs_f/ft^2)	$\bar{P}_f$ (lbs_f/ft^2)	σ (lbs_f/ft^2)	h_L (in. liq.)
841	19.9	0.0075	12.3	2.2	3.5	1.8	2.0
842	26.1	0.0023	13.6	2.7	4.1	2.0	2.0
843	22.7	0.0029	12.9	2.5	3.8	1.3	2.0
847	25.3	0.0024	13.4	2.7	4.0	1.9	2.0
851	18.1	0.0112	12.0	2.1	3.4	2.1	2.0
853	20.9	0.0075	12.6	2.3	3.6	2.1	2.0

Two-ft Column Data

Air-Water System

D_o = 0.25 in. D = 1.0 in. L = 0.25 in. n = 450 V_c = 25 ft.^{2}

V_L (ft/sec)	V_g^o (ft/sec)	$\Delta P - \rho_L h_L$ (lbs_f/ft^2)	h_L (in. liq.)	h_W (in.)	Q_L (gpm/ft weir)
0.0013	22.9	0.2	1.0	1.0	30
0.0217	16.7	0.2	1.0	1.0	30
0.0041	20.1	0.1	1.0	1.0	30
0.0124	18.3	0.1	1.0	1.0	28
0.0016	21.6	0.2	1.0	1.0	28
0.0534	12.7	0.1	1.0	1.0	28
0.0030	32.4	0.4	1.5	1.0	94
0.0054	26.6	0.3	1.5	1.0	71
0.0159	21.9	0.3	1.5	1.0	60
0.0078	24.1	0.3	1.5	1.0	65
0.0040	29.9	0.4	1.5	1.0	87
0.0064	26.7	0.3	1.5	1.0	73
0.0053	30.0	0.4	1.5	1.0	89
0.0028	32.1	0.4	1.5	1.0	90
0.0182	21.6	0.3	1.5	1.0	62
0.0923	12.1	0.2	1.5	1.0	40
0.0088	24.5	0.3	1.5	1.0	65
0.0034	29.9	0.4	1.5	1.0	80
0.0423	17.0	0.2	1.5	1.0	50
0.0266	18.8	0.2	1.5	1.0	50
0.0634	14.3	0.2	1.5	1.0	45
0.0019	27.0	0.2	1.5	1.5	34
0.0067	22.0	0.2	1.5	1.5	32
0.0033	24.3	0.2	1.5	1.5	32
0.0202	17.4	0.2	1.5	1.5	30
0.0569	13.0	0.1	1.5	1.5	29
0.0017	27.4	0.2	1.5	1.5	32
0.0094	21.4	0.2	1.5	1.5	27

V_L (ft/sec)	V_g^o (ft/sec)	$\Delta P - \rho_L h_L$ (lbs_f/ft^2)	h_L (in. liq.)	h_W (in.)	Q_L (gpm/ft weir)
0.0049	31.7	0.4	2.0	1.5	92
0.0028	33.9	0.4	2.0	1.5	92
0.0215	22.2	0.2	2.0	1.5	62
0.0514	17.5	0.2	2.0	1.5	54
0.0985	13.4	0.1	2.0	1.5	47
0.0084	27.1	0.3	2.0	1.5	68
0.0075	28.9	0.3	2.0	1.5	81
0.0131	24.4	0.2	2.0	1.5	66
0.0334	19.5	0.2	2.0	1.5	51
0.0783	15.0	0.1	2.0	1.5	49
0.0075	25.8	0.2	2.0	2.0	39
0.0107	23.3	0.2	2.0	2.0	37
0.0049	28.0	0.2	2.0	2.0	45
0.0026	31.1	0.3	2.0	2.0	34
0.0654	16.1	0.1	2.0	2.0	35
0.0307	18.9	0.2	2.0	2.0	37
0.0174	21.0	0.2	2.0	2.0	35
0.0082	33.3	0.4	2.5	2.0	102
0.0053	35.6	0.4	2.5	2.0	102
0.0083	30.6	0.3	2.5	2.0	95
0.0042	38.4	0.5	2.5	2.0	128
0.0088	29.8	0.3	2.5	2.0	90
0.0154	25.7	0.3	2.5	2.0	72
0.0398	21.9	0.2	2.5	2.0	64
0.0668	18.3	0.2	2.5	2.0	59
0.1060	15.3	0.1	2.5	2.0	53
0.0449	20.4	0.2	2.5	2.0	62
0.0250	23.4	0.2	2.5	2.0	68
0.0114	27.6	0.3	2.5	2.0	78
0.0867	16.4	0.1	2.5	2.0	57

V_L (ft/sec)	V_g^o (ft/sec)	$\Delta P - \rho_L h_L$ (lbs_f/ft^2)	h_L (in. liq.)	h_W (in.)	Q_L (gpm/ft weir)
0.0026	39.8	0.4	3.0	3.0	81
0.0041	37.0	0.4	3.0	3.0	78
0.0081	32.2	0.3	3.0	3.0	87
0.0324	25.4	0.2	3.0	3.0	66
0.0174	28.0	0.3	3.0	3.0	57
0.0804	19.9	0.2	3.0	3.0	60
0.0024	40.5	0.4	3.0	3.0	86
0.0036	37.6	0.4	3.0	3.0	80
0.0015	43.6	0.4	3.0	3.0	69
0.0080	31.9	0.3	3.0	3.0	52
0.0280	25.3	0.2	3.0	3.0	59
0.0153	28.2	0.2	3.0	3.0	49
0.0060	39.7	0.4	3.2	3.0	122
0.0085	32.8	0.3	3.2	3.0	93
0.0153	28.2	0.2	3.2	3.0	74
0.0309	24.9	0.2	3.2	3.0	74
0.0849	19.4	0.2	3.2	3.0	64
0.0057	39.8	0.5	3.2	3.0	122
0.0081	32.1	0.3	3.2	3.0	93
0.0209	33.9	0.3	4.0	5.0	62
0.0135	38.6	0.4	4.0	5.0	70
0.0077	43.6	0.5	4.0	5.0	82
0.0053	47.7	0.6	4.0	5.0	94
0.0045	51.6	0.7	4.0	5.0	110
0.0033	57.4	0.8	4.0	5.0	124
0.0423	28.2	0.2	4.0	5.0	48
0.0764	23.3	0.2	4.0	5.0	35
0.0181	35.9	0.4	4.5	5.0	108
0.0161	40.2	0.5	4.5	5.0	127
0.0141	43.5	0.6	4.5	5.0	128
0.0315	31.6	0.3	4.5	5.0	85
0.0277	33.2	0.3	4.5	5.0	97
0.0461	28.0	0.2	4.5	5.0	76
0.0788	23.4	0.2	4.5	5.0	65

NOMENCLATURE

A_f-- frontal area of the bubble, L^2.

A_o-- hole area, L^2.

b-- carried mass of liquid, M.

c-- sonic velocity, L/θ.

C-- modified orifice coefficient defined by $P = C(V_g^o)^2/2g_c$.

C_D-- drag coefficient.

C_o-- modified orifice coefficient for ideal fluid.

D-- distance between the holes, L.

D_b-- diameter of the bubble, L.

D_o-- diameter of the hole, L.

Eu-- Euler number, $(\Delta P_T - \rho_L h_L)/(\rho_g V_g^{o2}/2g_c)$.

F-- frequency of the pressure fluctuations in the chamber under the plate, $1/\theta$.

F_g-- flow factor $V_g^o \sqrt{\rho_g}$.

FR-- Froude number, $D_o g/V_g^{o2}$.

g-- acceleration of gravity, L/θ^2.

g_c-- conversion factor, $ML/F\theta^2$.

h_L-- head of liquid on the plate, L.

h_w-- height of the overflow weir, L.

L-- thickness of the plate, L.

n-- number of holes.

P_a-- atmosphereic pressure, F/L^2.

P_B-- time-average pressure in the chamber under the plate, F/L^2.

P_c-- instantaneous pressure in the chamber under the plate, F/L^2.

P'_f-- instantaneous fluctuating component of the chamber pressure, $P_c - P_B$, F/L^2.

P_f-- maximum drop in chamber pressure below the time average, F/L^2.

$\overline{P}_f$-- average maximum drop in chamber pressure below the time average, F/L^2.

P_o-- pressure in the chamber above the plate, F/L^2.

P_p-- pressure in the liquid at the plate surface, $P_o + h_L$, F/L^2.

P_t-- pressure inside the bubble, F/L^2.

ΔP-- pressure change, F/L^2.

NOMENCLATURE (cont'd.)

ΔP_T-- average total pressure drop across the plate, $P_B - P_o$, F/L^2.

$\Delta P'_T$-- instantaneous total pressure drop across the plate, $P_c - P_o$, F/L^2.

Q_g^o-- average volumetric gas-flow rate into the chamber, L^3/Θ.

Q_L-- volumetric liquid flow rate to the plate L^3/Θ.

Re_g-- Reynold's number based on gas properties, $D_o V_g^o \rho_g / \mu_g$.

Re_L-- Reynold's number based on liquid properties, $D_o V_g^o \rho_L / \mu_L$.

t-- time, Θ.

V_B-- volume of the bubble, L^3.

V_c-- volume of the chamber under the plate, L^3.

V'_g-- instantaneous gas velocity through the holes with all holes assumed to be operating equally, L/Θ.

V_g^o-- time-average gas velocity through the holes with all the holes operating equally, Q_g^o/nA_o, L/Θ.

V'_L-- instantaneous dumping rate with all the holes operating equally, L/Θ.

V_L-- time-average dumping rate with all the holes operating equally, L/Θ.

ΔV-- volume change, L^3.

We-- Weber number, $4\gamma/D_o (\rho_g V_g^{o\,2}/2g_c)$.

z-- $(P_f - \bar{P}_f)/\sigma$.

z-- $(\Delta P_T - \rho_L h_L - \rho_L L - \bar{P}_f)/\sigma$.

ϵ-- a factor that depends on the number of holes and measures the blocking effect of neighboring holes.

ϕ-- volume number (defined by Eq. 3).

γ-- surface tension, F/L.

μ_g-- viscosity of the gas, $M/L\Theta$.

μ_L-- viscosity of the liquid, $M/L\Theta$.

η-- a number of standard deviations.

ρ_g-- density of the gas, M/L^3.

$\bar{\rho}_g$-- average density of the gas, M/L^3.

ρ_L-- density of the liquid, M/L^3.

$\Delta\rho$-- density difference, M/L^3, $\rho_L - \rho_g$.

σ-- standard deviation of P_f, F/L^2.

LIST OF ILLUSTRATIONS

LIST OF ILLUSTRATIONS (cont'd.)

LIST OF ILLUSTRATIONS (cont'd.)

BIBLIOGRAPHY

1. D. S. Arnold, C. A. Plank, and E. M. Schoenborn, Chem. Eng. Progr. 48, 633 (1952).
2. F. D. Mayfield, W. L. Church, Jr., A. C Green, D. C. Lee, Jr., and R. W. Rasmussen, Ind. Eng. Chem. 44, 2238 (1952).
3. F. A. Zenz, Petrol. Refiner, 33, No. 2,99 (1954).
4. C. d'A. Hunt, D. N Hanson, and C. R. Wilke, A. I. Ch. E. Journal 1, 441 (1956).
5. J. B. Jones and C. Pyle, Chem. Eng. Progr. 51, 424 (1955).
6. C. d'A. Hunt, "Capacity Factors in the Performance of Perforated-Plate Columns", Ph.D. Thesis, University of California, Berkeley, California, or UCRL-2696, October 1954.
7. C. L. Umholtz, Humble Oil and Refining Co., Baytown, Texas, private communication (1956).
8. L. Davidson, "A Study of the Formation of Gas Bubbles from Horizontal Circular Submerged Orifices", Ph.D. Thesis, Columbia University, New York (1951).
9. P. H. Calderbank, Trans. Inst. Chem. Engrs. (London) 34, 79 (1956).
10. D. G. Robinson, "Mass Transfer within Bubbles", M.Sc. Thesis, University of Toronto, Toronto, Canada (1956).
11. C. J. Quigley, A. I. Johnson, and B L. Harris, Chem. Eng. Progr. Symposium Series No. 16, 51, 31 (1955).
12. D. W. van Krevelen and P. J. Hoftijzer, Chem. Eng. Progr. 46, 29 (1950).
13. R. R. Hughes, A. E. Handlos, H. D. Evans, and R. L. Maycock, Chem. Eng. Progr. 51, 557 (1955).
14. Lord Rayleigh, Theory of Sound, Second Edition (Dover, New York, 1945), Vol. 2, p. 188.
15. G. A. Hughmark and H. E. O'Connell, Chem. Eng. Progr. 53, 127M (1957).
16. International Critical Tables, Edward W. Washburn, Ed. (McGraw-Hill, New York, 1929), Vol. 5, p. 2.
17. International Critical Tables, Edward W. Washburn, Ed. (McGraw-Hill, New York, 1929), Vol. 6, p. 462.

BIBLIOGRAPHY (cont'd.)

18. The Refrigerating Data Book, B. H. Jennings, Ed. (Am. Soc. Refrigerating Engrs., New York, 1951), Seventh Edition, Basic Volume, p. 94, Table 2.

19. C. A. Bennett and N. L. Franklin, Statistics in Chemistry and the Chemical Industry (Wiley, New York, 1954), pp. 245-265, 273-283.

20. R. D. Lee, "Gas-Film Mass Transfer on Perforated Plates", Ph.D. Thesis, University of California, Berkeley, California, in preparation.

21. S. Kamei, T. Takamatsu, K. Goto, and A. Kometani, Chem. Eng. (Tokyo) 18, 308 (1954).

22. T. Leibson, R. E. Kelley, and L. A. Bullington, Petrol. Refiner 36, No. 2, 127 (1957).

23. A. S. Foss and J. A. Gerster, Chem. Eng. Progr. 52, 28J (1956).

24. C. J. Hwang and J. R. Hodson, Petrol. Refiner, 37, No. 2, 104-118 (1958).

25. A. P. Colburn, Ind. Eng. Chem. 28, 526 (1936).

26. C. L. Umholtz and M. Van Winkle, Petrol. Refiner 34, No. 7, 144 (1955).

27. C. L. Umholtz and M. Van Winkle, Ind. Eng. Chem. 49, 226 (1957).

28. V. L. Streeter, Fluid Dynamics (McGraw-Hill, New York, 1948), pp. 174-176.

29. H. S. Bean, E. Buckingham, and P. S. Murphys, J. Research Nat. Bur. Standards 2, No. 3, 561 (1929).